PB86-100807

CALIFORNIA INSTITUTE OF TECHNOLOGY

EARTHQUAKE ENGINEERING RESEARCH LABORATORY

CUMULATIVE DAMAGE OF STRUCTURES SUBJECTED TO RESPONSE SPECTRUM CONSISTENT RANDOM PROCESSES

By

Garrett Duane Jeong

Report No. EERL 85-03

A Report on Research Conducted Under a Grant
from the National Science Foundation

Pasadena, California
1985

This investigation was sponsored by Grant No. CEE81-19962 from the National Science Foundation under the supervision of Wilfred D. Iwan. Any opinions, findings, conclusions or recommendations expressed in this publication are those of the author and do not necessarily reflect the views of the National Science Foundation.

CUMULATIVE DAMAGE OF STRUCTURES SUBJECTED TO RESPONSE SPECTRUM CONSISTENT RANDOM PROCESSES

Thesis by

Garrett Duane Jeong

In Partial Fulfillment of the Requirements
for the Degree of
Doctor of Philosophy

California Institute of Technology
Pasadena, California

1985

(Submitted January 11, 1985)

ACKNOWLEDGMENTS

I wish to express my sincere appreciation to Professor W. D. Iwan, my thesis advisor, for his guidance and encouragement throughout the course of this investigation.

I would also like to thank the California Institute of Technology, the National Science Foundation, and the S. D. Bechtel, Jr. Foundation for their financial support during my years of graduate studies.

The technical assistance of Sharon Beckenbach and Gloria Jackson in the typing and preparation of this manuscript is gratefully acknowledged.

Lastly, I would like to thank my parents, to whom this thesis is dedicated, for making me realize the importance of learning and helping me whenever they could throughout my education.

ABSTRACT

A theoretical analysis of the effect of duration on the damage of structures subjected to earthquakes is presented. Earthquake excitation is modeled as a nonstationary random process. Estimates of the first-passage probability of a simple oscillator are employed to choose modulated Gaussian random processes consistent with a prescribed response spectrum. The response spectrum is assumed to be specified independent of the duration. Expressions for the mean damage of a structure are derived using an approach similar to the Miner-Palmgren rule for failure caused by cyclic loads. The expected damage expressions are then evaluated for a structure subjected to modulated Gaussian random processes of varying duration.

Two types of structures are examined: a steel structure and a reinforced concrete structure. Results are presented for systems with constant linear stiffness and a particular form of softening behavior. The nonlinearity of the softening system is accounted for by statistical linearization. The level of expected damage is found to be a strong function of both the duration of the excitation and the ductility of the response.

TABLE OF CONTENTS

TABLE OF CONTENTS (CONCLUDED)

CHAPTER I

INTRODUCTION

In many parts of the world, seismic considerations are the controlling factor in the design of structures. Building codes contain seismic elements which have been adopted for the safety and welfare of the public. For most structures, the building code recommends an equivalent lateral force analysis. Seismically induced loads are accounted for by equivalent static lateral loads. Although easy to implement and computationally efficient, such an approach may be inadequate for structures such as schools, hospitals, nuclear power plants, and other important structures where the integrity of the structure is of great importance.

Most important structures and special facilities are designed using a more detailed dynamic analysis in order to ensure their safety during a seismic event. Such a detailed analysis requires a specification of the anticipated nature of the ground motion as well as a complete description of the structure. If one or more characteristic earthquake accelerograms are specified as input, the equations of motion may be numerically integrated to give a detailed representation of the system response. However, numerical integration may be costly and the statistical nature of the seismic input makes specification of the input time histories difficult.

Due to the many uncertainties in predicting the precise nature of the time history of earthquake ground motion, the design response spectrum has received wide acceptance as a measure of the design input.

The design spectrum provides a direct measure of the anticipated peak response of a structure or system under consideration as a function of its natural frequency and damping. In some cases, it may be argued that the peak response is the predominant factor affecting the safety and reliability of the system. However, in most cases the performance of the system will depend upon more than just the peak response of various components. In particular, for system components which fail due to repeated cyclic loading, performance will be a function of the entire history of cyclic oscillations.

The failure of structures subjected to strong earthquake excitation is often caused by a low-cycle material failure. In this case, the structural components experience high strains and relatively few response cycles. For some materials, this type of failure is often referred to as low-cycle fatigue.

Using numerical integration of the equations of motion of a simple hysteretic steel structure, Kasiraj and Yao [35] showed that low-cycle failure is not predictable by considering only the maximum response. Using random vibration theory, Miles [34] derived an analytical expression for the mean damage of a structure subjected to a stationary random process based upon the cumulative damage hypothesis of Miner [31] and Palmgren [32]. Roberts [33] and Lin [1] generalized the mean damage expression to the nonstationary case, but did not apply it to the low-cycle failure of structures subjected to earthquakes. In order to implement the expressions for expected damage to seismic structures, empirical constants are required for the assumed cumulative damage

hypothesis. Bertero and Popov [27] and Yamada [28] have performed experimental tests on structural members to determine the necessary constants for structures experiencing a number of cycles of oscillation at large strains.

Design spectra may be defined either deterministically or probabilistically. It is the objective of this thesis to examine the effects of the duration of excitation on the reliability of a system when the response spectrum is specified probabilistically. Three basic elements are combined to achieve this goal. First, the first-passage probability for a simple harmonic oscillator is used to define a nonstationary random process which corresponds statistically to a desired response spectrum. Although the first-passage problem for the simple oscillator has not been solved exactly, reasonably accurate approximations have been obtained by Vanmarcke [6] and Mason and Iwan [8]. Secondly, a model is postulated for the incremental damage of a system. Damage to the structure is based on the simple cumulative damage hypothesis proposed by Miner and Palmgren. Finally, random vibration theory is used to compute the accumulated damage of a simple structure and to determine the degree of total damage.

In Chapter II, the relevant concepts from random vibration theory are reviewed. Analytical approaches to the first-passage problem and the method of statistical linearization are also discussed.

In Chapter III, the accuracy of one approach to the first-passage problem is assessed through simulation and then applied to define a response spectrum consistent process. The probabilistic nonlinear

response spectrum of a softening nonlinear elastic system is also examined.

In Chapter IV, an incremental damage model is assumed based on the Miner-Palmgren failure rule for damage due to repeated cyclic loads. Through the further application of random vibration theory, a measure of the damage to a system subjected to a deterministically modulated Gaussian random process is derived.

Damage in a simple structure is calculated in Chapter V for the response spectrum consistent random process defined in Chapter III. The effects of variations in duration of the excitation and ductility ratio of the response are discussed. Damage in a softening nonlinear elastic system is also computed through the use of statistical linearization.

CHAPTER II

RELEVANT CONCEPTS OF RANDOM VIBRATIONS, THE FIRST PASSAGE PROBLEM, AND STATISTICAL LINEARIZATION

2.1 Random Response of a Linear System to a Class of Nonstationary Excitation

The system to be considered is described by its equation of motion

$$\ddot{x} + 2\xi\omega_0\dot{x} + \omega_0^2 x = \theta(t)w(t) \qquad (2.1)$$

where ξ is the fraction of critical damping, ω_0 is the undamped natural frequency in radians per second, and $\theta(t)$ is a deterministic modulating function for $w(t)$, a stationary Gaussian white-noise process with mean zero.

The initial conditions for the system may be posed in one of two ways. First, they can be specified deterministically. A special case of this is the zero start where the system is assumed to be at rest when the excitation is applied. Alternatively, a probability distribution may be specified for the initial conditions. For the system described by equation (2.1) with $\theta(t)$ set to a constant, the stationary response may be described by a stationary probability distribution. If this stationary probability distribution is used to specify initial conditions, this situation is known as a stationary start. In light of the fact that structural response to earthquake-like excitation is to be studied, a zero start will be assumed.

Equation (2.1) may be solved in 2n-space by first considering a system of n first-order ordinary differential equations written in matrix form as

$$\begin{aligned} \dot{\underset{\sim}{y}}(t) &= \underline{\underline{A}}(t)\underset{\sim}{y}(t) + \underline{\underline{B}}(t)w(t) \\ \underset{\sim}{y}(0) &= \underset{\sim}{y}_0 \end{aligned} \tag{2.2}$$

where $\underline{\underline{A}}(t)$ is a time-varying n by n matrix, $\underline{\underline{B}}(t)$ is a time-varying vector of order n, and w(t) is a stationary Gaussian white-noise process with mean zero. The fundamental matrix solution for this system is a time-varying n by n matrix denoted by $\underline{\underline{Y}}(t)$ which satisfies

$$\begin{aligned} \dot{\underline{\underline{Y}}}(t) &= \underline{\underline{A}}(t)\underline{\underline{Y}}(t) \\ \underline{\underline{Y}}(0) &= \underline{\underline{I}} \end{aligned} \tag{2.3}$$

where $\underline{\underline{I}}$ is an n by n identity matrix. The solution to equation (2.2) may be expressed in terms of the fundamental matrix solution as

$$\underset{\sim}{y}(t) = \underline{\underline{Y}}(t)\underset{\sim}{y}_0 + \underline{\underline{Y}}(t)\int_0^t \underline{\underline{Y}}^{-1}(\tau)\underline{\underline{B}}(\tau)w(\tau)d\tau \quad . \tag{2.4}$$

The function w(t) is a stationary white-noise process with mean zero which implies

$$\begin{aligned} E[w(t)] &= 0 \\ E[w(t_1)w(t_2)] &= 2\pi S_0 \delta(t_2 - t_1) \end{aligned} \tag{2.5}$$

where S_0 is a constant spectral density and $\delta(.)$ is the dirac delta

function. Furthermore, since $w(t)$ is Gaussian and $\underset{\sim}{y}(t)$ is related to $w(t)$ through a linear operation, $\underset{\sim}{y}(t)$ is a Gaussian random vector process. It is assumed that the process is specified at a given time by its mean vector and its covariance matrix; however, the autocorrelation matrix $E[\underset{\sim}{y}(t+\tau)\underset{\sim}{y}^T(t)]$ is also needed to completely define the process.

By taking expected values of both sides of equation (2.4) and using equation (2.5), the mean vector $\mu_y(t)$ may be written as

$$\mu_y(t) = E[\underset{\sim}{y}(t)] = \Upsilon(t)\underset{\sim}{y}_0 \quad . \tag{2.6}$$

The covariance matrix $\mathcal{Q}(t)$ is defined as

$$\mathcal{Q}(t) \equiv E\{[\underset{\sim}{y}(t)-\mu_y(t)][\underset{\sim}{y}(t)-\mu_y(t)]^T\} \quad . \tag{2.7}$$

Substituting equations (2.4) and (2.6) into equation (2.7) and taking expected values yields

$$\mathcal{Q}(t) = \Upsilon(t)\{\int_0^t\int_0^t \Upsilon^{-1}(\tau')\mathcal{B}(\tau')E[w(\tau')w(\tau)]\mathcal{B}^T(\tau)[\Upsilon^{-1}(\tau)]^T d\tau' d\tau\}\Upsilon^T(t). \tag{2.8}$$

Using equation (2.5) and performing the integration on τ' gives the covariance matrix as

$$\mathcal{Q}(t) = 2\pi S_0\Upsilon(t)\{\int_0^t \Upsilon^{-1}(\tau)\mathcal{B}(\tau)\mathcal{B}^T(\tau)[\Upsilon^{-1}(\tau)]^T d\tau\}\Upsilon^T(t) \quad . \tag{2.9}$$

An alternative to equation (2.9) for computing the covariance matrix can be obtained [1] by first taking the expected value of equation (2.2)

$$\frac{d}{dt}E[\underset{\sim}{y}(t)] = \underset{\sim}{A}(t)E[\underset{\sim}{y}(t)] \quad . \tag{2.10}$$

Subtracting equation (2.10) from equation (2.2) and letting $\underset{\sim}{z}(t) = \underset{\sim}{y}(t) - E[\underset{\sim}{y}(t)]$ gives

$$\frac{d}{dt}\underset{\sim}{z}(t) = \underset{\sim}{A}(t)\underset{\sim}{z}(t) + \underset{\sim}{B}(t)w(t) \quad . \tag{2.11}$$

Post-multiplying equation (2.11) by $\underset{\sim}{z}^T(t)$ leads to

$$[\frac{d}{dt}\underset{\sim}{z}(t)]\underset{\sim}{z}^T(t) = \underset{\sim}{A}(t)\underset{\sim}{z}(t)\underset{\sim}{z}^T(t) + \underset{\sim}{B}(t)\underset{\sim}{z}^T(t)w(t) \quad . \tag{2.12}$$

Transposing equation (2.12) and adding the result to equation (2.12) yields

$$\frac{d}{dt}[\underset{\sim}{z}(t)\underset{\sim}{z}^T(t)] = \underset{\sim}{A}(t)\underset{\sim}{z}(t)\underset{\sim}{z}^T(t) + \underset{\sim}{z}(t)\underset{\sim}{z}(t)^T\underset{\sim}{A}^T(t) + \underset{\sim}{B}(t)\underset{\sim}{z}^T(t)w(t) + w(t)\underset{\sim}{z}(t)\underset{\sim}{B}^T(t) \quad . \tag{2.13}$$

Taking expected values of both sides of equation (2.13) and noting that $\underset{\sim}{Q}(t) = E[\underset{\sim}{z}(t)\underset{\sim}{z}^T(t)]$, one finds

$$\frac{d}{dt}\underset{\sim}{Q}(t) = \underset{\sim}{A}(t)\underset{\sim}{Q}(t) + [\underset{\sim}{A}(t)\underset{\sim}{Q}(t)]^T + \underset{\sim}{B}(t)E[\underset{\sim}{z}^T(t)w(t)] + E[w(t)\underset{\sim}{z}(t)]\underset{\sim}{B}^T(t) \quad . \tag{2.14}$$

Using equations (2.4) and (2.5), the expected values in the third and fourth terms may be evaluated as

$$\begin{aligned} E[w(t)\underset{\sim}{z}(t)] &= \pi S_0 \underset{\sim}{B}(t) \\ E[\underset{\sim}{z}^T(t)w(t)] &= \pi S_0 \underset{\sim}{B}^T(t) \quad . \end{aligned} \tag{2.15}$$

Hence, equation (2.14) becomes

$$\frac{d}{dt}\underline{\underline{Q}}(t) = \underline{\underline{A}}(t)\underline{\underline{Q}}(t) + [\underline{\underline{A}}(t)\underline{\underline{Q}}(t)]^T + 2\pi S_0 \underline{\underline{\theta}}(t)\underline{\theta}^T(t) \quad . \qquad (2.16)$$

Since the initial conditions are specified deterministically, equation (2.16) has zero initial conditions.

Note that using equation (2.9) requires solving n^2 first-order differential equations for the fundamental matrix solution and $\frac{n(n+1)}{2}$ integrals for the covariance matrix. On the other hand, using equation (2.16), the covariance matrix is directly computed by solving $\frac{n(n+1)}{2}$ first-order differential equations. Except in the simplest cases where one can express the covariance matrix explicitly through equation (2.9), the use of equation (2.16) is probably numerically more efficient.

Having defined the mean vector $\underline{\mu}_y(t)$ and the covariance matrix $\underline{\underline{Q}}(t)$, the joint probability density for the Gaussian vector process $\underset{\sim}{y}(t)$ may now be written as

$$p(\underset{\sim}{y}(t)) = \frac{1}{\sqrt{(2\pi)^n \det \underline{\underline{Q}}(t)}} \exp\{-\frac{1}{2}[\underset{\sim}{y}(t)-\underline{\mu}_y(t)]^T \underline{\underline{Q}}^{-1}(t)[\underset{\sim}{y}(t)-\underline{\mu}_y(t)]\}. \qquad (2.17)$$

The system described by equation (2.1) may be put in the form of equation (2.2) by letting

$$\underset{\sim}{y} = \begin{Bmatrix} x \\ \dot{x} \end{Bmatrix}, \quad \underline{\underline{A}} = \begin{bmatrix} 0 & 1 \\ -\omega_0^2 & -2\xi\omega_0 \end{bmatrix}, \text{ and } \underline{\theta}(t) = \begin{Bmatrix} 0 \\ \theta(t) \end{Bmatrix} \quad . \qquad (2.18)$$

The fundamental matrix solution is given by

$$\underline{\Psi}(t) = \begin{bmatrix} e^{-\xi\omega_0 t}(\cos\omega_d t + \frac{\xi\omega_0}{\omega_d}\sin\omega_d t) & \frac{1}{\omega_d}e^{-\xi\omega_0 t}\sin\omega_d t \\ -\frac{\omega_0^2}{\omega_d}e^{-\xi\omega_0 t}\sin\omega_d t & e^{-\xi\omega_0 t}(\cos\omega_d t - \frac{\xi\omega_0}{\omega_d}\sin\omega_d t) \end{bmatrix} \tag{2.19}$$

where $\omega_d = \omega_0\sqrt{1-\xi^2}$. Since a zero start is assumed, equation (2.6) implies that the mean vector $\underline{\mu}_y(t)$ is the zero vector. Using equation (2.9) and the fundamental matrix solution, the covariance matrix $\underline{Q}(t)$ may be calculated.

Choosing the alternative method, equation (2.16) and the definitions in equation (2.18) require the elements of the covariance matrix to satisfy

$$\begin{aligned} \dot{q}_{11} &= 2q_{12} \\ \dot{q}_{12} &= q_{22} - [\omega_0^2 q_{11} + 2\xi\omega_0 q_{12}] \\ \dot{q}_{22} &= -2[\omega_0^2 q_{12} + 2\xi\omega_0 q_{22}] + 2\pi S_0\theta^2(t) \quad . \end{aligned} \tag{2.20}$$

Equation (2.20) is a simple set of first-order differential equations where q_{ij} is the element of $\underline{Q}(t)$ in the ith row and the jth column.

With the zero mean vector and the specified covariance matrix, the joint probability density for x and $\dot{x}$ at a given time t may be derived from equation (2.17) as

$$p(x,\dot{x},t) = \frac{1}{2\pi\sqrt{\det\ \underline{Q}(t)}}\ \exp\left[-\frac{1}{2}(\phi_{11}x^2+2\phi_{12}x\dot{x}+\phi_{22}\dot{x}^2)\right] \tag{2.21}$$

where

$$\mathcal{\phi} = (\phi_{ij}) = \mathcal{Q}^{-1} \quad .$$

Another important statistic of this system is the average number of times per unit time the random process x(t) crosses a given positive threshold level from below. Let the threshold level be x = b where b is a positive constant and denote this statistic by $\nu(b,t)$. The expected frequency of up-crossing of a level b is related to the joint probability of x and $\dot{x}$ through [2]

$$\nu(b,t) = \int_0^\infty \dot{x}\, p(b,\dot{x},t)\, d\dot{x} \quad . \tag{2.22}$$

Substituting equation (2.21) into equation (2.22) and performing the integration yields

$$\nu(b,t) = \frac{\sqrt{\det \mathcal{Q}(t)}}{2\pi q_{11}(t)} \left\{ \exp\left[-\frac{1}{2}\phi_{11}(t)b^2\right] - b\phi_{12}(t)\sqrt{\frac{\pi}{2\phi_{22}(t)}}\, \exp\left[-\frac{1}{2}\frac{b^2}{q_{11}(t)}\right] \operatorname{erfc}\left[\frac{\phi_{12}(t)b}{\sqrt{2\phi_{22}(t)}}\right] \right\} \quad . \tag{2.23}$$

Letting b = 0 in equation (2.23) one arrives at the expected frequency of zero crossings with positive slope as

$$\nu(0,t) = \frac{\sqrt{\det \mathcal{Q}(t)}}{2\pi q_{11}(t)} \quad . \tag{2.24}$$

The steady-state solution for the situation where $\theta(t)$ is unity may be found by setting the left side of equation (2.20) to zero. This specifies the covariance matrix as

$$\mathbf{Q} = \begin{bmatrix} \dfrac{\pi S_0}{2\xi\omega_0^3} & 0 \\ 0 & \dfrac{\pi S_0}{2\xi\omega_0} \end{bmatrix} . \tag{2.25}$$

This reduces equations (2.23) and (2.24) to

$$\nu(b) = \frac{\omega_0}{2\pi} \exp\left[-\frac{b^2}{2q_{11}}\right] \tag{2.26}$$

$$\nu(0) = \frac{\omega_0}{2\pi} . \tag{2.27}$$

2.2 The First-Passage Problem for a Lightly Damped Simple Oscillator

The first-passage problem involves determining the probability that a random process exceeds a specified threshold level during a given time interval. Since first-passage probabilities are often associated with failure probabilities, it is appropriate to use the terms "safe" or "unsafe" to refer to the domain where the random process is respectively below or above the threshold.

For a lightly damped simple oscillator subjected to stationary Gaussian white noise described by equation (2.1) with $\theta(t)$ set to unity, the displacement response is the random process of interest. Because of the relationship between the response spectrum and the response time history, a symmetric double barrier is considered. Figure 2.1

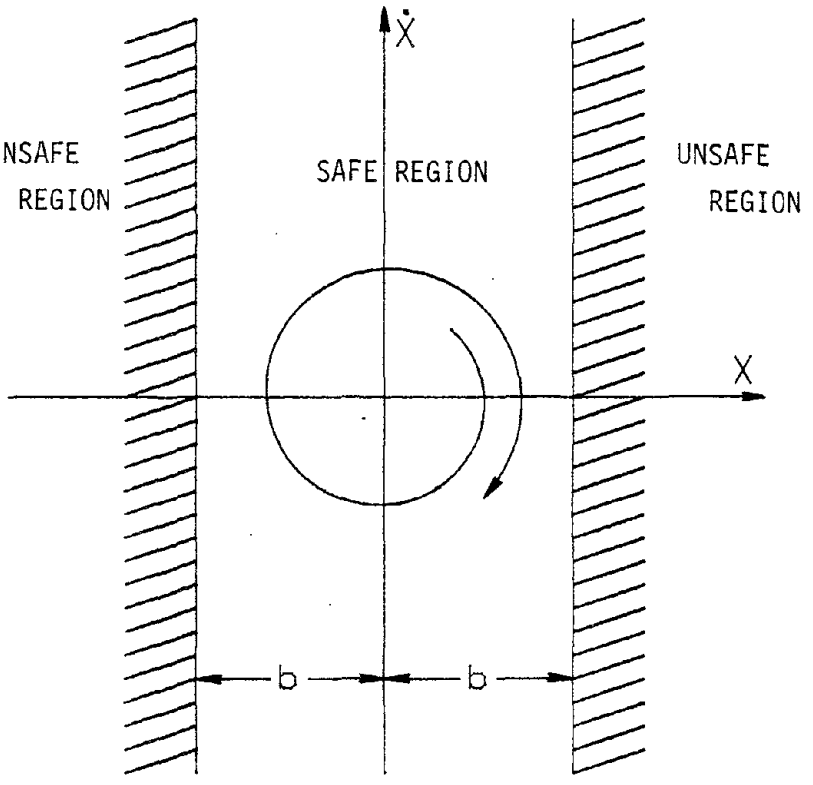

Figure 2.1 Phase Plane Representation of the First Passage Problem with Symmetric Double Barrier.

illustrates this configuration in the phase plane. The safe domain is characterized by the region between two barriers at x = b and x = -b. The first-passage problem consists of determining the probability distribution of the time when the trajectory of the response first leaves the safe region and enters the unsafe region.

Let W(T) be the probability that the magnitude of x(t) does not exceed a level b throughout the interval [0,T]. Hence,

$$W(T) \equiv \Pr\left[|x(t)|_{max} < b \;\; ; \;\; 0 \leq t \leq T \right] \tag{2.28}$$

where Pr[A] denotes the probability that the expression A is true. W(T) is called the reliability function and is related to the first-passage probability density through

$$p(T) = - \frac{dW}{dT} \tag{2.29}$$

where p(T)dT is the probability that first passage occurs on the interval [T,T+dT].

It has been observed [4] that for small values of T, the reliability function depends highly on its initial conditions. However, for large values of T, W(T) tends to a decaying exponential regardless of the initial conditions. Mark [5] proposed a linear combination of n decaying exponentials of the form

$$W(T) = \sum_{i=1}^{n} A_i e^{-\alpha_i T} \tag{2.30}$$

as an approximation for W(T), but this requires a substantial amount of

numerical computation to use. When T is large, W(T) may be approximated by the dominant term of equation (2.30). Therefore, W(T) is assumed to be of the form

$$W(T) = e^{-\alpha T} \tag{2.31}$$

where α is the smallest α_i in equation (2.30). The parameter α is known as the limiting decay rate of the first crossing density or the average crossing rate. A great deal of effort has been directed toward finding a good approximation for this decay rate.

The assumption of independent level crossings leads to the simplest approximation for the limiting decay rate. The average rate of up-crossing of a level b is $\nu(b)$, and is equal to the average rate of down-crossing of the level -b. Hence, the average crossing rate is given by

$$\alpha = 2\nu(b) \tag{2.32}$$

where $\nu(b)$ is given by equation (2.26). The number of level crossings that occur constitute a Poisson process with average crossing rate α. The assumption of independent level crossings works well for high barrier levels. However, for low barrier levels, this approximation breaks down since the response is narrow-banded and the crossings are not independent.

Other simple approximations for the limiting decay rate involve assuming independent peaks, independent envelope crossings, or independent envelope peaks. Each of these assumptions offers varied degrees of success in approximating the limiting decay rate. Those

assumptions involving the envelope statistics are better approximations since they take into account the narrow-bandedness of the system.

Reasonably good results have been obtained for the limiting decay rate by considering the response as a two-state Markov process. Because of the narrow-bandedness of the response, the peaks above the threshold occur in clumps of duration T_1. The peaks are spaced at approximately $\frac{1}{2\nu(0)}$; therefore, the expected value of the duration of a clump is given by

$$E[T_1] = \frac{E[N_c]}{2\nu(0)} \tag{2.33}$$

where N_c is the number of peaks in a clump. Between each clump there is a period T_0 where the peaks remain below the threshold that is taken to be an independent exponentially distributed random variable with parameter α. Therefore,

$$E[T_0] = \frac{1}{\alpha} \quad . \tag{2.34}$$

Since there are N_c level crossings during the period T_0+T_1, the expected value of that period may be taken as

$$E[T_0+T_1] = \frac{E[N_c]}{2\nu(b)} \quad . \tag{2.35}$$

Vanmarcke [6] combines equations (2.33), (2.34), and (2.35) and arrives at

$$\alpha = \frac{2\nu(b)}{E[N_c]}\left[1 - \frac{\nu(b)}{\nu(0)}\right]^{-1} \quad . \tag{2.36}$$

He then estimates the expected number of peaks in the clump as

$$E[N_c] = \left[1 - \exp\left(-\sqrt{\frac{\pi}{2}}\gamma\frac{b}{\sigma}\right)\right]^{-1} \tag{2.37}$$

where σ is the standard deviation of the response. The parameter γ is a measure of the bandwidth of the response and is defined by the spectral moments of the response as

$$\gamma = \left[1 - \frac{\lambda_1^2}{\lambda_0\lambda_2}\right]^{1/2} \tag{2.38}$$

where

$$\lambda_i = \int_0^\infty \omega^i \, G(\omega) \, d\omega$$

and $G(\omega)$ is the one-sided spectral density of the response. It has been shown [7] that γ varies between 0 and 1 and is small for narrow-banded processes and relatively large for broad-banded processes. Substituting equation (2.37) into equation (2.36) yields

$$\alpha = \frac{2\nu(b)\left[1 - \exp\left(\sqrt{\frac{\pi}{2}}\gamma\frac{b}{\sigma}\right)\right]}{1 - \frac{\nu(b)}{\nu(0)}} \quad . \tag{2.39}$$

An alternate approach is chosen by Mason and Iwan [8]. Using equations (2.33), (2.34), and (2.35), the average crossing rate is written

as

$$\alpha = \frac{1}{E[T_1]} \frac{\mathcal{V}(b)}{\mathcal{V}(0)}\left[1 - \frac{\mathcal{V}(b)}{\mathcal{V}(0)}\right]^{-1} \quad . \tag{2.40}$$

Assuming a probability density for T_1 as

$$p_{T_1}(t) = \frac{1}{C}\, t \exp(-\beta t) \tag{2.41}$$

where C is a normalizing constant and β is a parameter of the density, the expected value of T_1 is given by

$$E[T_1] = \frac{2}{\beta} \quad . \tag{2.42}$$

The limiting value as $n \to \infty$ of the conditional probability that a clump which already contains n crossings will continue for at least one more crossing is found from the probability density of T_1 to be

$$P^* = \exp\left(-\frac{\beta}{2\mathcal{V}(0)}\right) \tag{2.43}$$

where P^* denotes that limiting value. By considering the response of the system for one-half cycle of oscillation after a peak greater than the threshold b, an integral equation for the stationary probability density for successive peaks greater than the threshold is obtained for which $\frac{1}{P^*}$ is the eigenvalue. The eigenvalue is approximated and the limiting decay rate is given by

$$\alpha = -\mathcal{V}(b)\left[1 - \frac{\mathcal{V}(b)}{\mathcal{V}(0)}\right]^{-1} \ln(P^*) \tag{2.44}$$

where

$$P^* = \frac{1}{\operatorname{erfc}\left(\frac{b}{\sqrt{2}\sigma}\right)} \left\{ \frac{1}{2}\left[1 - \sqrt{\frac{2}{\pi(1-c^2)}}\,\frac{b}{\sigma}\right][\operatorname{erf}(y_1) - \operatorname{erf}(y_2)] \right.$$

$$\left. + \frac{c}{\pi\sqrt{1-c^2}}[\exp(-y_2^2) - \exp(-y_1^2)] + \operatorname{erfc}(y_1) \right\}$$

for which

$$c = \exp\left(-\frac{\pi\xi}{\sqrt{1-\xi^2}}\right)$$

$$y_1 = \frac{1}{c}\left(\frac{b}{\sqrt{2}\sigma} + \frac{1}{2}\sqrt{\pi(1-c^2)}\right)$$

$$y_2 = \max\left[\frac{b}{\sqrt{2}\sigma}\ ,\ \frac{1}{c}\left(\frac{b}{\sqrt{2}\sigma} - \frac{1}{2}\sqrt{\pi(1-c^2)}\right)\right] \quad .$$

It has been observed that the Mason and Iwan approach is somewhat less conservative than Vanmarcke's approach and corresponds well with numerical simulations.

In the case of nonstationary excitations, the modulating function $\theta(t)$ is allowed to vary in time. The approximations of the limiting decay rate found for stationary excitation along with the instantaneous response statistics are used to compute an instantaneous limiting decay rate, $\alpha(t)$. Equation (2.31) is then replaced by

$$W(t_d) = \exp\left(-\int_0^{t_d} \alpha(t)\, dt\right) \qquad (2.45)$$

where t_d is the duration of the excitation. The two-state Markov process may be extended in this fashion.

Using Vanmarcke's approximation [9], the spectral density is allowed to vary in time. The moments may then be calculated based on this evolving spectral density and used to calculate an instantaneous $\gamma(t)$. The limiting decay rate is then given by

$$\alpha(t) = \frac{2\nu(b,t)\left[1 - \exp\left(-\sqrt{\frac{\pi}{2}}\gamma(t)\frac{b}{\sigma(t)}\right)\right]}{1 - \frac{\nu(b,t)}{\nu(0,t)}} \quad . \tag{2.46}$$

For modulated white noise, $\gamma(t)$ is a constant and the nonstationary behavior is accounted for by the time dependence of $\sigma(t)$, $\nu(b,t)$, and $\nu(0,t)$.

Mason and Iwan [8] propose the use of an alternate probability density for T_1 when using their method for nonstationary excitation. That density is given by

$$p_{T_1}(t) = \frac{1}{C}\, t^{\frac{\sigma^4(t)}{\sigma_s^4(t)}} \exp(-\beta t) \tag{2.47}$$

where $\sigma^2(t)$ is the instantaneous variance of the response and $\sigma_s^2(t)$ is the stationary response variance associated with the instantaneous value of the excitation. The $\frac{\sigma^4(t)}{\sigma_s^4(t)}$ term reflects the nonstationarity by accounting for the greater independence of barrier level crossings when the response is broad-banded. Note that for stationary response this term is equal to unity, thus reducing the density to that for the stationary case. Using a derivation analogous to that for stationary excitation yields

$$\alpha(t) = \frac{-2\nu(b,t)\ \ln[P^*(t)]}{\left[1 + \frac{\sigma^4(t)}{\sigma_s^4(t)}\right]\left[1 - \frac{\nu(b,t)}{\nu(0,t)}\right]} \tag{2.48}$$

where $\nu(0,t)$, $\nu(b,t)$, and $P^*(t)$ are implicitly time-varying, based on the instantaneous covariance values.

2.3 Extension of the First-Passage Problem to a Nonlinear Simple Oscillator

The foregoing analysis may be extended to a nonlinear simple oscillator by using the method of statistical linearization to compute approximate response statistics from which estimates may be made of the first-passage probability. Independently introduced by Booton [11] and Caughey [12] at about the same time, the method of statistical linearization is an extension of the equivalent linearization technique of Kryloff and Bogoliuboff [13]. Since the simple oscillator is a special case of an n-degree of freedom system, the n-degree of freedom system will be discussed.

Caughey used modal decomposition to uncouple the linear part of a nonlinear system of equations, and applied the linearization technique to each of the resulting single-degree-of-freedom equations. Foster [14] generalized the method by developing an approximate closed form solution for the equivalent linear damping and stiffness matrices, but this required inversion of a 2n by 2n matrix for an n-degree of freedom system. Using a simple physical interpretation for the effective linear

parameters, Iwan and Yang [15] determined the terms of the equivalent linear damping and stiffness matrices as simple scalar equations.

Using 2n-space notation a nonlinear n-degree of freedom system may be written as

$$\dot{\underset{\sim}{y}} = \underset{\sim}{h}(\underset{\sim}{y}) + \underset{\sim}{f}(t) \tag{2.49}$$

where $\underset{\sim}{h}(\underset{\sim}{y})$ is a nonlinear vector function of $\underset{\sim}{y}$ and $\underset{\sim}{f}(t)$ is a random excitation vector. Consider an auxiliary system of linear differential equations of the form

$$\dot{\underset{\sim}{y}} = \underline{\underline{A}}[S(t)]\underset{\sim}{y} + \underset{\sim}{f}(t) \tag{2.50}$$

where $\underline{\underline{A}}[S(t)]$ is an arbitrary matrix dependent on the time-varying response statistic S(t) chosen such that the solution to equation (2.50) approximates the solution to equation (2.49). The error in estimating the nonlinear system by a linear system may be defined by the difference between the equations involved. Hence from equations (2.49) and (2.50),

$$\underset{\sim}{\varepsilon} = \underset{\sim}{h}(\underset{\sim}{y}) - \underline{\underline{A}}[S(t)]\underset{\sim}{y} \tag{2.51}$$

where $\underset{\sim}{\varepsilon}$ is the vector of the equation differences.

The appropriate choices for the elements of $\underline{\underline{A}}[S(t)]$ will be those that minimize $\underset{\sim}{\varepsilon}$ in some sense. A criterion for minimizing $\underset{\sim}{\varepsilon}$ is to require the mean of the scalar product $\underset{\sim}{\varepsilon}^T\underset{\sim}{\varepsilon}$ to be a minimum, i.e.,

$$E[\underset{\sim}{\varepsilon}^T\underset{\sim}{\varepsilon}] = \text{minimum} \quad . \tag{2.52}$$

It is noted that minimization of the equation difference does not imply

minimization of the solution difference. However, widespread usage of the method in conjunction with experiment or numerical simulation suggest that the technique approximates the nonlinear response well. The necessary condition for equation (2.52) is

$$\frac{\partial}{\partial a_{ij}} E[\underline{\varepsilon}^T \underline{\varepsilon}] = -2E[y_j \varepsilon_i] = 0 \qquad i,j=1,2,\ldots,n \quad . \tag{2.53}$$

It has been shown [16] that for $\underline{f}(t)$ Gaussian this will be a true minimum (as opposed to a maximum). Applying the definition of $\underline{\varepsilon}$ leads to

$$E[\underset{\sim}{y}\underline{\varepsilon}^T] = E[\underset{\sim}{y}\underline{h}^T(\underset{\sim}{y})] - \underline{A}[S(t)]E[\underset{\sim}{y}\underset{\sim}{y}^T] = 0 \quad . \tag{2.54}$$

Atalik and Utku [17] showed that if $\underset{\sim}{y}$ is a jointly Gaussian random vector process with mean zero and $\underline{h}(\underset{\sim}{y})$ is sufficiently smooth so that first partials with respect to y_i for $i=1,2,\ldots,2n$ exist, the condition in equation (2.54) reduces to the elements of $\underline{A}[S(t)]$ being given by

$$a_{ij} = E\left[\frac{\partial}{\partial y_j} h_i(\underset{\sim}{y})\right] \qquad i,j=1,2,\ldots,2n \quad . \tag{2.55}$$

$\underline{A}[S(t)]$ is an implicitly time-varying matrix. If we assume $\underline{A}[S(t)]$ is actually continuous in time, a unique fundamental matrix solution exists and equation (2.9) defines the approximate covariance matrix. For Gaussian excitation the response statistic S(t) may be taken as the covariance matrix $\underline{Q}(t)$ and equation (2.16) becomes a system of nonlinear differential equations easily implemented numerically.

For a nonlinear simple oscillator, obtaining an approximation for the covariance matrix allows one to arrive at approximations for the response statistics necessary to compute a limiting decay rate and estimate the first-passage probability.

CHAPTER III

RESPONSE SPECTRUM CONSISTENT RANDOM PROCESSES

In the following applications of the first-passage problem for a simple oscillator, the Mason and Iwan two-state Markov process approach has been used to compute first-passage probabilities. Vanmarcke's two-state Markov process approach or any other method of estimating first-passage probabilities may have been chosen. The accuracy of any application of the first-passage problem will depend upon the accuracy of the first-passage probability estimate.

3.1 Probabilistic Determination of the Maximum Response of a Simple Oscillator Subjected to Modulated White Noise

The solution for the first-passage problem for a simple oscillator may be used to give the probabilistic specification of the maximum response of the oscillator subjected to modulated white-noise excitation. Recall from equation (2.1) that the equation of motion of the oscillator is given by

$$\ddot{x} + 2\xi\omega_0\dot{x} + \omega_0^2 x = \theta(t)w(t) \qquad (3.1)$$

where ξ is the fraction of critical damping, ω_0 is the undamped natural frequency, and $\theta(t)w(t)$ is a modulated white noise. Zero initial conditions will be assumed.

The probability, $W(t_d)$, that the maximum response of the oscillator is less than or equal to a level b after a time t_d is the reliability function defined in equation (2.28). Hence,

$$W(t_d) = Pr\left[|x(t)|_{max} < b \;\; ; \;\; 0 \leq t \leq t_d \right] \tag{3.2}$$

where t_d is the duration of the modulating envelope, $\theta(t)$. The reliability function is evaluated using the analytical approach of Mason and Iwan.

To check the accuracy of the analytical approach used to determine the reliability function, a Monte Carlo simulation study of equation (3.1) was performed. An ensemble of sample functions was generated to represent stationary Gaussian white noise. Each sample function was constructed from a sequence of independent normally distributed numbers with zero mean and unit variance. The numbers were used as ordinates of the function at equally spaced time intervals, Δt. The function was assumed to vary linearly over each interval. The time scale was chosen such that the initial point was uniformly distributed on the interval $[-\Delta t, 0]$. The numerically generated unit variance sample functions were multiplied by $\left[\frac{2\pi S_0}{\Delta t}\right]^{1/2}$ to give a process with a power spectral density of [18]

$$S(\omega) = S_0 \frac{6 - 8\cos(\omega\Delta t) + 2\cos(2\omega\Delta t)}{(\omega\Delta t)^4} \; . \tag{3.3}$$

$S(\omega)$ approaches a constant S_0 as $\omega\Delta t$ approaches zero. The expression for $S(\omega)$ remains within 5% of S_0 for $\omega\Delta t < 0.57$, and within 10% for

$\omega\Delta t < 0.76$. Thus, the time interval may be chosen sufficiently small to approximate a white-noise process to within a given tolerance out to any desired frequency. In this study, Δt was set equal to $\frac{T}{20}$ where T is the undamped natural period of the oscillator.

Since the applied excitation is assumed to be a straight line segment on each time interval, the solution to equation (3.1) may be solved by digital computer in a purely arithmetical way [19]. The exact analytical expression for the response of a damped single-degree-of-freedom system with arbitrary initial conditions was written for a linearly varying excitation. The total response for a time interval was then obtained by analytically matching the initial conditions of the current interval to the final conditions of the previous interval. In this way, no numerical approximations were introduced other than the white-noise approximation and the round off due to the digital representation of the response.

The simplest modulating envelope is a rectangular pulse of unit amplitude and duration, t_d (Figure 3.1a). In Figures 3.2-3.4, the probability that the maximum response will be less than a given threshold level is plotted versus duration of excitation for several threshold levels and several values of damping based on analytical first-passage estimates. The results are displayed in a dimensionless form. The durations are expressed in multiples of the natural period. The threshold levels are normalized by the stationary standard deviation of the system described by equation (3.1) with $\theta(t) = 1$. The stationary standard deviation, σ_s, may be written from equation (2.25) as

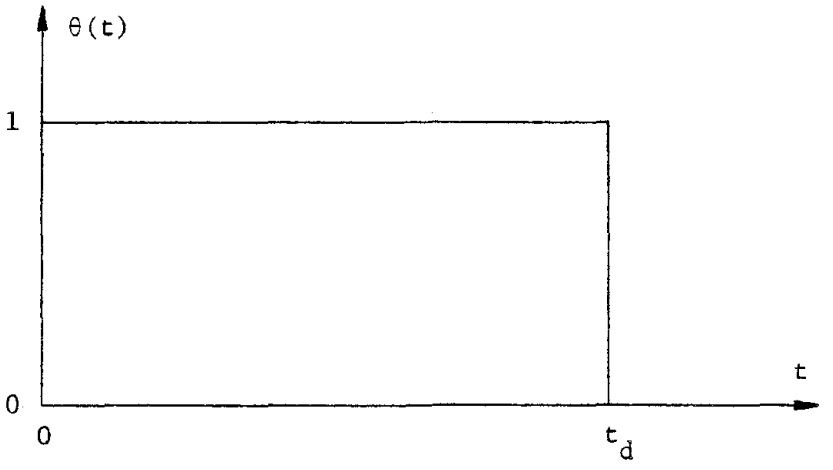

(a) Rectangular Envelope

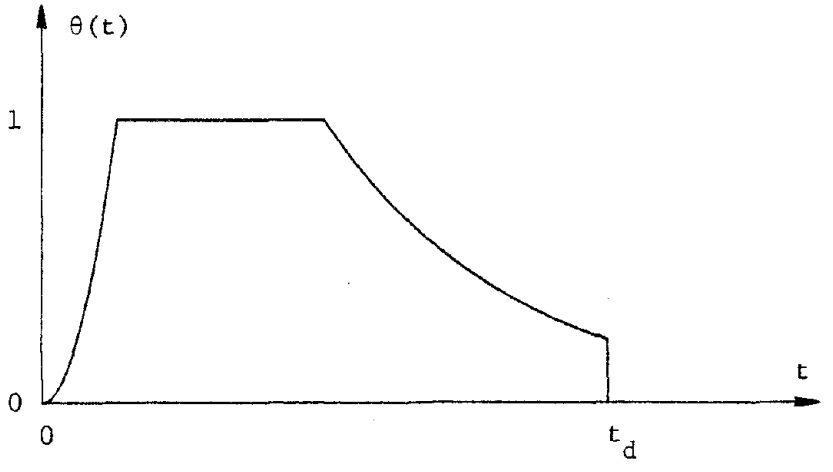

(b) Earthquake-like Envelope

Figure 3.1 Modulating Envelopes for the Stationary Gaussian Random Process

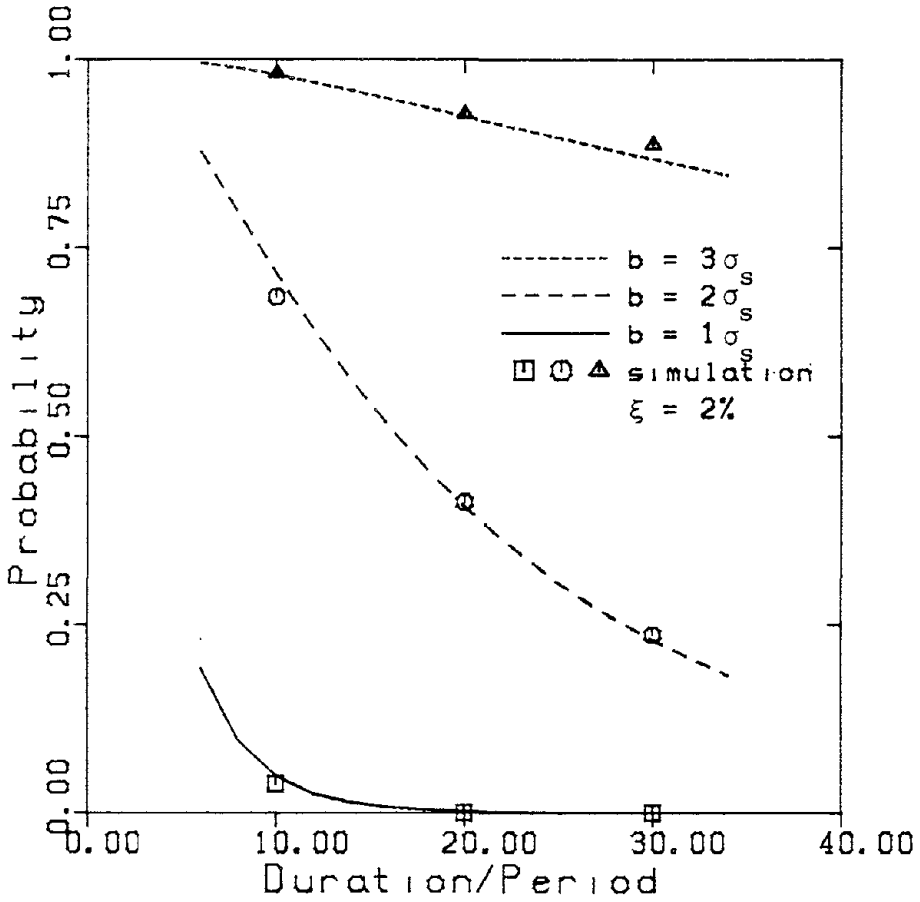

Figure 3.2 Probability of Not Exceeding the Threshold Level versus Normalized Duration for Rectangular Modulating Envelope, ξ = 2%.

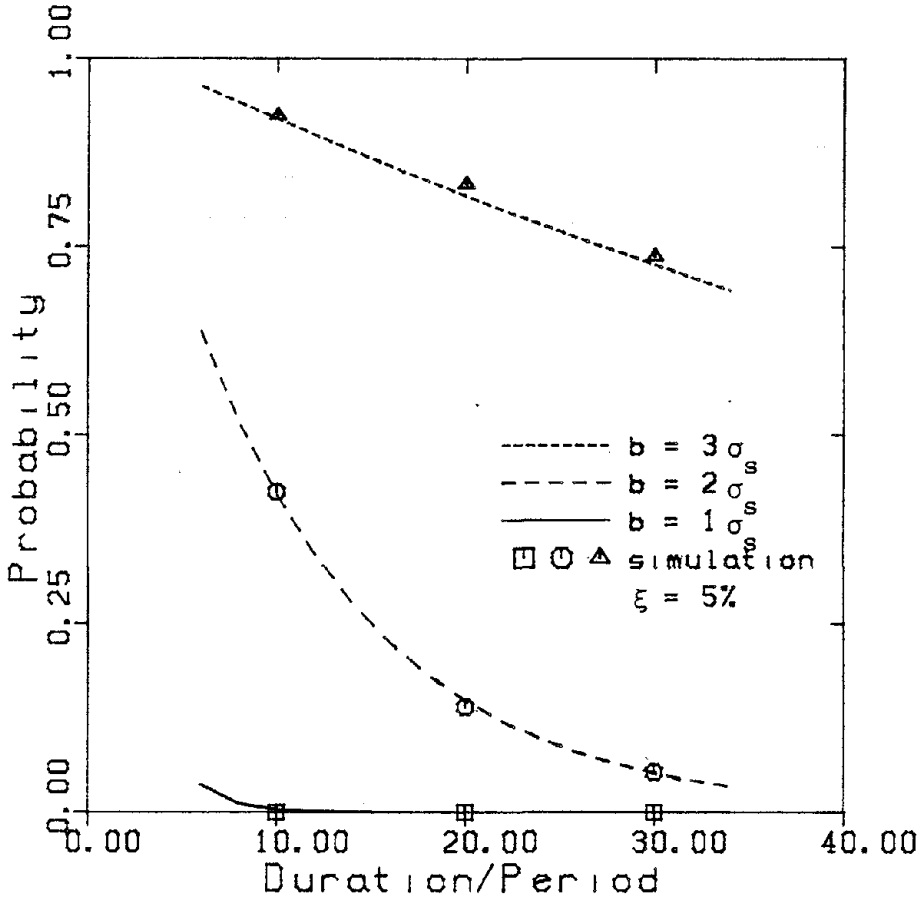

Figure 3.3 Probability of Not Exceeding the Threshold Level versus Normalized Duration for Rectangular Modulating Envelope, ξ = 5%.

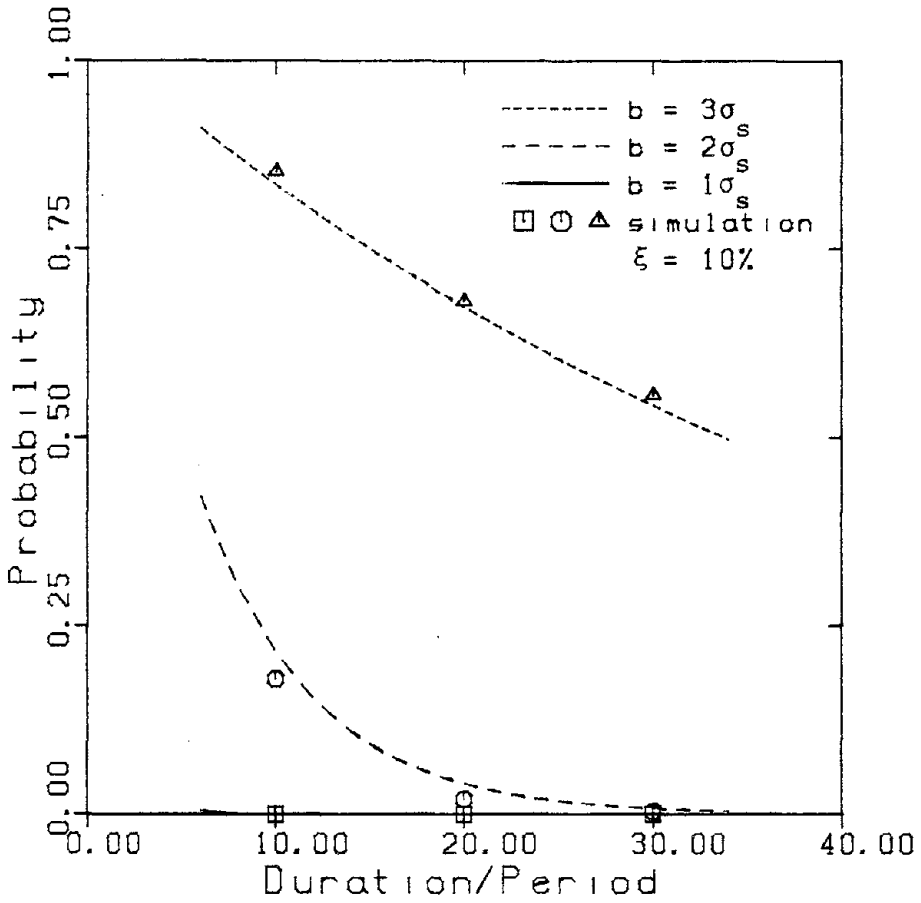

Figure 3.4 Probability of Not Exceeding the Threshold Level versus Normalized Duration for Rectangular Modulating Envelope, ξ = 10%.

$$\sigma_s = \left[\frac{\pi S_0}{2\xi\omega_0^3} \right]^{1/2} = \left[\frac{S_0 T^3}{16\xi\pi^2} \right]^{1/2} \tag{3.4}$$

where S_0 is the constant power spectral density of the Gaussian white noise, w(t). Also shown in Figures 3.2-3.4 are the results of the simulation study for the same threshold levels and damping values using an ensemble of 1000 sample functions.

It is observed that the probability that the maximum response is less than a given threshold level decreases with increasing duration. Therefore, the probability distribution of the maximum response varies with duration. This suggests that duration is an important parameter when probabilistically determining the maximum response. The analytical method agrees reasonably well with simulation.

From Figures 3.2-3.4, it may appear that the response of a system with more damping is more likely to surpass a given absolute level. However, this is not the case. The stationary standard deviation of the response is inversely proportional to the square root of the damping ratio. Therefore, the normalized threshold levels which are constant multiples of the stationary standard deviation of the response become smaller as the damping ratio increases. In Figure 3.5 the probability that the maximum response is less than a constant threshold level is plotted versus the duration of the excitation for several damping values. From this figure it is evident that the probability that the response of a system will not exceed a given threshold increases as the damping in the system increases.

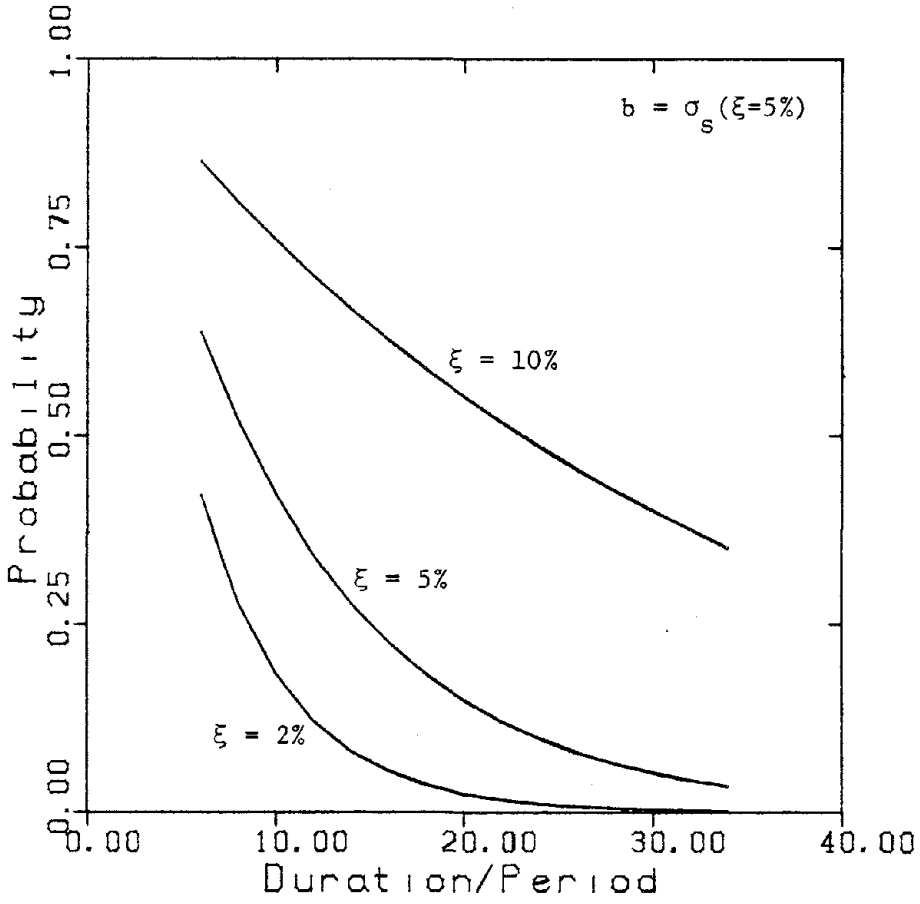

Figure 3.5 Probability of Not Exceeding the Threshold Level versus Normalized Duration for Rectangular Modulating Envelope. Threshold Level held constant, independent of damping ratio.

To represent earthquake-like excitation, it is appropriate to choose a modulating envelope that models the nonstationary character of actual accelerograms. Specific forms for such envelopes have been suggested by a number of authors (e.g., [20], [21]). Real accelerograms often consist of three phases: a phase where the excitation builds, a strong motion phase where the shaking remains fairly constant, and a phase where the motion dies out. Earthquakes of larger magnitude tend to have envelopes of longer duration.

One form of modulating envelope which has been suggested [20] is shown in Figure 3.1b. This envelope may be expressed as

$$\theta(t) = \begin{cases} 56.25\left(\frac{t}{t_d}\right)^2 & ; \quad 0 \leq t \leq \frac{2}{15}t_d \\ 1.0 & ; \quad \frac{2}{15}t_d < t \leq \frac{1}{2}t_d \\ \exp\left[-2.976\left(\frac{t}{t_d} - \frac{1}{2}\right)\right] & ; \quad \frac{1}{2}t_d < t \leq t_d \end{cases} \tag{3.5}$$

where t_d is defined as the duration of the excitation. When $t_d = 30$ seconds, the modulating envelope, $\theta(t)$, is similar to the Caltech B-type earthquake envelope given in Reference [20] which was designed to represent shaking close to the fault in a Richter Magnitude 7 or greater earthquake.

Figures 3.6-3.8 show the probability that the maximum response of the simple oscillator is below a specified level for several threshold levels and several values of damping using the envelope of equation (3.5). Results from Monte Carlo simulation are also shown. The analytical approach agrees well with the simulation results. As in the case of

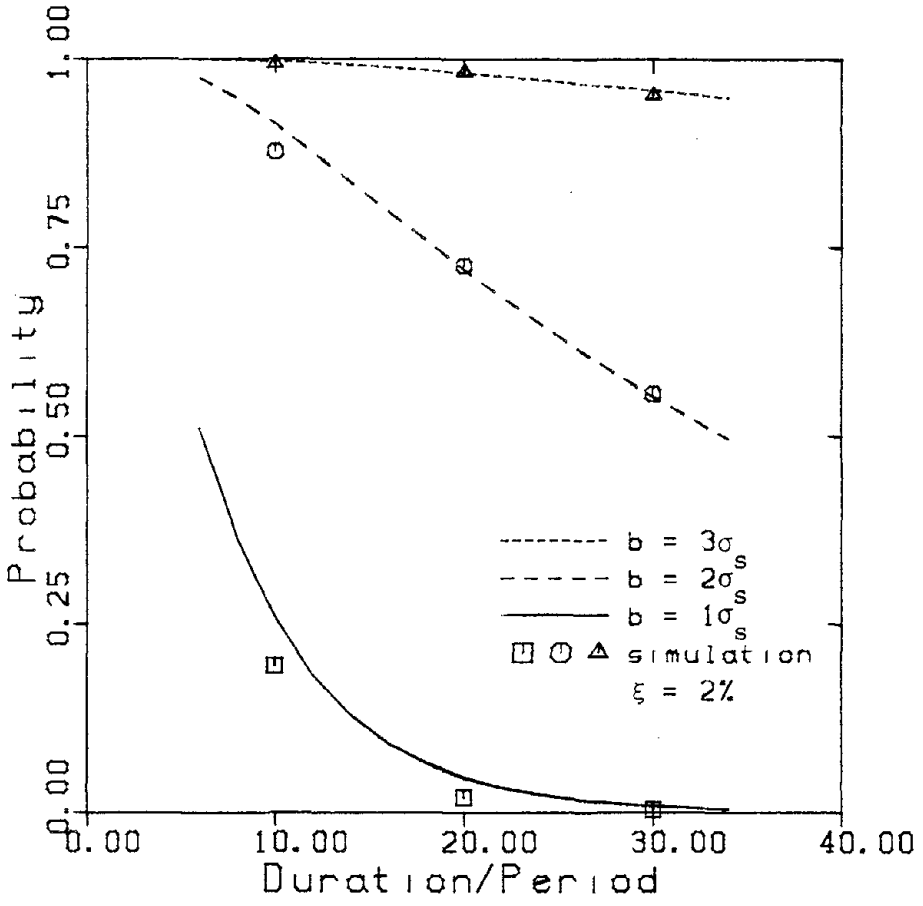

Figure 3.6 Probability of Not Exceeding the Threshold Level versus Normalized Duration for Earthquake-like Modulating Envelope, ξ = 2%.

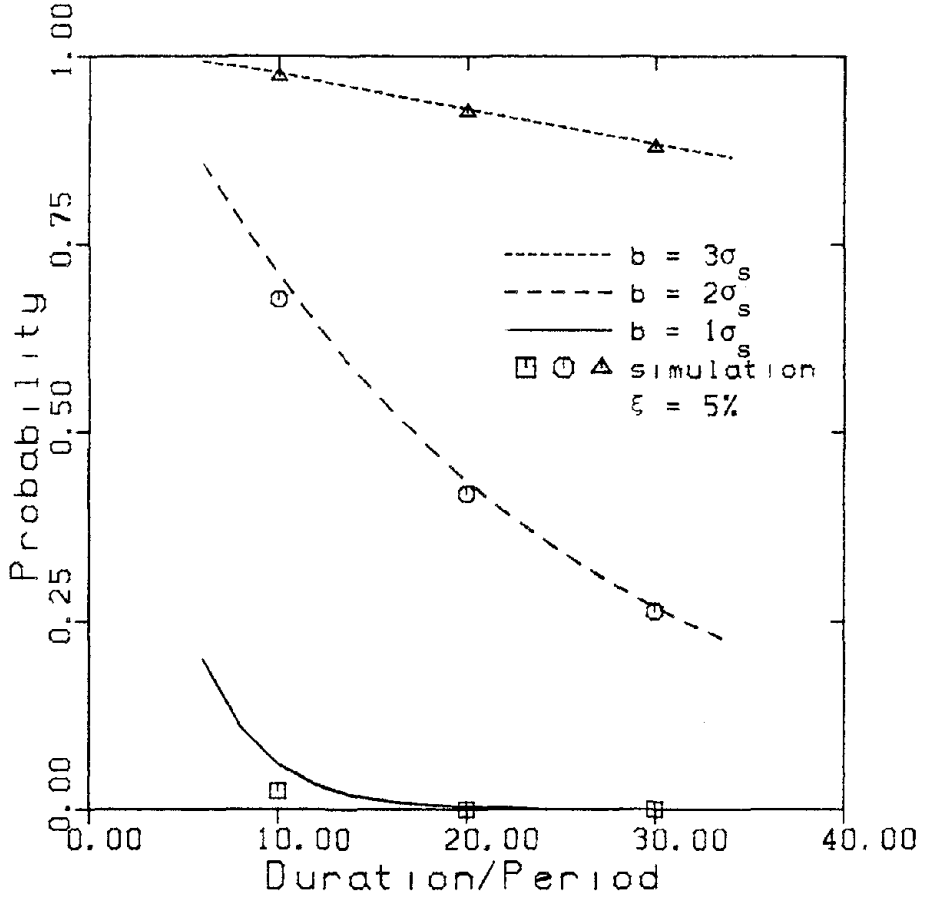

Figure 3.7 Probability of Not Exceeding the Threshold Level versus Normalized Duration for Earthquake-like Modulating Envelope, ξ = 5%.

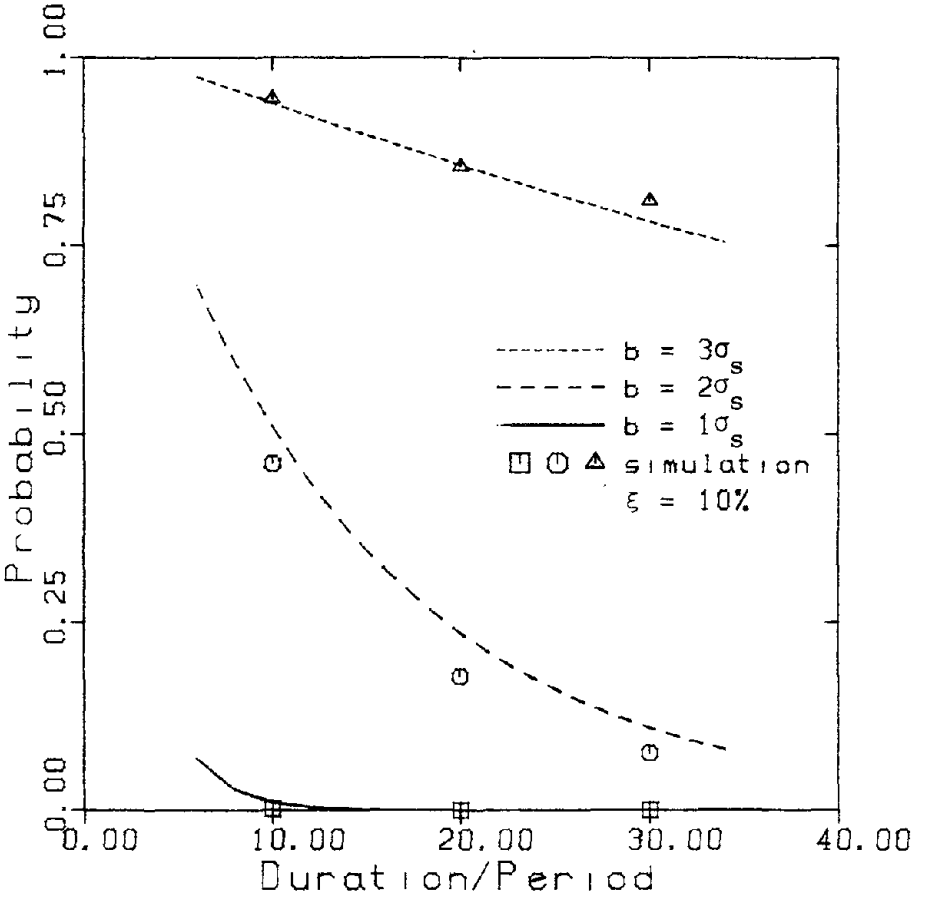

Figure 3.8 Probability of Not Exceeding the Threshold Level versus Normalized Duration for Earthquake-like Modulating Envelope, ξ = 10%.

the rectangular modulating envelope, the apparent variation in the probability distribution suggest that duration of excitation is an important parameter when probabilistically specifying the maximum response of a simple oscillator.

In Figure 3.9, the probability that the peak response does not exceed a constant threshold level is plotted versus the duration of excitation for several values of damping using the earthquake-like envelope. Like the results for the rectangular envelope, the likelihood that the threshold level will not be exceeded increases as the damping in the system increases.

3.2 Determination of Response Spectrum Consistent Random Processes

The response spectrum has been widely accepted as a way of describing some of the aspects of earthquake ground motion that are of interest to the engineer. The response spectrum is defined from the behavior of a single-degree-of-freedom system. The given ground acceleration is applied to the base of a simple oscillator and the maximum displacement is measured or calculated. The maximum displacement depends on the applied excitation, the value of damping in the system, and the natural frequency of the system. The family of curves, for various values of damping, of the maximum displacement plotted versus the natural frequency make up the response spectrum for the ground motion.

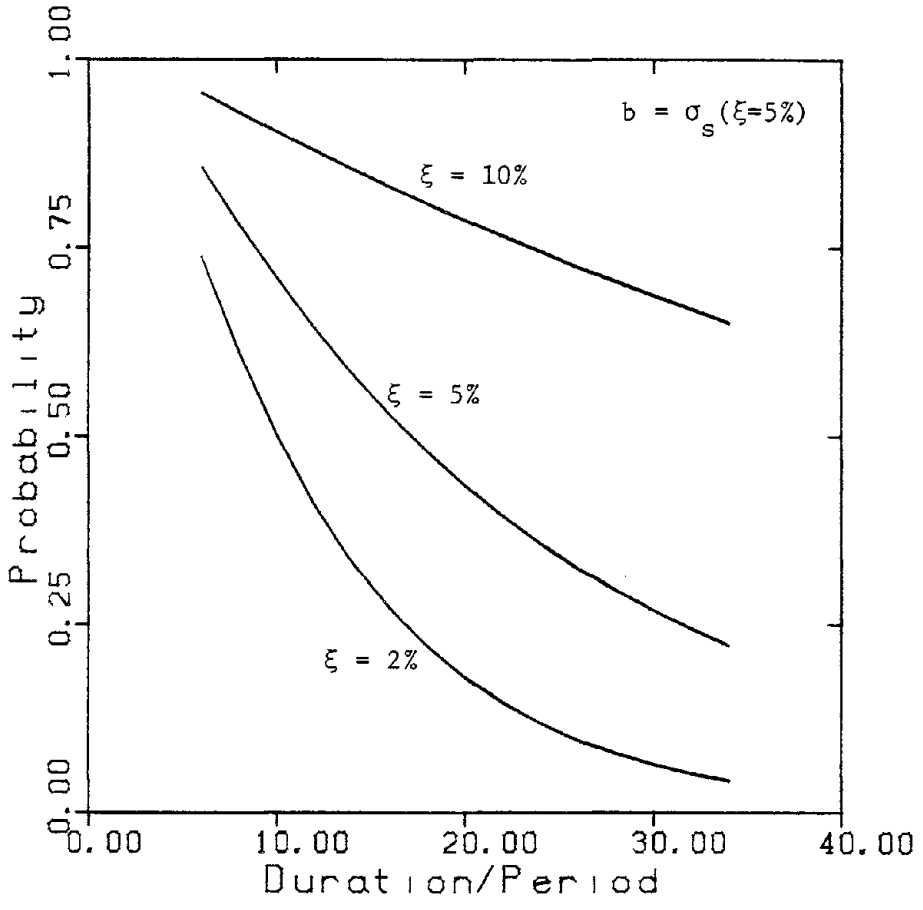

Figure 3.9 Probability of Not Exceeding the Threshold Level versus Normalized Duration for Earthquake-like Modulating Envelope. Threshold Level held constant, independent of damping ratio.

Studies of response spectra for actual accelerograms [22] have shown that important features of the response spectra can be represented by simplified smoothed curves for design purposes. These curves are derived by computing the response spectra for a number of earthquakes and then normalizing the spectra in such a way that the spectra may be compared. The mean and the standard deviation of the normalized response spectrum values are calculated over the entire frequency range and used to compute parameters of a probability distribution. Smooth curves are then chosen to describe the shape and normalized level of the response spectrum for a given confidence level. The curves make up the design response spectra. When scaled to reflect the maximum ground motion, they are used to specify seismic input for structural design.

Design response spectra of the type discussed above have been adopted by the U.S. Nuclear Regulatory Commission (NRC) for the seismic design of nuclear power plants [23]. The NRC design response spectrum is made up of straight line segments when plotted on logarithmic tripartite graph paper. The vertices or control points of the straight line segments for each value of damping are specified by the frequency at which the points occur and the ratio of the response pseudo acceleration to the maximum ground acceleration. Based on the work reported in Reference [24], these design response spectra have a confidence level of 84.1%.

Analytically, it is convenient to model earthquake excitation as a Gaussian random process defined by its power spectral density and a deterministic modulating envelope. If the seismic input is specified in

this way, it should correspond statistically to the design response spectrum. This may be achieved by performing a first-passage probability analysis for a simple oscillator in order to select power spectral density ordinates of the process from the design response spectrum.

A linear oscillator subjected to the artificial earthquake process may be described by

$$\ddot{x} + 2\xi\omega_0\dot{x} + \omega_0^2 x = \theta(t)g(t) \qquad (3.6)$$

where $\theta(t)$ is the deterministic modulating envelope and $g(t)$ is a stationary Gaussian random process with spectral density $S(\omega)$. Response spectra are usually constructed only for lightly damped systems where the response is narrow-banded about the natural frequency. Hence, for ξ sufficiently small, a good approximation for the response of the system described by equation (3.6) may be obtained by replacing $g(t)$ with a stationary Gaussian white-noise process, $w(t)$, with constant spectral density $S_0 = S(\omega_0)$ for each ω_0.

Since the analytical approach of Mason and Iwan for calculating first-passage probabilities of a simple oscillator was directed toward modulated Gaussian white-noise processes, it may be used here to compute the power spectral density ordinates. The design response spectrum may be described by

$$\Pr\left[\, |x(t)|_{max} < SD(\omega_0,\xi) \;\; ; \;\; 0 \leq t \leq t_d \,\right] = P_s \qquad (3.7)$$

where $SD(\omega_0,\xi)$ is the target spectrum value for natural frequency ω_0 and

fraction of critical damping, ξ, and P_s is the confidence level of the spectrum. The confidence level, P_s, corresponds to the reliability function defined in equation (2.28), with the threshold level b replaced by the value of the target response spectrum, $SD(\omega_0,\xi)$. Hence, equation (2.45) may be written as

$$W(t_d) = \exp\left[-\int_0^{t_d} \alpha(SD,S_0,\omega_0,\xi,t)\, dt\right] \tag{3.8}$$

where t_d is the duration of the excitation, α is the limiting decay rate, and S_0 is the constant power spectral density of the excitation. An increase in S_0 causes a decrease in $W(t_d)$ and vice versa. Using a simple iterative process, S_0 may be varied in equation (3.8) until $W(t_d)$ is within some predetermined tolerance, for example, 0.5%, of P_s. The value of S_0 is then assigned to $S(\omega_0)$.

In Figure 3.10, the NRC design response spectra outlined in Regulatory Guide 1.60 are shown for a maximum ground acceleration of 50% g. Power spectra were derived for several durations and are shown in Figures 3.11 and 3.12 for damping values of 2% and 10% of critical damping. A confidence level of 84.1% was assumed.

The overall shape of the power spectrum is somewhat similar as duration is varied. For a fixed response spectrum and fixed confidence level, the level of the power spectrum increases as the duration decreases. and vice versa. A shift in the distribution of the power toward the lower frequencies as duration decreases is evident from the

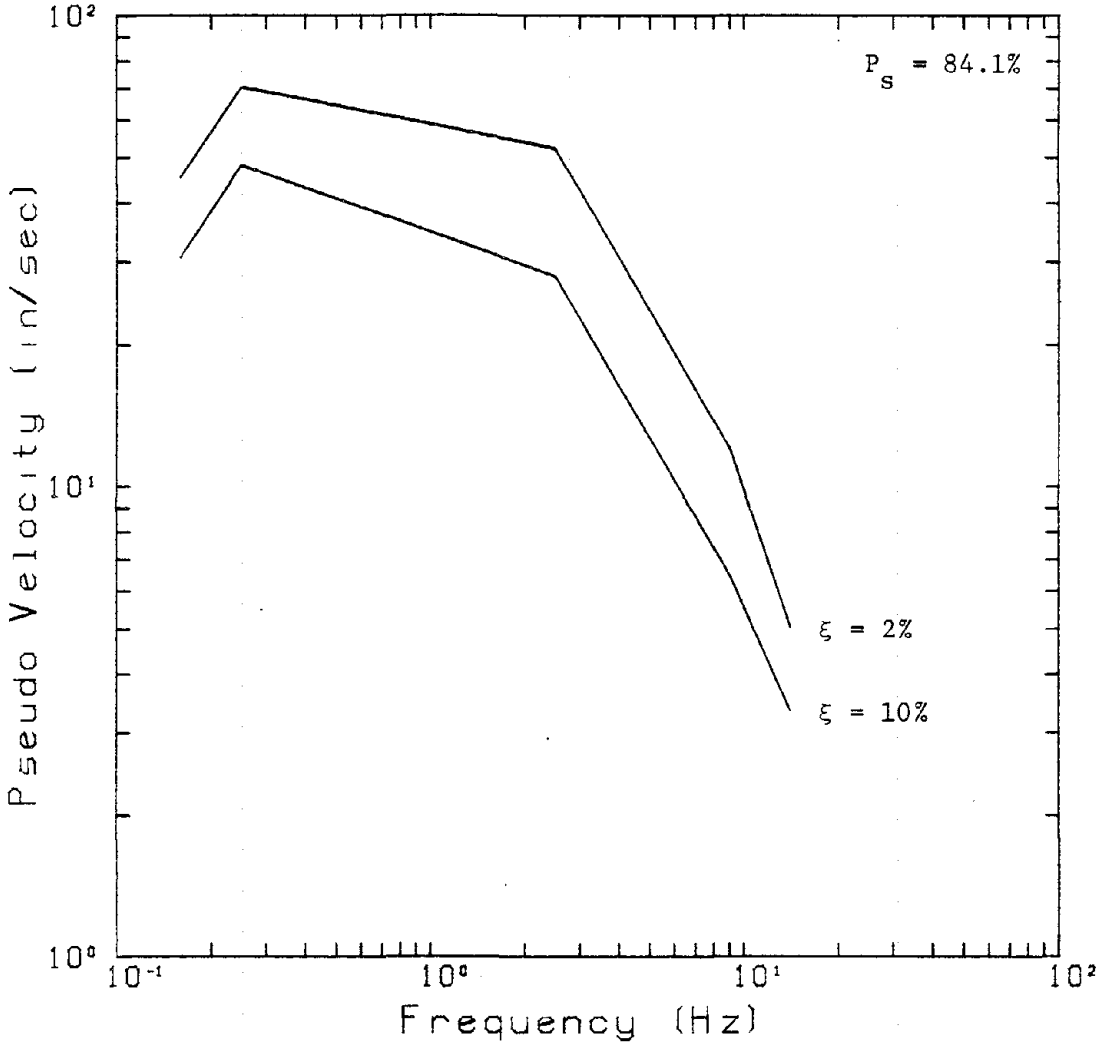

Figure 3.10 NRC Horizontal Design Response Spectra, scaled to 0.5g Maximum Ground Motion.

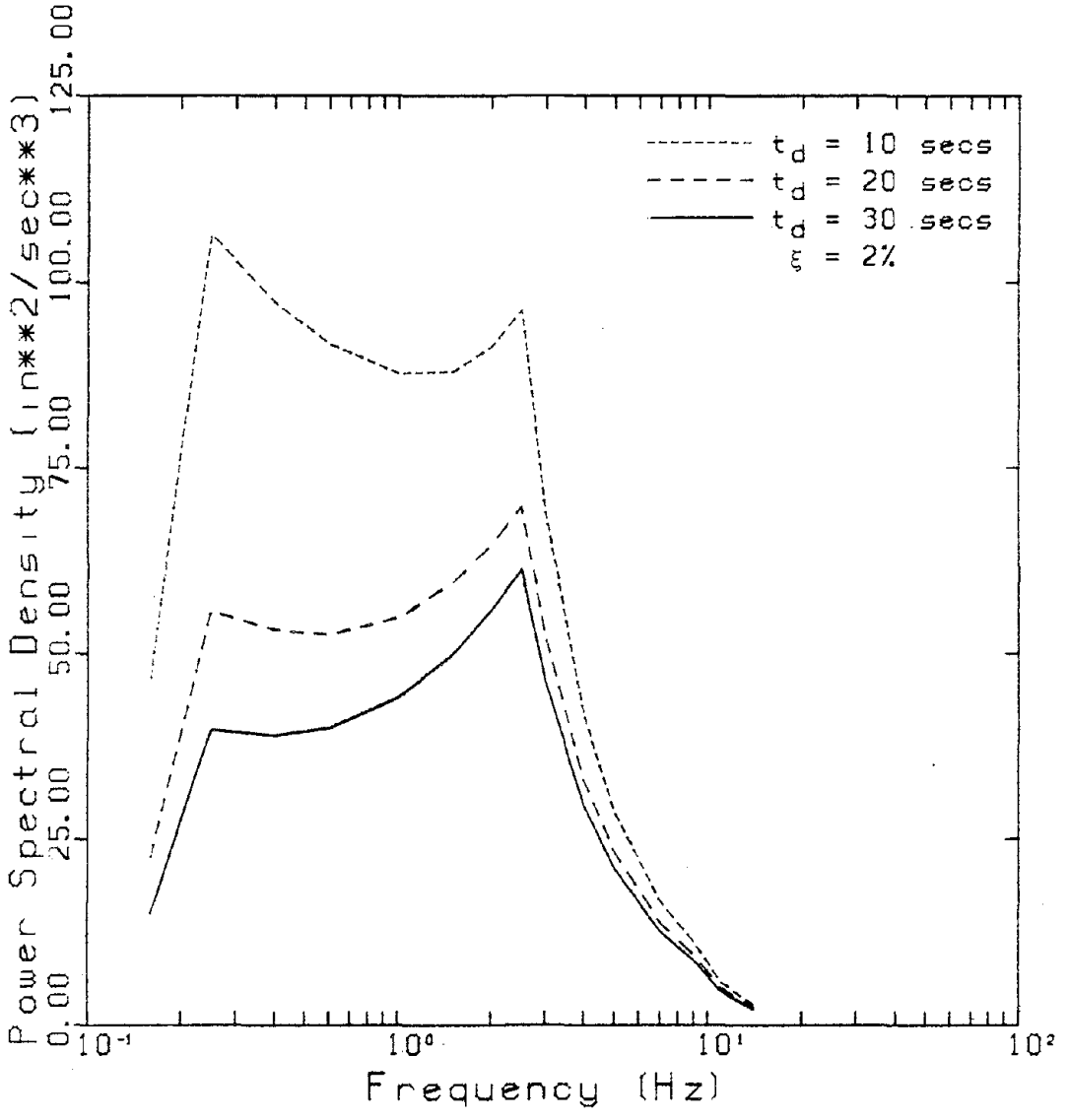

Figure 3.11 Comparison of Derived Power Spectra for three Durations, ξ = 2%.

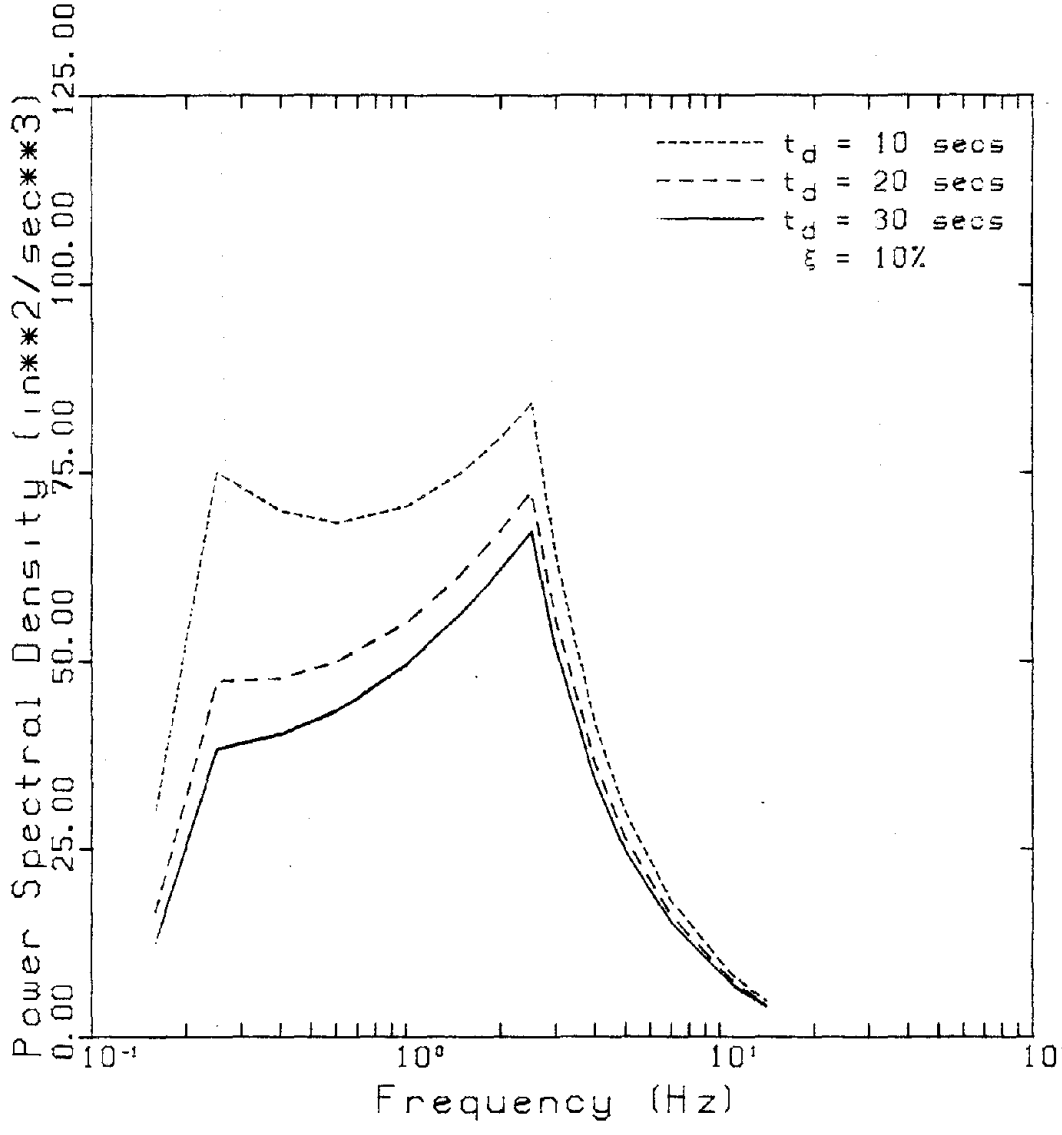

Figure 3.12 Comparison of Derived Power Spectra for three Durations, ξ = 10%.

peak that occurs at 0.25 Hertz.

Since the response spectra for different values of damping are derived from a single earthquake time history, one might expect that a single process may be derived from the design response spectrum for different values of damping. This is not the case for the power spectra derived above. The design response spectra for different values of damping produce slightly different power spectra. This may be expected since the design response spectra are constructed from a number of real accelerograms each with its own duration, frequency content, etc. In Figures 3.13-3.15, the power spectra are replotted for each duration to compare their agreement for different values of damping. Better agreement is found at the high frequencies for shorter durations and at the low frequencies for longer durations. Figures 3.13-3.15 suggest a duration slightly longer than 20 seconds will give good agreement between the power spectrum derived using 2% damping and the power spectrum derived using 10% damping for the design spectra considered here. This may be expected since the earthquakes upon which the design response spectrum is based have durations primarily between 20 and 30 seconds.

3.3 Maximum Response of a Nonlinear Simple Oscillator Subjected to Earthquake-like Excitation

If a structure behaves nonlinearly, the customary linear response spectrum may not characterize the response of the structure. In Section 3.2, a Gaussian random process was constructed to agree statistically

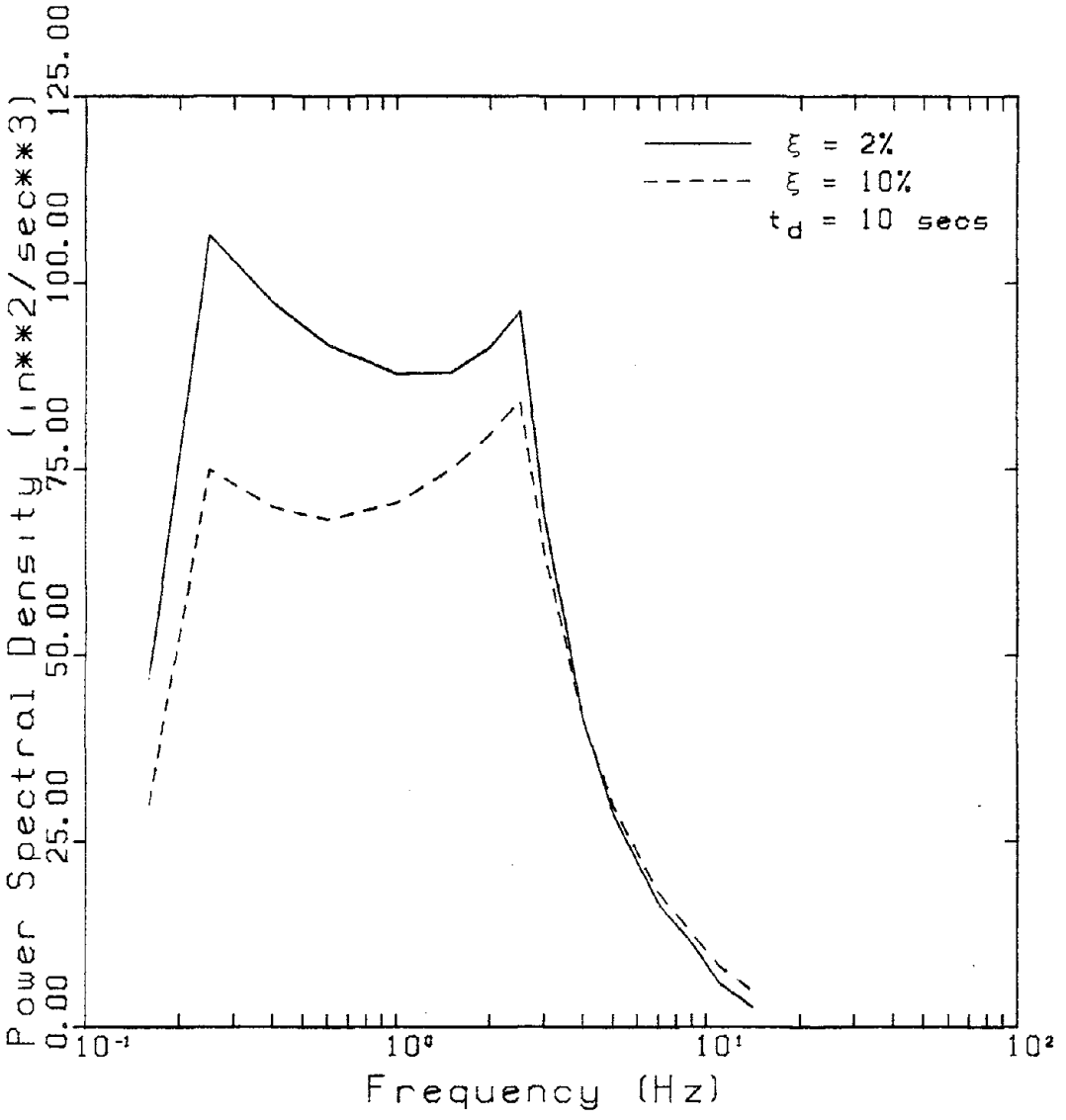

Figure 3.13 Comparison of Derived Power Spectra for two values of Damping, t_d = 10 seconds.

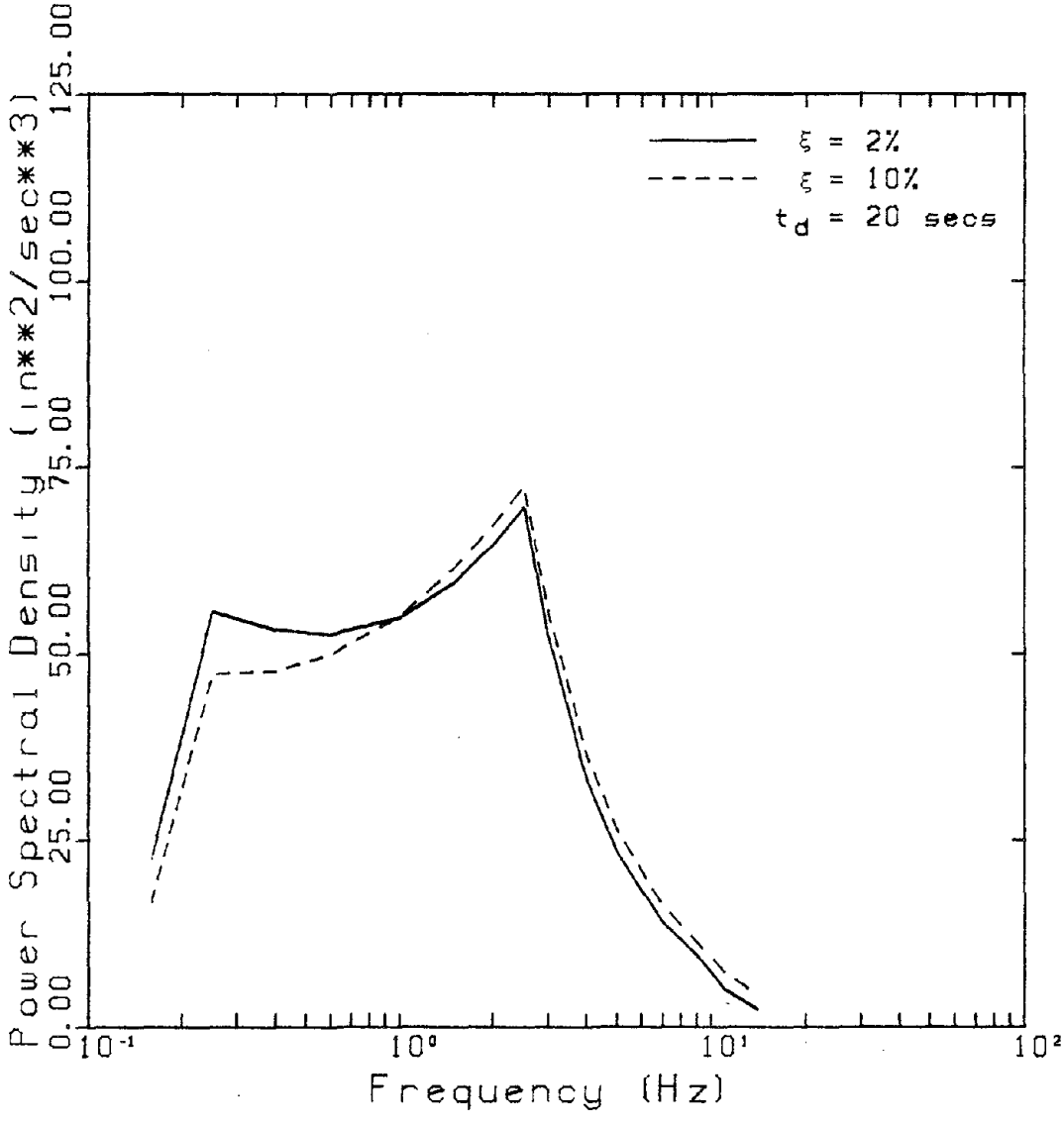

Figure 3.14 Comparison of Derived Power Spectra for two values of Damping, t_d = 20 seconds.

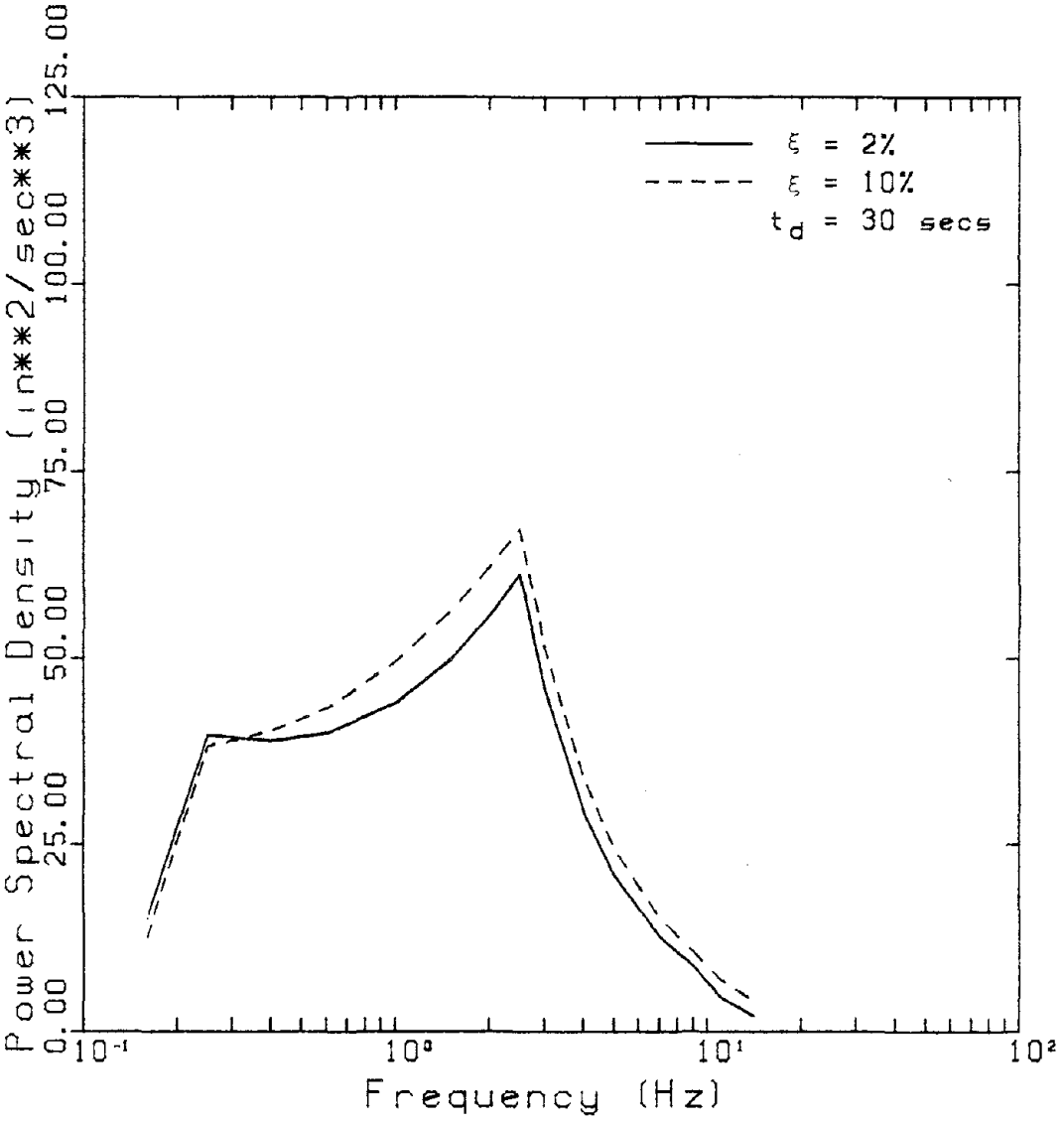

Figure 3.15 Comparison of Derived Power Spectra for two values of Damping, t_d = 20 seconds.

with a specified design response spectrum. Using that process, statistical linearization, and the analytical approach to the first-passage problem for a simple oscillator, the maximum response of a nonlinear simple oscillator may be obtained statistically for excitation defined by a design response spectrum.

As an example of a nonlinear simple oscillator, consider a softening elastic restoring force that has a force-deflection relationship described by

$$f = \frac{2}{\pi} f_u \tan^{-1}\left(\frac{\pi k_0 x}{2 f_u}\right) \tag{3.9}$$

where f_u is the ultimate force and k_0 is the small displacement stiffness. The nature of this restoring force characteristic is shown in Figure 3.16.

Let the quantity $\frac{f_u}{k_0}$ be denoted by x_y and the ratio of the maximum response, x_{max}, to x_y be denoted by μ. Then, the value of μ is a measure of the nonlinearity of the system and may vary from 0 to ∞ with $\mu = 0$ corresponding to a linear system. x_y represents the displacement corresponding to a restoring force f_u for a linear system with stiffness k_0, and is similar to the elastic limit displacement of a yielding system (see Figure 3.16). Equation (3.9) may be expressed in terms of μ and x_{max} as

$$f = \frac{2}{\pi} \frac{k_0 x_{max}}{\mu} \tan^{-1}\left(\frac{\pi}{2\mu} \frac{x}{x_{max}}\right) \quad . \tag{3.10}$$

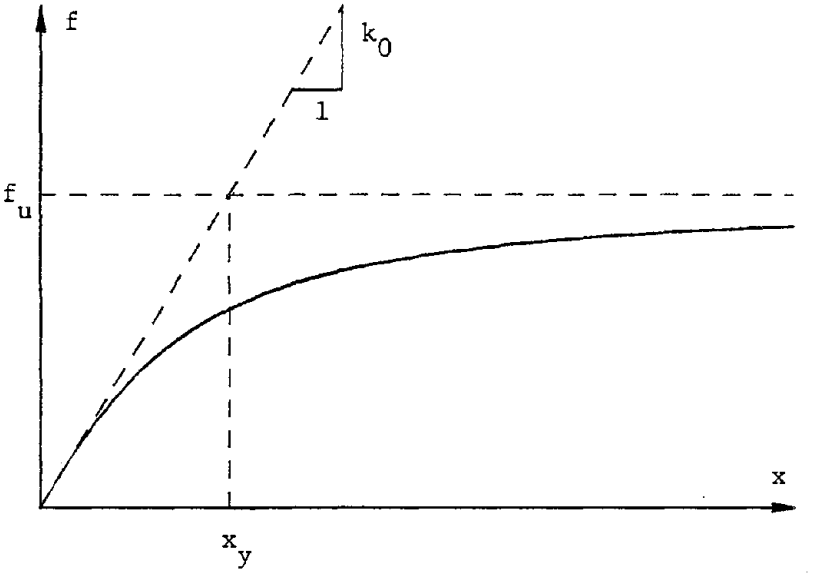

Figure 3.16 Softening Elastic Restoring Force Characteristic

The nonlinear force-deflection relationship described above is similar to the backbone curve of a yielding system in that the stiffness softens as the displacement increases. However, when a yielding system is loaded beyond some point, the unloading path differs from the loading path. This inelastic behavior is not modeled by the nonlinear relationship described by equation (3.10). However, the nonlinear relationship is a better approximation to a yielding system than a linear relationship and is useful to assess the effects of softening on system response. The response of the yielding system is often described by the ductility ratio; i.e., the ratio of the maximum response to the maximum elastic response. The nonlinearity parameter μ, defined herein, is similar to the ductility ratio of the yielding system.

The equation of motion for a simple oscillator with the particular softening behavior discussed above may be written as

$$\ddot{x} + 2\xi\omega_0\dot{x} + \frac{2}{\pi}\omega_0^2\frac{x_{max}}{\mu}\tan^{-1}\left(\frac{\pi}{2\mu}\frac{x}{x_{max}}\right) = \theta(t)w(t) \qquad (3.11)$$

where ξ and ω_0 are the fraction of critical damping and undamped natural frequency, respectively, associated with small displacements. Writing the equation of motion in 2n-space notation yields

$$\dot{\underset{\sim}{y}} = \underset{\sim}{h}(\underset{\sim}{y}) + \underset{\sim}{g}(t)w(t) \qquad (3.12)$$

where

$$\underset{\sim}{y} = \begin{Bmatrix} x \\ \dot{x} \end{Bmatrix}$$

$$\underset{\sim}{h}(\underset{\sim}{y}) = \begin{Bmatrix} y_2 \\ -2\xi\omega_0 y_2 - \frac{2}{\pi}\omega_0^2 \frac{x_{max}}{\mu} \tan^{-1}\left(\frac{\pi}{2}\mu \frac{y_1}{x_{max}}\right) \end{Bmatrix}$$

and

$$\underset{\sim}{\mathcal{Q}}(t) = \begin{Bmatrix} 0 \\ \theta(t) \end{Bmatrix} \quad .$$

Assuming that $\underset{\sim}{y}$ is a jointly Gaussian random vector process with mean zero, equation (2.55) leads to the equivalent linear system given by

$$\dot{\underset{\sim}{y}} = \mathbb{A}[\mathcal{Q}(t)]\underset{\sim}{y} + \underset{\sim}{\mathcal{Q}}(t)w(t) \tag{3.13}$$

where

$$\mathbb{A}[\mathcal{Q}(t)] = \begin{bmatrix} 0 & 1 \\ -\omega_0^2\sqrt{\pi}\gamma \exp(\gamma^2)\,\mathrm{erfc}(\gamma) & -2\xi\omega_0 \end{bmatrix}$$

and

$$\gamma = \frac{\sqrt{2}}{\pi\mu} \frac{x_{max}}{\sqrt{q_{11}(t)}} \quad .$$

Hence, the instantaneous equivalent linear natural frequency ω_e and damping ratio ξ_e are

$$\omega_e = \omega_0 \left[\sqrt{\pi}\gamma \exp(\gamma^2) \operatorname{erfc}(\gamma)\right]^{1/2}$$
$$\xi_e = \xi \left[\sqrt{\pi}\gamma \exp(\gamma^2) \operatorname{erfc}(\gamma)\right]^{-1/2} \quad . \tag{3.14}$$

Substituting $\underline{A}[Q(t)]$ into equation (2.16), it is seen that the covariance matrix approximation for the nonlinear system satisfies

$$\begin{aligned}
\dot{q}_{11} &= 2q_{12} \\
\dot{q}_{12} &= q_{22} - [\omega_0^2 q_{11}\sqrt{\pi}\gamma \exp(\gamma^2) \operatorname{erfc}(\gamma) + 2\xi\omega_0 q_{12}] \\
\dot{q}_{22} &= -2[\omega_0^2 q_{12}\sqrt{\pi}\gamma \exp(\gamma^2) \operatorname{erfc}(\gamma) + 2\xi\omega_0 q_{22}] + 2\pi S_0 \theta^2(t)
\end{aligned} \tag{3.15}$$

with zero initial conditions.

Using the equivalent linear system and the analytical approach to the first-passage problem outlined in Section 2.2, a statistical design response spectrum may be calculated for the nonlinear system excited by a Gaussian random process defined by its power spectral density $S(\omega)$ and modulating envelope $\theta(t)$. An equation analogous to equation (3.8) may be written for the equivalent linear system as

$$W(t_d) = \exp\left[-\int_0^{t_d} \alpha(x_{max}, S(\omega_e), \omega_e, \xi_e, t)\, dt\right] \tag{3.16}$$

where t_d is the duration of the excitation, α is the limiting decay rate, x_{max} is the unknown maximum response, and $S(\omega_e)$ is the spectral density of the excitation evaluated at the equivalent natural frequency. An increase in x_{max} causes an increase in $W(t_d)$. It is a simple matter

to vary x_{max} in equation (3.16) until $W(t_d)$ is within some tolerance of the confidence level, P_s.

Statistical design response spectra have been calculated for softening nonlinear elastic systems with μ equal to 0, 2, 5, and 10 for the Gaussian random process generated with the linear system from the NRC design response spectrum of Section 3.2 with a duration of 30 seconds. In Figures 3.17 and 3.18, the statistical maximimum response of the softening nonlinear elastic system is plotted against the small displacement frequency. The curve for $\mu = 0$ is the NRC design response spectrum from which the excitation process was derived since $\mu = 0$ corresponds to a linear system.

The instantaneous equivalent linear natural frequency, ω_e, of the softening nonlinear elastic system described in equation (3.14) is always less than or equal to the small displacement natural frequency, ω_0. A frequency shift occurs in the statistical maximum response spectrum for the softening nonlinear elastic oscillator due to the downward shift in the natural frequency. This frequency shift is most noticeable in Figures 3.17 and 3.18 at the control points in the response spectrum.

The maximum response of the nonlinear simple oscillator is affected by two factors. First, an overall increase in the maximum response occurs due to the assumed level of softening, μ, in the system. Secondly, the frequency shift can cause a variation in the maximum response by increasing or decreasing the value of the power spectral density of the excitation corresponding the instantaneous effective

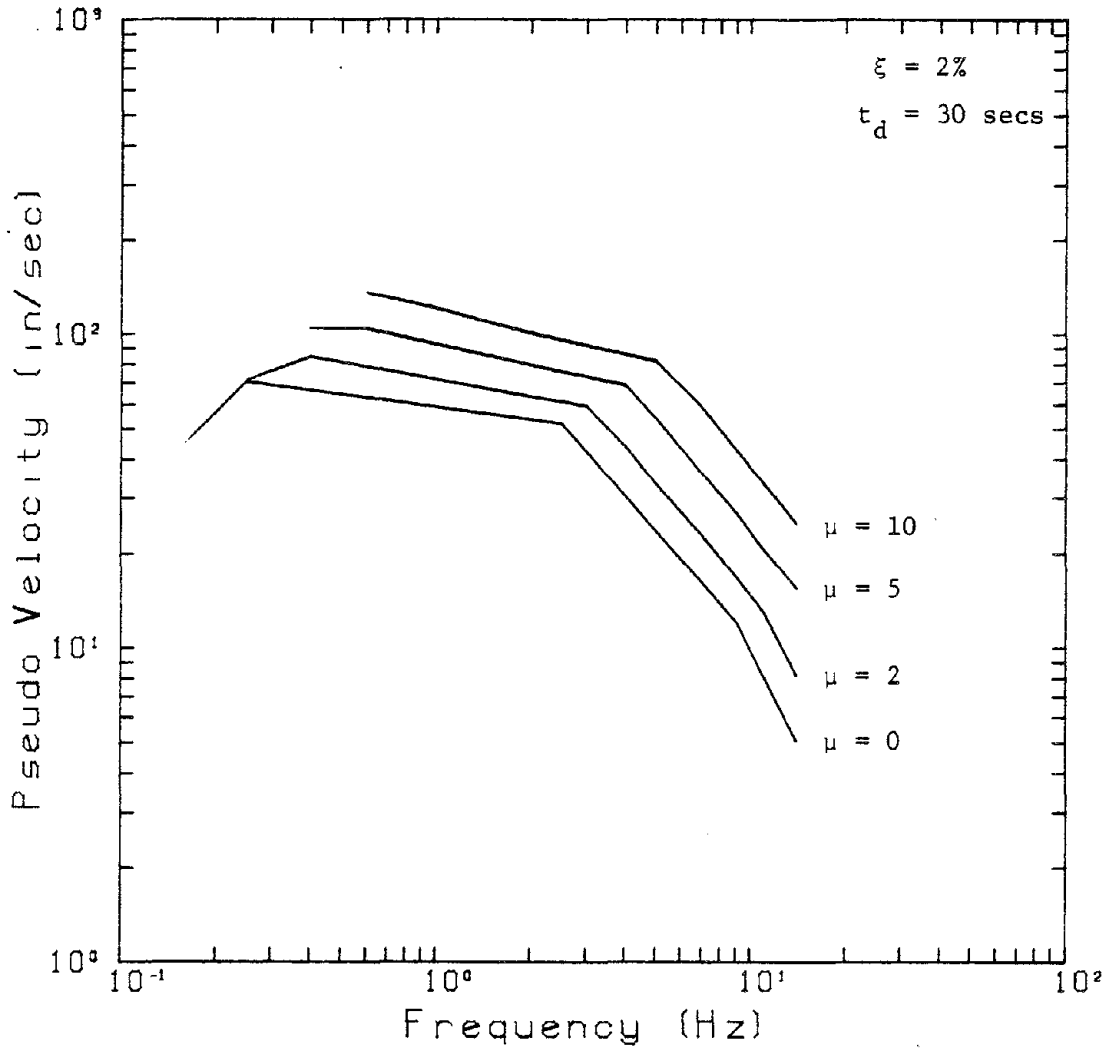

Figure 3.17 Statistical Maximum Response of the Softening Elastic System, ξ = 2%, t_d = 30 seconds.

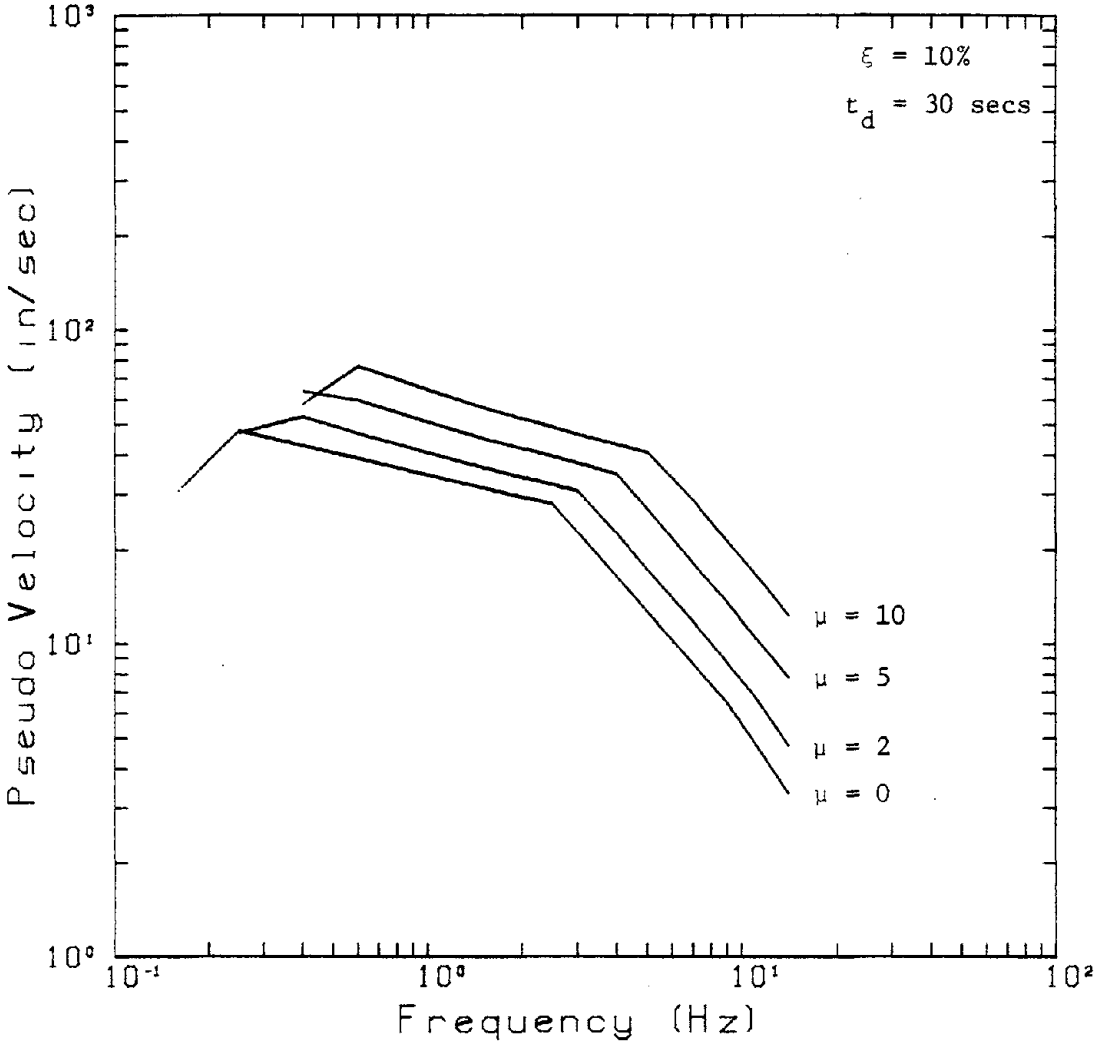

Figure 3.18 Statistical Maximum Response of the Softening Elastic System, ξ = 10%, t_d = 30 seconds.

natural frequency. This variation depends on the shape of the power spectral density of the excitation process. In Figures 3.17 and 3.18, variation in the maximum response are most evident for frequencies less than 0.25 Hertz where the frequency shift causes a sharp decrease in the power spectral density and for frequencies greater than 9 Hertz where the frequency shift causes a sharp increase in the power spectral density. An increase in the structural damping decreases the response for the nonlinear system in the same manner as for the linear system.

The net effect of the softening nonlinear elastic restoring force is that the statistical maximum response spectrum resembles a linear response spectrum which has been translated along an axis of constant spectral displacement (a line with a slope of one on the log-log pseudo-velocity diagram). These results are similar to the inelastic response spectra for the hysteretic system described by Iwan and Gates [25] and Iwan [26].

CHAPTER IV

AN ANALYTICAL METHOD FOR COMPUTATION OF CUMULATIVE DAMAGE

4.1 Failure of Structural Members under Cyclic Loading

When a structure is subjected to strong earthquake ground motion, large displacements can occur. The displacements may be associated with large strains in the structural members. The repeated application of large strains may cause failure in the structural members.

Experimental tests to determine the behavior of structural members under large cyclic strains have been performed by Bertero and Popov [27] and Yamada [28,29]. The structural members were subjected to cyclic bending deflections of constant amplitude until fracture occurred. The relationship between the number of cycles to failure, N, and the deflection amplitude may be expressed as

$$N\mu^{s} = C_{\mu} \tag{4.1}$$

where μ is the ductility factor of the deformation, defined as the ratio of the maximum deflection to the maximum elastic deflection, and s and C_{μ} are the empirical constants determined from the experimental tests.

Yamada [29] defines the failure constants for steel structural members from tests on wide-flange steel columns. The columns were axially loaded in compression to $\frac{1}{3}$ of the ultimate strength of the centrally loaded column and cycled in bending to failure. Failure was described as local flange buckling followed by local buckling of the web leading to torsion about the member axis and loss of axial resistance.

The damage law may be expressed approximately as

$$Nb^{1.85} = 81.93 \tag{4.2}$$

where b is the amplitude of the cycling in terms of the displacement of the actual test specimen. The yield displacement may be found using simple beam theory. Normalizing the displacement in equation (4.2) by the yield displacement, the damage law may be written in terms of the ductility factor as

$$N\mu^{1.85} = 167.1 \quad . \tag{4.3}$$

The exponent in equations (4.2) and (4.3) is approximately equal to 2, a widely accepted value for steel.

It has been observed that failure of reinforced concrete members may also be described by equation (4.1). Data from bending tests performed on rectangular reinforced concrete columns axially loaded in compression to $\frac{1}{3}$ of the yield load are given in Reference [28]. Using the method of least squares to fit the data, the relationship between the constant deflection amplitude of the test specimen and the number of cycles to failure may be written as

$$Nb^{5.88} = 239.1 \quad . \tag{4.4}$$

Here, failure was described as when the concrete fell down due to the buckling of the longitudinal reinforcement. By considering a reinforced concrete column as a beam of two materials, namely concrete and steel, the yield displacement in bending may be computed. Hence, in terms of

the ductility ratio, the damage law becomes

$$N\mu^{5.88} = 416.3 \quad . \tag{4.5}$$

The damage laws discussed for steel and reinforced concrete are shown in Figure 4.1. Note that the steel requires more cycles to fail than the reinforced concrete for the same level of ductility. The value of the ductility for N = 1 provides an upper limit to the allowable ductility factor of the structure. The damage laws are similar to some of those that are used to describe low-cycle fatigue failure of materials.

4.2 Damage Accumulation for Narrow-banded Random Response

Cyclic failure in a material may be of two basic types. High-cycle failure occurs from repeated application of stresses below the yield stress of the material. The number of cycles to failure for high-cycle failure is of the order 10^4. Low-cycle failure occurs when the material is strained repeatedly beyond the yield point. Less than 10^3 cycles are typically required for a low-cycle failure. When low-cycle failure is of concern, it is more meaningful to relate the number of cycles to failure to the strain amplitude rather than the stress amplitude.

One approach, used to predict fatigue failure, is to model the relationship between the number of cycles to failure and the cyclic strain amplitude for a material under constant strain amplitude loading.

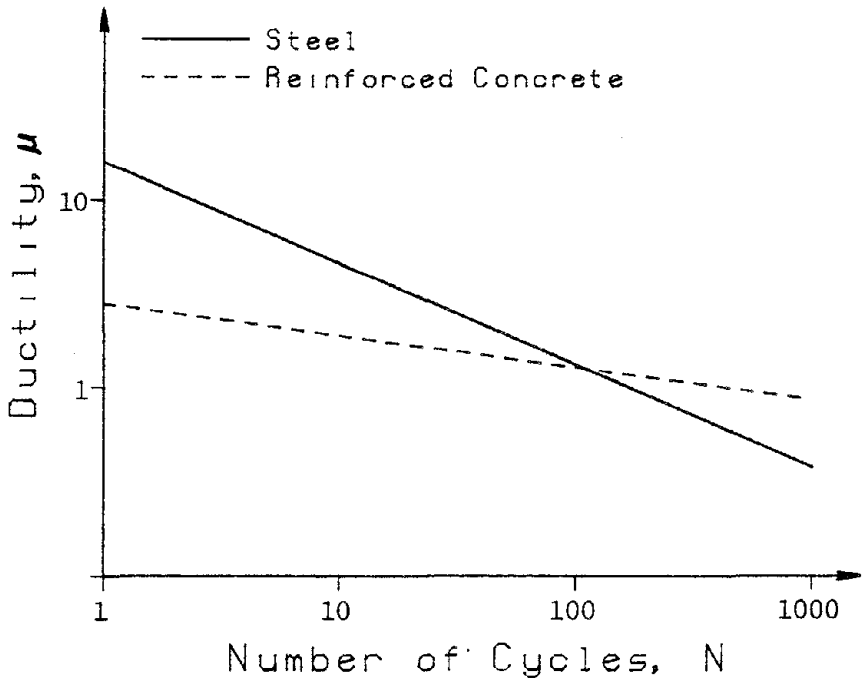

Figure 4.1 Damage Laws for Steel and Reinforced Concrete.

A widely accepted formula, proposed by Travernelli, Coffin and Manson [30] is given by

$$\varepsilon = \frac{\sigma_f}{E} (2N)^{\beta} + \varepsilon_f (2N)^{\gamma} \tag{4.6}$$

where N is the number of cycles to failure at the constant principal strain amplitude ε, E is the modulus of elasticity, and the other variables are empirical constants determined from experimental test data. The first term on the right-hand side of equation (4.6) dominates when ε is in the elastic range and reflects the classical S-N curve known as the Basquin equation for high-cycle fatigue. The second term is equal to the amount of strain beyond the elastic strain range at which the material must be cycled to fail in N cycles. The second term dominates for high-strain low-cycle fatigue.

During an earthquake, a lightly damped structure may be subjected to severe random forces causing cyclic nonstationary response. High strains may develop within members of the structure such that the second term of equation (4.6) governs the failure. In such a situation, the first term of the right-hand side of equation (4.6) may be neglected, and the failure relationship may be written as

$$N\varepsilon^{s} = C_{\varepsilon} \tag{4.7}$$

where N is the number of cycles to failure at the constant strain amplitude ε, and s and C_{ε} are positive empirical constants. By normalizing the strain by the elastic limit strain, equation (4.7) is

equivalent to equation (4.1).

A cumulative damage hypothesis may be used to relate the failure of a system with varying response amplitude to a system with constant response amplitude. The simple rule proposed independently by Miner [31] and Palmgren [32] assumes damage accumulation to be a linear function of the number of cycles of constant strain amplitude cyclic loading. Hence, the incremental damage due to the application of n_i cycles at a strain level ε_i is

$$D_i = \frac{n_i}{N(\varepsilon_i)} \quad . \tag{4.8}$$

Furthermore, it is assumed that the order of application of different strain levels has no effect on the total damage.* Thus, the total damage for varying strain levels is

$$D = \sum_I D_i = \sum_I \frac{n_i}{N(\varepsilon_i)} \quad . \tag{4.9}$$

Failure occurs when D reaches unity. Substituting equation (4.7) in equation (4.9) yields

$$D = C_\varepsilon^{-1} \sum_I n_i \varepsilon_i^s \quad . \tag{4.10}$$

The concept of total damage may easily be extended to random strain response by assuming the number of peaks occurring in the strain response is synonymous with the number of cycles in the strain response.

* There is evidence that this assumption may not be valid for all systems. However, it is employed herein because it allows the Palmgren-Miner theory to be used in the case of random strains.

This assumption is reasonable for lightly damped structures where the response is a narrow-banded nonstationary cyclic process.

Let m be the total number of peaks per unit time and $p(\varepsilon;t|m)$ be the conditional probability density for the strain amplitude of the response given the number of peaks per unit time. The quantity $m\ p(\varepsilon;t|m)$ represents the number of peaks at a level ε given m peaks per unit time. Hence, the expected number of peaks per unit time at a level ε is given by

$$E[n_\varepsilon(t)] = \int_0^\infty m\ p(\varepsilon;t|m)\ p(m;t)\ dm \tag{4.11}$$

where $p(m;t)$ is the time-varying probability density for the total number of peaks per unit time.

Based on equation (4.8) with equation (4.7) substituted and using equation (4.11) the expected rate of damage accumulation due to peaks of strain amplitude ε may be written as

$$E\left[\frac{dD}{dt}(\varepsilon;t)\right] = \frac{\varepsilon^s}{C_\varepsilon} \int_0^\infty m\ p(\varepsilon;t|m)\ p(m;t)\ dm \quad . \tag{4.12}$$

Integrating equation (4.12) over all levels of strain yields the expected rate of damage as

$$E\left[\frac{dD}{dt}(t)\right] = \frac{1}{C_\varepsilon} \int_0^\infty \varepsilon^s \int_0^\infty m\ p(\varepsilon;t|m)\ p(m;t)\ dm\ d\varepsilon \quad . \tag{4.13}$$

If the total number of peaks per unit time is assumed independent of the amplitude of the peaks, the following relationship holds

$$\int_0^\infty m\, p(\varepsilon;t|m)\, p(m;t)\, dm = p(\varepsilon;t) \int_0^\infty m\, p(m;t)\, dm = p(\varepsilon;t)\, E[M(t)] \qquad (4.14)$$

where E[M(t)] is the expected number of peaks per unit time. Substituting equation (4.14) into equation (4.13) yields

$$E\left[\frac{dD}{dt}(t)\right] = \frac{E[M(t)]}{C_\varepsilon} \int_0^\infty \varepsilon^s\, p(\varepsilon;t)\, d\varepsilon \qquad (4.15)$$

which may be integrated over the duration of the excitation to give the expected value of the total damage as

$$E[D(t_d)] = E\left[\int_0^{t_d} \frac{dD}{dt}(t)dt\right] = \frac{1}{C_\varepsilon} \int_0^{t_d} E[M(t)] \int_0^\infty \varepsilon^s\, p(\varepsilon;t)\, d\varepsilon\, dt \quad . \qquad (4.16)$$

4.3 Damage Accumulation Applied to a Simple Oscillator

A lightly damped system is classified as a narrow-banded system. The predominant frequency components of the response are contained in a narrow band near the natural frequency of the system. The response appears to be a slightly distorted sine function with slowly varying amplitude and phase. The cumulative damage of a lightly damped system

may be computed by considering the cyclic nonstationary response of a simple oscillator.

Assuming strain is proportional to displacement, equation (4.15) may be written in terms of displacement as

$$E\left[\frac{dD}{dt}(t)\right] = \frac{E[M(t)]}{C_b} \int_0^\infty b^s \, p(b;t) \, db \quad . \tag{4.17}$$

The damage model may be expressed in terms of displacement as

$$Nb^s = C_b \quad . \tag{4.18}$$

For the cyclic nonstationary response of a lightly damped simple oscillator, the number of peaks per unit time is approximately equal to the number of zero crossings per unit time. Hence,

$$E[M(t)] = \nu(0,t) \tag{4.19}$$

where $\nu(0,t)$ is the frequency of zero crossings defined by equation (2.24).

The probability density $p(b;t)$ may be found by considering the frequency of up-crossing of a simple oscillator at a level b at time t, $\nu(b,t)$, which is given by equation (2.23). Since the number of up-crossings at a level b is approximately equal to the number of peaks above the level b, $\nu(b,t)$ is approximately equal to the expected number of peaks above b per unit time. The expected total number of peaks per unit time is equal to the frequency of zero crossings, $\nu(0,t)$. Hence, the expected fraction of peaks above the level b is approximately

$\nu(b,t)/\nu(0,t)$, and the probability distribution of the peak magnitudes at time t may be approximated as

$$\Pr[\text{peaks} < b;\ t] = 1 - \frac{\nu(b,t)}{\nu(0,t)} \quad . \tag{4.20}$$

The average probability density of the peak magnitudes at time t may be obtained by differentiating equation (4.20) with respect to b. This yields

$$p(b;t) = -\frac{1}{\nu(0,t)} \frac{\partial \nu(b,t)}{\partial b} \quad . \tag{4.21}$$

Substituting equation (4.19) and (4.21) into equation (4.17), the expected rate of damage accumulation is given by

$$E\left[\frac{dD}{dt}(t)\right] = -\frac{1}{C_b} \int_0^\infty b^s \frac{\partial \nu(b,t)}{\partial b}\, db \quad . \tag{4.22}$$

$\frac{\partial \nu(b,t)}{\partial b}$ is found by differentiating equation (2.23) to be

$$\frac{\partial \nu(b,t)}{\partial b} = \frac{\sqrt{\det Q(t)}}{2\pi q_{11}(t)} \left\{ \frac{-b}{q_{11}(t)} \exp\left(-\frac{\phi_{11}(t) b^2}{2}\right) \right.$$

$$\left. - \frac{\phi_{12}(t)\sqrt{\pi}}{\sqrt{2\phi_{22}(t)}} \left[1 - \frac{b^2}{q_{11}(t)}\right] \exp\left(-\frac{b^2}{2q_{11}(t)}\right) \operatorname{erfc}\left(\frac{\phi_{12}(t) b}{\sqrt{2\phi_{22}(t)}}\right) \right\} \quad . \tag{4.23}$$

4.4 A Closed Form Expression for a Special Case of the Damage Law

The expected rate of damage accumulation given by equation (4.22) may be easily evaluated numerically for any appropriate value of s. For integer values of s, equation (4.22) may be evaluated in closed form. This was shown by Roberts [33] for odd integers and can be extended to even integers by the evaluation of a single integral.

It is convenient to introduce the correlation coefficient $\rho(t)$ defined as

$$\rho(t) = \frac{q_{12}(t)}{\sqrt{q_{11}(t)q_{22}(t)}} \tag{4.24}$$

where $q_{ij}(t)$ are the elements of the covariance matrix $\underline{Q}(t)$. It is also helpful to normalize the displacement by the root mean square value of the response and denote this new dimensionless variable by η where

$$\eta = \frac{b}{\sqrt{q_{11}(t)}} \quad . \tag{4.25}$$

Substituting equation (4.23) into equation (4.22) then yields

$$E\left[\frac{dD}{dt}(t)\right] = \frac{q_{11}^{\frac{s-1}{2}} q_{22}^{1/2}(1-\rho^2)^{1/2}}{2\pi C_b} \int_0^\infty \eta^s \exp\left(-\frac{\eta^2}{2}\right) \left\{ \eta \exp\left(\frac{-\rho^2\eta^2}{2(1-\rho^2)}\right) - \sqrt{\frac{\pi}{2}} \frac{\rho(1-\eta^2)}{\sqrt{1-\rho^2}} \left[1 - \operatorname{erf}\left(\frac{\rho\eta}{\sqrt{2(1-\rho^2)}}\right)\right] \right\} d\eta \tag{4.26}$$

where the functional dependence of ρ and q_{ij} on t has been omitted for

brevity.

Integrating equation (4.26) by parts gives

$$E\left[\frac{dD}{dt}(t)\right] = \frac{q_{11}^{\frac{s-1}{2}} q_{22}^{1/2}(1-\rho^2)^{1/2}}{2\pi C_b}\left\{[2(1-\rho^2)]^{\frac{s}{2}}\,\Gamma\left(\frac{s+2}{2}\right)\right.$$

$$\left. + \sqrt{\frac{\pi}{2}}\,\frac{s\rho}{\sqrt{1-\rho^2}}\left[2^{\frac{s-1}{2}}\,\Gamma\left(\frac{s+1}{2}\right) + J(\rho,s)\right]\right\} \qquad (4.27)$$

where

$$J(\rho,s) = \int_0^\infty \eta^s \exp\left(-\frac{\eta^2}{2}\right) \operatorname{erf}\left(\frac{\rho\eta}{\sqrt{2(1-\rho^2)}}\right) d\eta \qquad (4.28)$$

and the gamma function $\Gamma(a)$ is defined as

$$\Gamma(a) = \int_0^\infty x^{a-1} \exp(-x)\, dx \quad .$$

The function $J(\rho,s)$ cannot easily be expressed in a simple manner as a function of ρ and s. However, it does satisfy a reduction formula obtained by integrating equation (4.28) by parts to give

$$J(\rho,s) = (s-1)J(\rho,s-2) + \frac{\rho}{\sqrt{\pi}}[2(1-\rho^2)]^{\frac{s-1}{2}}\,\Gamma\left(\frac{s}{2}\right) \quad . \qquad (4.29)$$

Hence, to define the expected damage rate for all integral values of s, one needs only to evaluate equation (4.28) for $s = 0$ and $s = 1$. Performing this operation yields

$$J(\rho,0) = \int_0^\infty \exp\left(-\frac{\eta^2}{2}\right) \operatorname{erf}\left(\frac{\rho\eta}{\sqrt{2(1-\rho^2)}}\right) d\eta$$

$$= \operatorname{sgn}(\rho)\left[\sqrt{\frac{\pi}{2}} - \sqrt{\frac{2}{\pi}}\tan^{-1}\left(\frac{\sqrt{1-\rho^2}}{|\rho|}\right)\right] \qquad (4.30)$$

and

$$J(\rho,1) = \int_0^\infty \eta \exp\left(-\frac{\eta^2}{2}\right) \operatorname{erf}\left(\frac{\rho\eta}{\sqrt{2(1-\rho^2)}}\right) d\eta$$

$$= \rho \quad . \qquad (4.31)$$

The expected rate of damage accumulation may now be expressed as

$$E\left[\frac{dD}{dt}(t)\right] = \frac{2^{\frac{s}{2}}\,\Gamma\left(\frac{s+2}{2}\right)}{2\pi C_b}\, q_{11}^{\frac{s-1}{2}}(t)\, q_{22}^{s/2}(t)\, K(\rho(t),s) \qquad (4.32)$$

where

$$K(\rho(t),s) = (1-\rho^2)^{\frac{s+1}{2}} + \frac{s\rho\sqrt{\pi}}{\Gamma\left(\frac{s+2}{2}\right)}\left[\Gamma\left(\frac{s+1}{2}\right) + \left(\frac{1}{2}\right)^{\frac{s+1}{2}} J(\rho,s)\right] \quad . \qquad (4.33)$$

$K(\rho(t),s)$ is shown in Figure 4.2. $K(\rho(t),s)$ is positive for all values of ρ. Hence, the expected damage rate is positive. Note that $K(0,s)$ is equal to unity for all values of s.

A characteristic of the stationary response of a simple oscillator is that the displacement response and the velocity response are uncorrelated (i.e., $\rho = 0$). Thus the expected damage rate for stationary response is given by

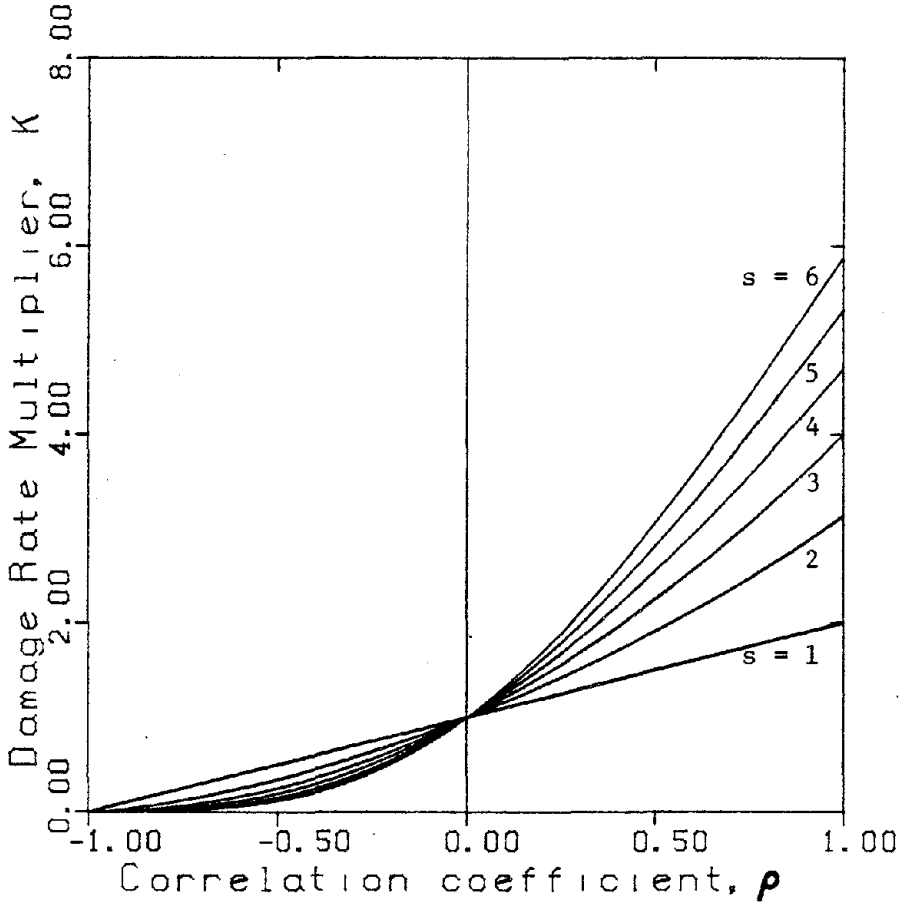

Figure 4.2 Damage Rate Multiplier versus Correlation Coefficient.

$$E\left[\frac{dD}{dt}(t)\right]_{\rho=0} = \frac{2^{\frac{s}{2}}\,\Gamma\left(\frac{s+2}{2}\right)}{2\pi C_b}\, q_{11}^{\frac{s-1}{2}}(t)\; q_{22}^{\frac{1}{2}}(t) \tag{4.34}$$

which is consistent with the results given by Miles [34].

4.5 Normalization of the Expected Total Damage for a Linear System Subjected to Modulated White Noise

Integrating equation (4.22) with respect to time, the expected total damage may be written as

$$E[D(t_d)] = -\frac{1}{C_b}\int_0^{t_d}\int_0^{\infty} b^s\,\frac{\partial \nu}{\partial b}(b,t)\; db\; dt \quad . \tag{4.35}$$

Consider the special case where a simple linear oscillator with natural period T is subjected to modulated white-noise excitation. If the modulating envelope is a function of only the normalized time, $\tau = \frac{t}{T}$, given the duration t_d of the excitation, a convenient normalization of the expected total damage problem exists.

In the situation described above, the covariance matrix $\underline{Q}(\tau)$ may be expressed as

$$\underline{Q}(\tau) = \begin{bmatrix} S_0 T^3 f_{11}(\tau) & S_0 T^2 f_{12}(\tau) \\ S_0 T^2 f_{21}(\tau) & S_0 T f_{22}(\tau) \end{bmatrix} \tag{4.36}$$

where the $f_{ij}(\tau)$'s are dimensionless functions and S_0 is the power

spectral density of the white-noise excitation. Using this form of the covariance matrix, the derivative of the frequency of up-crossings with respect to the crossing level may be written as

$$\frac{\partial \nu}{\partial b}(b,t) = \sqrt{S_0 T^3}\ \frac{\partial \nu^*}{\partial \beta}(\beta,\tau) \tag{4.37}$$

where

$$\beta = \frac{b}{\sqrt{S_0 T^3}} \quad .$$

Performing a change of variables on equation (4.35) yields

$$E\left[D\left(\frac{t_d}{T}\right)\right] = -\frac{(S_0 T^3)^{\frac{s}{2}}}{C_b} \int_0^{\frac{t_d}{T}} \int_0^{\infty} \beta^s\ \frac{\partial \nu^*}{\partial \beta}(\beta,\tau)\ d\beta\ d\tau \quad . \tag{4.38}$$

It may be shown that the first-passage problem defining the power spectral density from the response spectrum given in equation (3.8) may be written as

$$P_s = \exp\left[-\int_0^{\frac{t_d}{T}} \alpha(r,\xi,\tau)\ d\tau\right] \tag{4.39}$$

where P_s is the confidence level of the response spectrum, α is the limiting decay rate, and r is the response spectrum normalized by the excitation level given by

$$r = \frac{SD}{\sqrt{S_0 T^3}} \quad .$$

The expected total damage may be expressed in terms of r as

$$E\left[D\left(\frac{t_d}{T}\right)\right] = -\frac{SD^s}{C_b}\frac{1}{r^s}\int_0^{\frac{t_d}{T}}\int_0^{\infty}\beta^s\frac{\partial\Psi^*}{\partial\beta}(\beta,\tau)\,d\beta\,d\tau \quad . \tag{4.40}$$

Recall from equation (4.7) that for low-cycle failure the damage law is given by

$$N\varepsilon^s = C_\varepsilon$$

where ε is a strain which is greater than the elastic limit strain ε_y of the material. If the strain is normalized by the elastic limit strain, the damage law may be written as

$$N\mu^s = C_\mu \tag{4.41}$$

where μ is known as the ductility factor given by

$$\mu = \frac{\varepsilon}{\varepsilon_y}$$

and

$$C_\mu = \frac{C_\varepsilon}{\varepsilon_y^s} \quad .$$

Since strains are assumed proportional to displacements, it follows that

$$\frac{SD^s}{C_b} = \frac{SD^s/S_y^s}{C_b/S_y^s} = \frac{\mu^s}{C_\mu} \tag{4.42}$$

where S_y is the displacement corresponding to the elastic limit strain, ε_y. Using this relationship in equation (4.40) yields

$$E\left[D\left(\frac{t_d}{T}\right)\right] = -\frac{\mu^s}{C_\mu}\frac{1}{r^s}\int_0^{\frac{t_d}{T}}\int_0^{\infty}\beta^s\frac{\partial V^*}{\partial\beta}(\beta,\tau)\,d\beta\,d\tau \tag{4.43}$$

where r is implicitly defined by equation (4.39).

The expected total damage may be computed given the duration of the excitation in natural periods of the system, the ductility factor of the system, and the confidence level associated with the ductility and the damage model. Note that the overall shape of the response spectrum is not important. Only the value of the response spectrum at the natural frequency of the system matters in its relationship to the ductility factor, μ, of the response.

For the softening nonlinear elastic system of section 3.3, the power spectral density of the excitation is not a constant with respect to the time because of the time-varying frequency shift. The expected total damage of the nonlinear system depends on the shape of the power spectral density. In this case, it is better to use equation (4.35) directly to compute the expected total damage.

CHAPTER V

ASSESSMENT OF THE EFFECTS OF DURATION ON THE DAMAGE OF A SIMPLE SYSTEM

5.1 Introduction

In order to assess the effects of various system parameters on the expected total damage of a structure, consider the simple frame shown in Figure 5.1. When the frame is subjected to strong earthquake ground motion, large displacements can occur. Large bending moments develop at the top and the bottom of the columns of the frame. The large bending moments cause large strains which may be associated with low-cycle failure.

A simple analytical model for earthquake excitation is a modulated stationary Gaussian random process. The equation of motion for the simple frame subjected to such a process is that of a simple oscillator and given by

$$\ddot{x} + 2\xi\omega_0\dot{x} + \omega_0^2 x = \theta(t)g(t) \qquad (5.1)$$

where ξ is the fraction of critical damping, ω_0 is the natural frequency of the system, $\theta(t)$ is the deterministic modulating envelope, and $g(t)$ is a stationary Gaussian random process with spectral density $S(\omega)$. Zero initial conditions are assumed.

The modulating envelope will be taken to be the earthquake-like modulating envelope used in Section 3.2. The envelope may be written in terms of the dimensionless time, τ, as

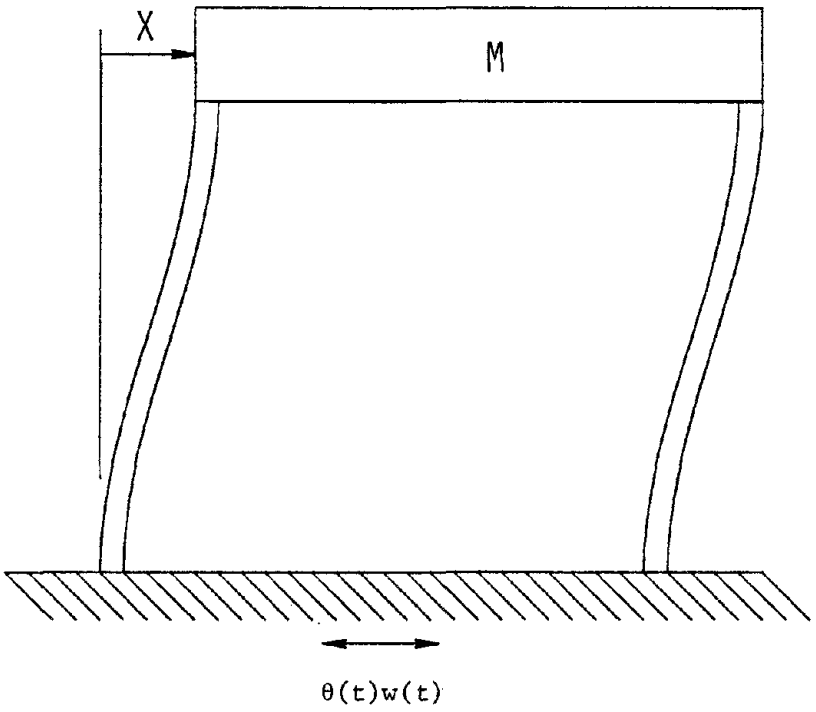

Figure 5.1 Simple Frame Structure.

$$\theta(\tau) = \begin{cases} \dfrac{56.25}{(t_d/T)^2}\,\tau^2 & ; \quad 0 \leq \tau \leq \dfrac{2t_d}{15T} \\ 1.0 & ; \quad \dfrac{2t_d}{15T} < \tau \leq \dfrac{t_d}{2T} \\ \exp\left[-2.976\left(\dfrac{\tau}{t_d/T} - \dfrac{1}{2}\right)\right] & ; \quad \dfrac{t_d}{2T} < \tau \leq \dfrac{t_d}{T} \end{cases} \tag{5.2}$$

where

$$\tau = \frac{t}{T}$$

and T is the natural period of the system.

Response statistics of the system, in particular the covariance matrix, are needed to evaluate the expected total damage. If the system is lightly damped, the response will be narrow-banded about the natural frequency. Hence, the same approximation used in Section 3.2 for ξ sufficiently small may be used here. The process g(t) may be replaced with a stationary Gaussian white-noise process, w(t), with constant spectral density $S_0 = S(\omega_0)$.

The methods discussed in Section 2.1 may be used to compute the response statistics of the system. The response statistics may then be applied to equations (4.39) and (4.43) to compute the expected total damage.

5.2 Expected Total Damage - Linear Model

Equation (4.22) may be evaluated numerically for any value of the damage law exponent, s. However, to study the effects of duration on the expected total damage, it is computationally more efficient to use integer values of s. In that case the closed form solution described in Section 4.4 may be applied to evaluate the expected rate of damage accumulation. Numerical integration in time may then be used to compute the total expected damage. For steel, the damage law exponent will be taken to be 2 and equation (4.3) becomes

$$N\mu^2 = 167.1 \quad . \tag{5.3}$$

For reinforced concrete, s is approximately 6 in equation (4.5) so the damage law will be taken as

$$N\mu^6 = 416.3 \quad . \tag{5.4}$$

The normalization discussed in Section 4.5 for the linear elastic system will be applied here. Time variables will be normalized by the natural period of the system. The earthquake-like modulating envelope described by equation (5.2) will be used. The duration of excitation will be expressed a $\frac{t_d}{T}$ natural periods; hence, varying the natural period is equivalent to varying the duration.

The expected total damage is given in equation (4.43) as

$$E\left[D\left(\frac{t_d}{T}\right)\right] = -\frac{\mu^s}{C_\mu}\frac{1}{r^s}\int_0^{\frac{t_d}{T}}\int_0^{\infty}\beta^s\frac{\partial\psi^*}{\partial\beta}(\beta,\tau)\,d\beta\,d\tau \qquad (5.5)$$

where r satisfies

$$P_s = \exp\left[-\int_0^{\frac{t_d}{T}}\alpha(r,\xi,\tau)\,d\tau\right] . \qquad (5.6)$$

The integration over β is performed by applying equation (4.32) and the integration over τ is performed numerically.

Since large amounts of yielding are assumed, the system will behave in a nonlinear manner. However, the effects of a system nonlinearity can often be accounted for approximately by a simple shift in the damping factor and natural frequency of a linear structure. Therefore, by studying a linear system, a fundamental understanding of the effects of duration and ductility ratio on damage may be obtained even for a nonlinear system.

In Figures 5.2 and 5.3, the expected total damage is shown for a linearly elastic system. Curves are shown for several levels of ductility and two values of damping. Figure 5.2 represents a damage behavior close to that of a steel structure and Figure 5.3 approximates the behavior of a reinforced concrete structure.

For a fixed ductility level, the expected total damage is primarily a function which initially increases rapidly with increasing duration,

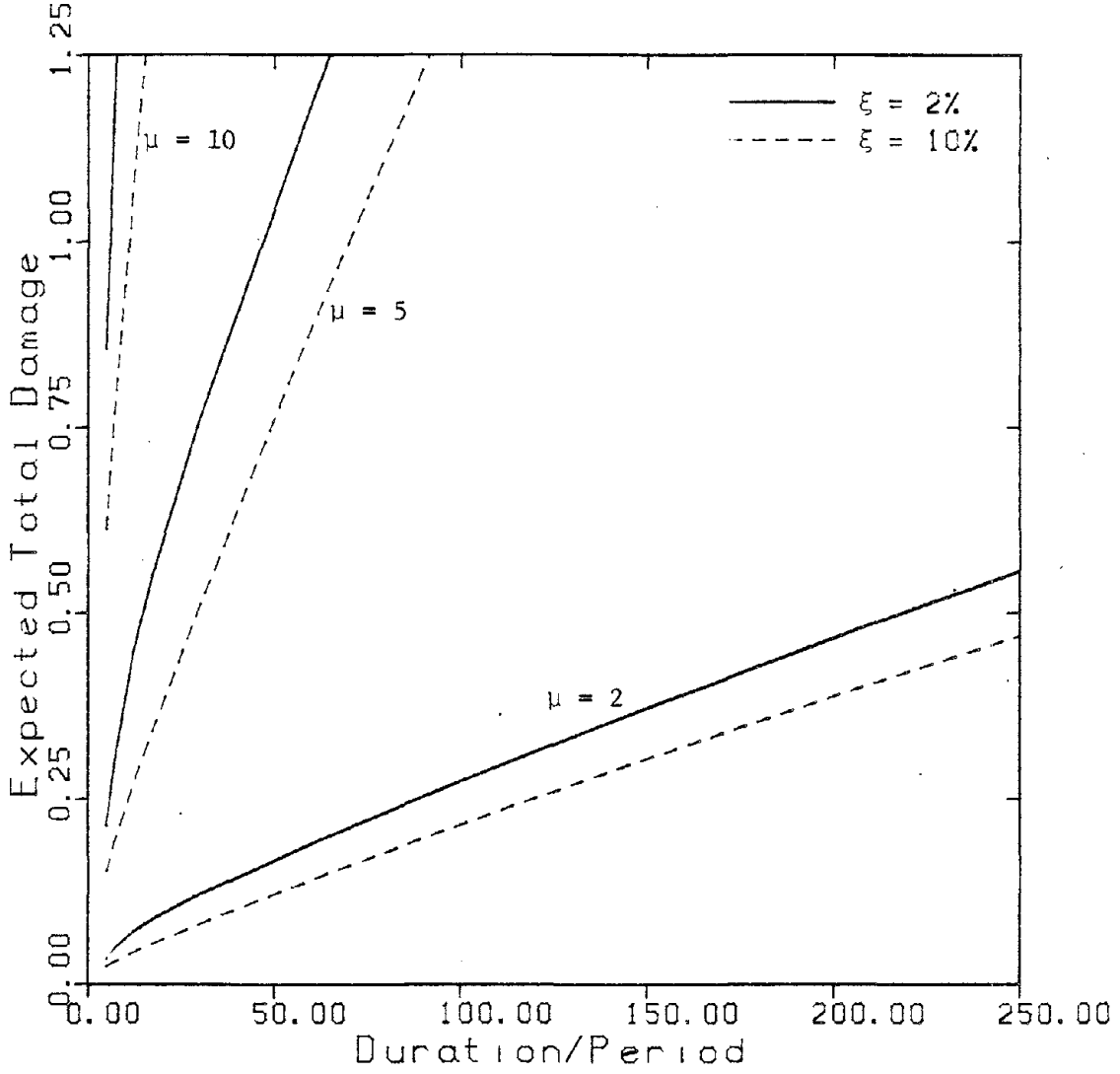

Figure 5.2 Expected Total Damage versus Normalized Duration for a Linear Steel Structure.

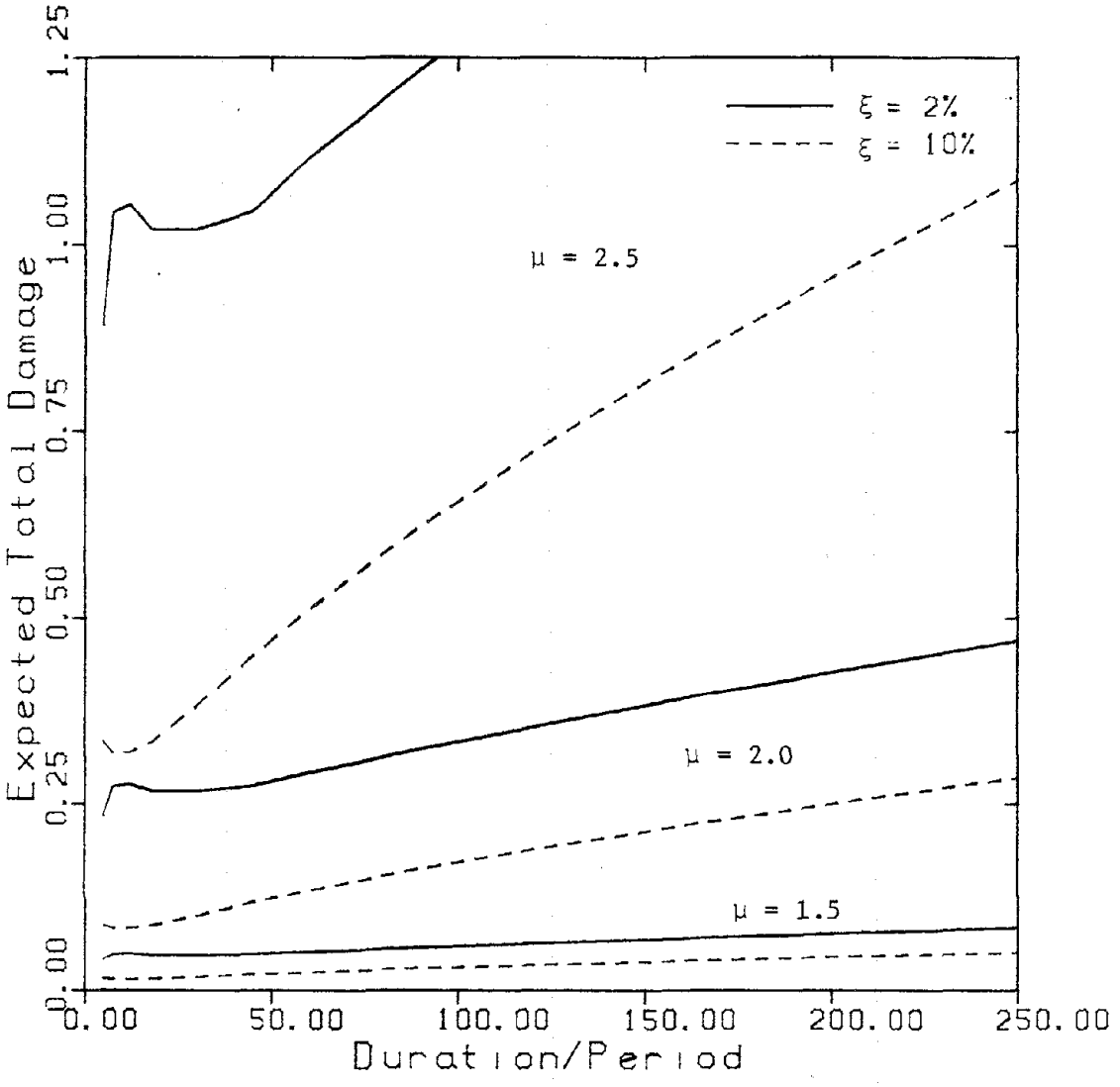

Figure 5.3 Expected Total Damage versus Normalized Duration for a Linear Reinforced Concrete Structure.

then approaches a nearly constant positive slope corresponding to the stationary damage rate. For a steel structure the expected damage is a somewhat uniformly increasing function of duration. However, for a reinforced concrete structure, there is a region below 50 periods where the expected damage is rather insensitive to duration.

As the ductility level increases, the material is cycled further into its plastic range, and the expected total damage increases. From equation (5.5), it is apparent that E[D] is proportional to μ^s for a linear system. Therefore, the damage is a stronger function of the ductility ratio for the reinforced concrete structure than for the steel structure. The steel structure is capable of sustaining much greater levels of ductility than the reinforced concrete structure without failure.

In Figures 5.2 and 5.3, structural damping is treated independently of the ductility factor. Realistically, however, an increase in damping reduces the system response, thereby also reducing the ductility factor. Hence, the net reduction in the damage due to an increase in damping is greater than the reduction implied in the figures.

5.3 Expected Total Damage - Softening Nonlinear Model

The effect of system softening may be included to better approximate a yielding system by considering a simple oscillator with a softening nonlinear elastic spring. Using the same system as in Section 3.3,

the equation of motion for such a simple oscillator is given by

$$\ddot{x} + 2\xi\omega_0\dot{x} + \frac{2}{\pi}\omega_0^2\frac{x_{max}}{\mu}\tan^{-1}\left(\frac{\pi}{2}\mu\frac{x}{x_{max}}\right) = \theta(t)w(t) \qquad (5.7)$$

where ξ and ω_0 are the fraction of critical damping and the undamped natural frequency, respectively, associated with small displacements, x_{max} is the maximum response of the system, and μ is the nonlinearity parameter.

Statistical linearization techniques may be used to define an equivalent linear system for which response statistics and expected total damage are computed. Equation (4.35) is used directly to compute the expected total damage due to the variation in the power spectral density caused by the time-varying frequency shift.

In Figures 5.4-5.7, the expected total damage for the softening nonlinear elastic system subjected to the processes derived in Section 3.2 from the NRC design response spectrum is shown for several values of the nonlinearity parameter μ. Recall that μ may vary from 0 to any finite value with $\mu = 0$ corresponding to a linear system, and that μ is similar to the ductility ratio of a yielding system for values greater than unity.

Figures 5.4 and 5.5 represent damage behavior based on the damage law for steel [equation (5.3)], and Figures 5.6 and 5.7 represent damage behavior based on the damage law for reinforced concrete [equation (5.4)]. The results are shown for various combinations of duration, ductility ratio, and damping ratio and plotted against the undamped

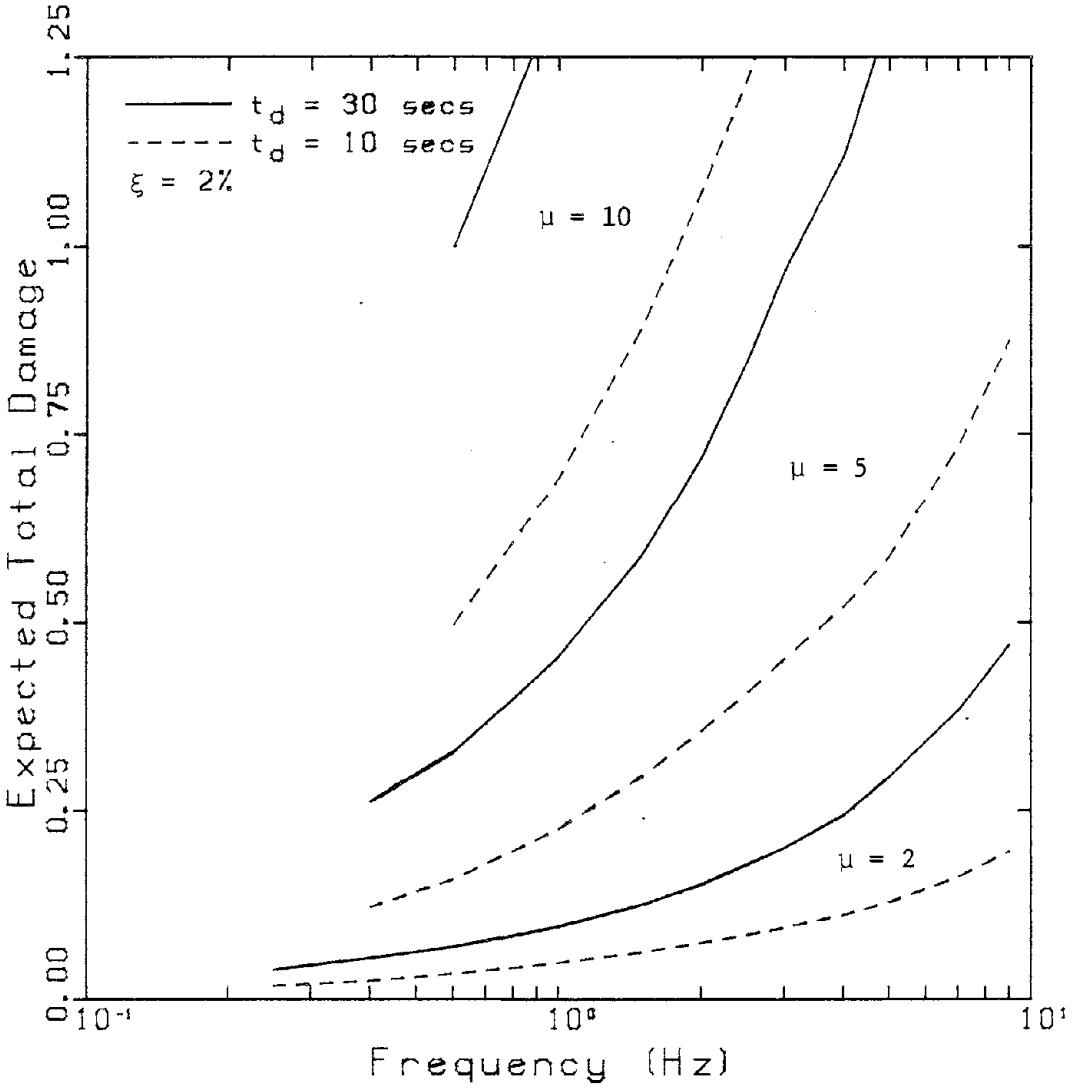

Figure 5.4 Expected Total Damage versus Natural Frequency for a Softening Steel Structure, ξ = 2%. (NRC Design Response Spectrum)

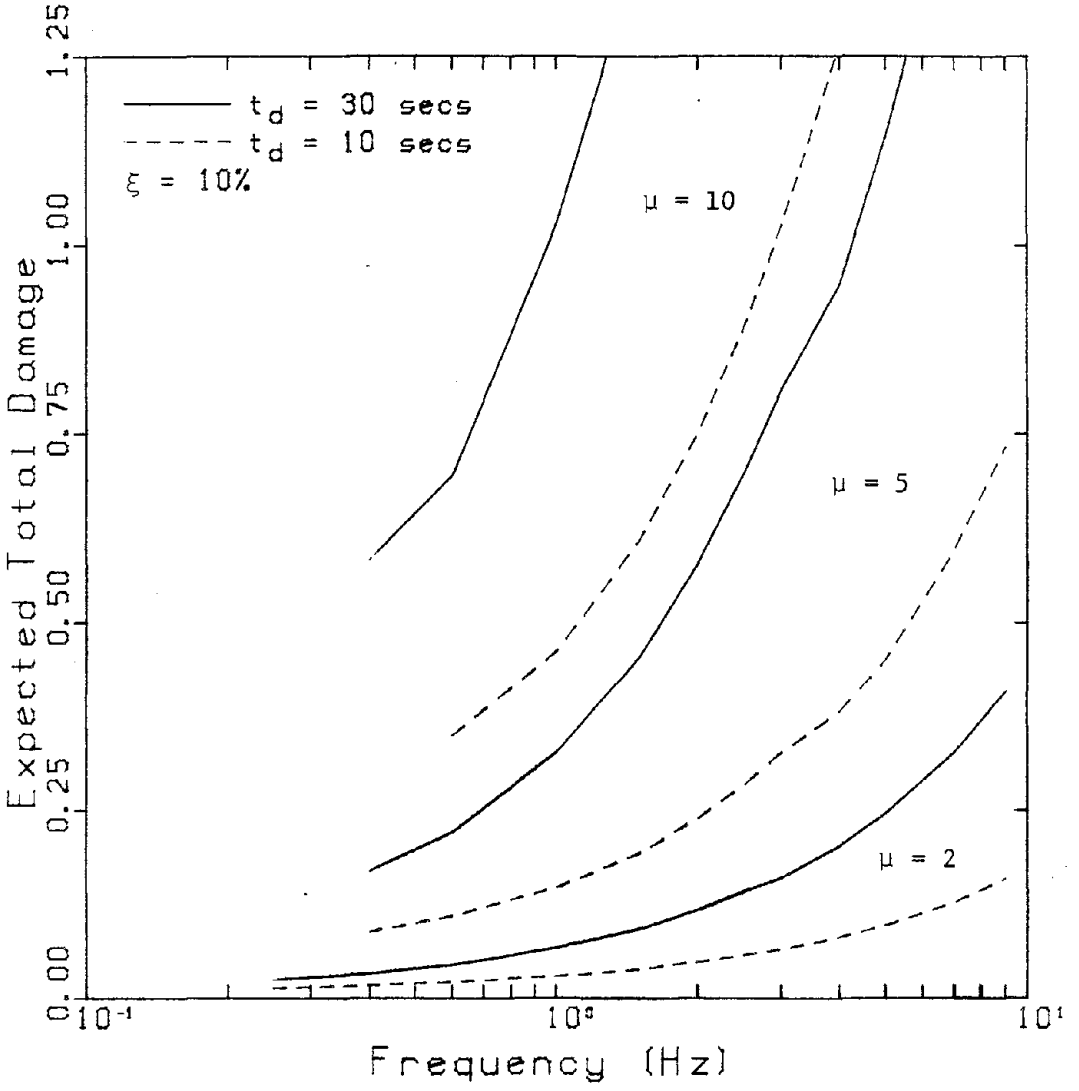

Figure 5.5 Expected Total Damage versus Natural Frequency for a Softening Steel Structure, ξ = 10%. (NRC Design Response Spectrum)

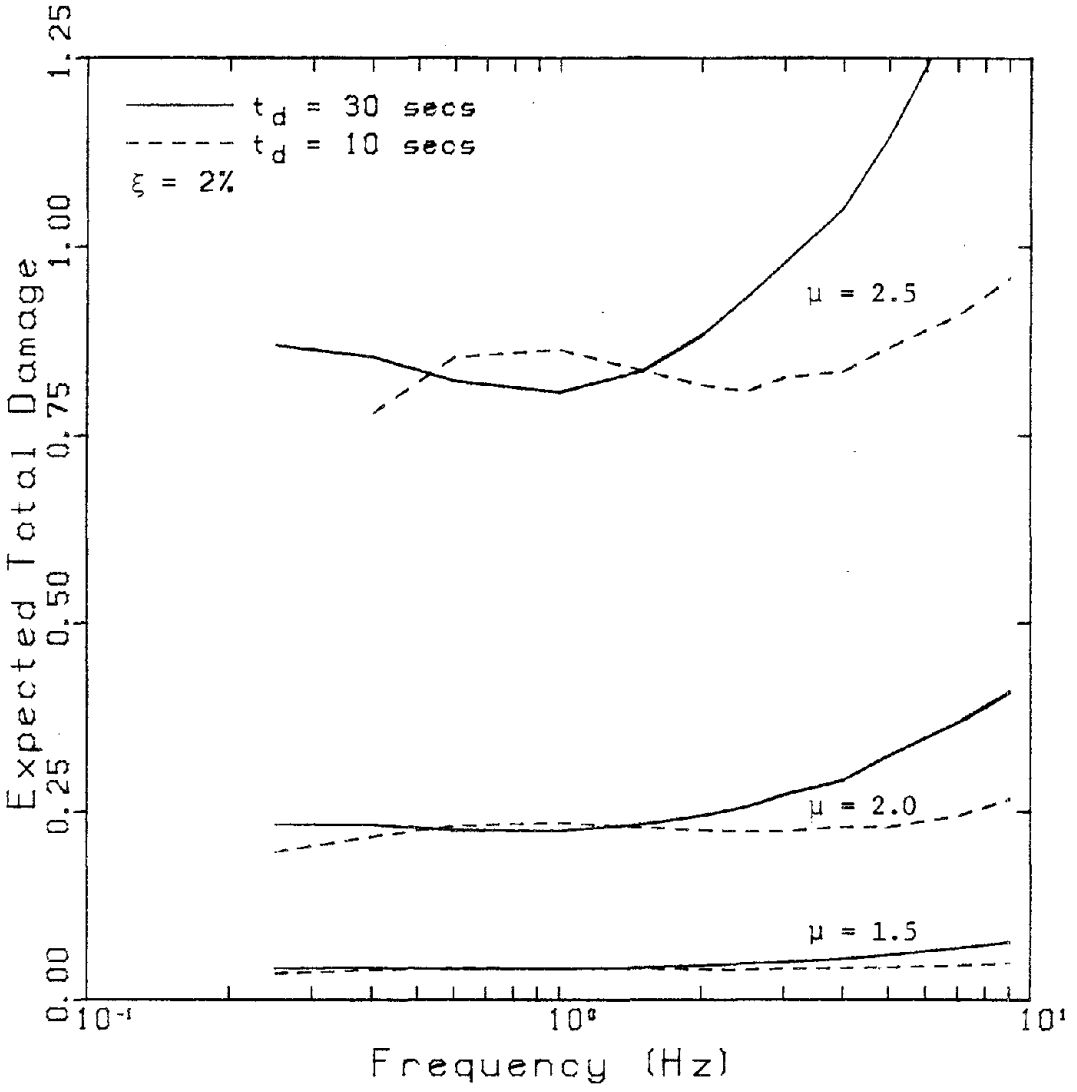

Figure 5.6 Expected Total Damage versus Natural Frequency for a Softening Reinforced Concrete Structure, ξ = 2%. (NRC Design Response Spectrum)

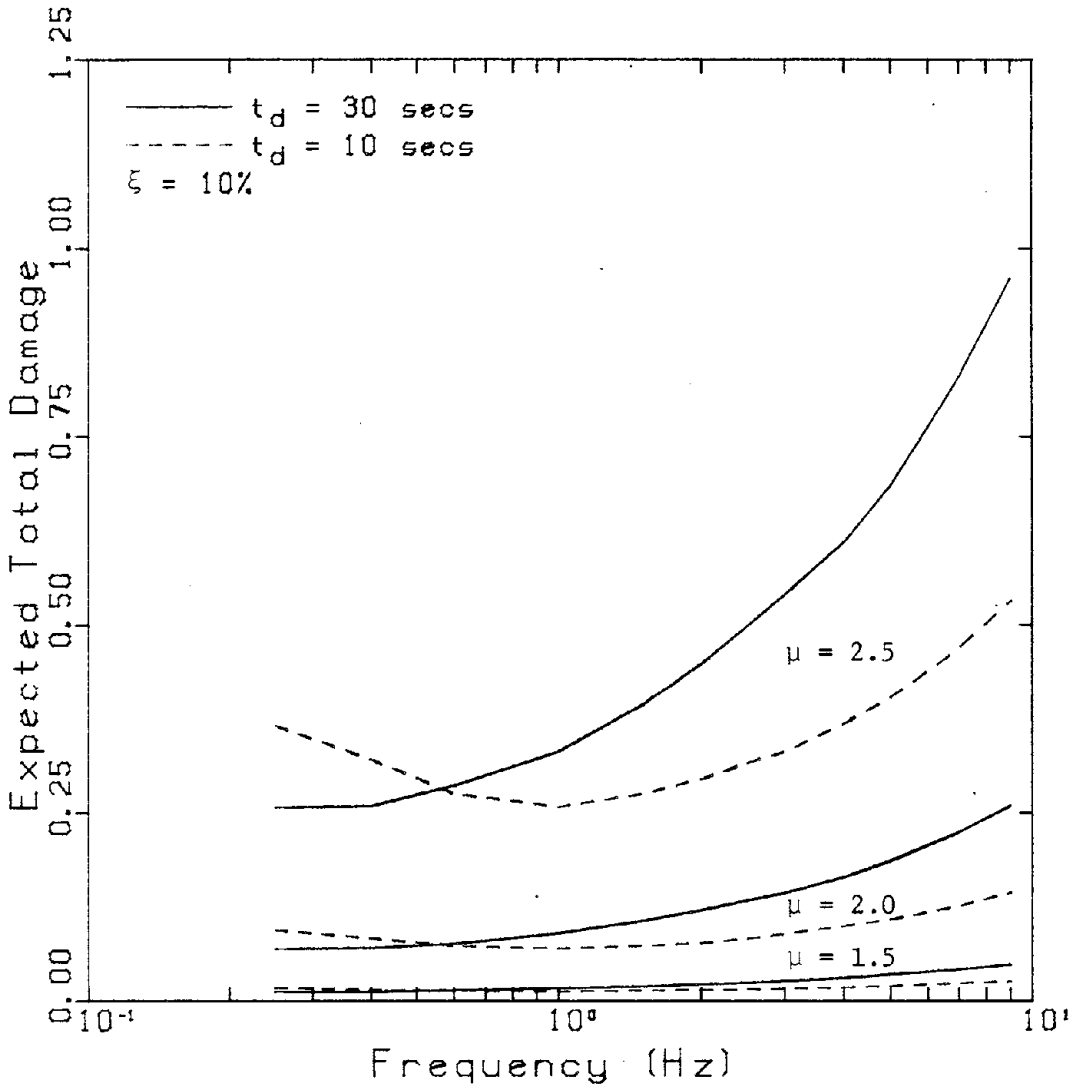

Figure 5.7 Expected Total Damage versus Natural Frequency for a Softening Reinforced Concrete Structure, ξ = 10%. (NRC Design Response Spectrum)

natural frequency associated with small displacements.

The expected total damage of the softening nonlinear elastic system is qualitatively the same as that of the linear system. The nonlinearity affects the expected total damage in three ways. First, an increase in the response amplitude occurs because of the assumed level of softening in the system resulting in an increase in the amount of damage per cycle of response. Secondly, the downward frequency shift reduces the number of response cycles executed for a fixed duration of excitation. Finally, the frequency shift also changes the effective power spectral density of the input excitation. The power input to the system may increase or decrease depending on the slope of the power spectrum near the small displacement natural frequency of the system. This, in turn, modifies the response amplitude accordingly.

5.4 Expected Damage Contours

A useful way to display expected damage information is shown in Figure 5.8. Based on the system which behaves linearly, contours for expected total damage equal to unity may be presented as a relationship between the ductility factor of the response and the duration of excitation. In this way, combinations of duration and ductility factor for which the expected total damage is greater than or less than unity may readily be identified.

From Figure 5.8 it is evident that the range of the allowable

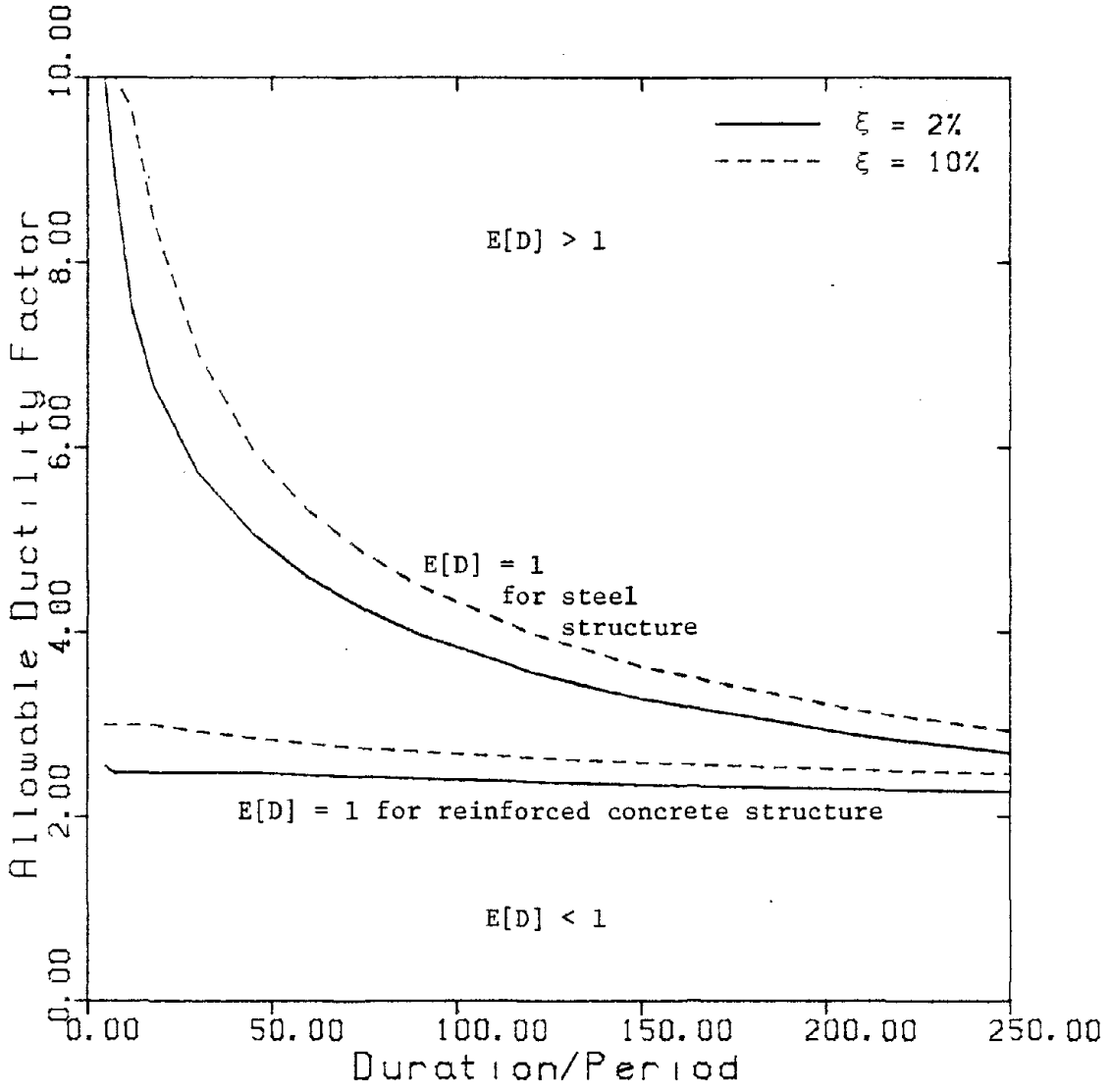

Figure 5.8 Contours of Expected Total Damage equal to unity versus Allowable Ductility Factor and Normalized Duration for Linear Steel and Reinforced Concrete Structures.

ductility factor is much smaller for the reinforced concrete structure than for the steel structure. The rapid increase in damage associated with short durations, along with the strong dependence upon the ductility ratio, leads to the existence of a sharp threshold for failure in the reinforced concrete structure.

The expected total damage reflects a mean value of the damage of a structure. Hence, the allowable ductility factor for a given duration shown in Figure 5.8 may be taken to be an upper bound of the design ductility factor of the structure. The value of the damage is, of course, a function of the failure model employed in the analysis and may not be applicable to all structures. However, the functional dependence of the expected damage on the ductility factor and duration is thought to be representative.

A considerable amount of computation is required to compute expected damage contours for a nonlinear system. Since the expected total damage of the softening nonlinear system is less than that for the linear system, the contours for the linear system may be conservatively used in place of the contours for the nonlinear system.

CHAPTER VI

SUMMARY AND CONCLUSIONS

In Chapter I, it was proposed that three basic elements be combined in order to study the effects of duration on the damage of structures. The first element was to define a nonstationary random process which models earthquake excitation and corresponds statistically to a desired response spectrum. The second element was to postulate a model for the incremental damage of a system. The last element was to compute a measure of the damage in a simple structure.

In Chapter II the necessary tools to accomplish these tasks were reviewed. In the first section, random vibration theory was discussed including methods to compute the response statistics needed to implement the first-passage probability estimates and cumulative damage expressions. The second section dealt with analytical approaches to the first-passage probability of a simple oscillator and defined the equations which would later be used to synthesize the response spectrum consistent processes. The last section recalled the method of statistical linearization in order that a nonlinear system could be considered by the first-passage probability and accumulated damage estimates.

In Chapter III, modulated Gaussian random processes were assumed to model earthquake-like excitation. The modulating envelope was assumed fully defined by its duration. Analytical estimates of the first-passage probability of a simple oscillator were calculated for several threshold levels. The result were found to be reasonably accurate when

compared to Monte Carlo simulation. Using the analytical first-passage probability estimates, power spectrum ordinates were chosen such that the maximum response exceeded the design spectrum with a predetermined probability. Actual random processes were computed consistent to the NRC design response spectrum. The magnitude of the power spectrum found in this manner varied significantly with duration.

The maximum response of a nonlinear softening system to excitation specified by a response spectrum was discussed. The role of the first-passage problem was reversed to find the maximum response of a statistically linearized nonlinear system. The maximum response of the softening nonlinear system as function of frequency was found to be similar to a linear response spectrum which had been translated along an axis of constant displacement on a log-log pseudo-velocity diagram.

In Chapter IV, the behavior of structural members under cyclic loads was discussed. A rule analogous to the Miner-Palmgren rule approach to fatigue was postulated. The rule was used to compute the mean damage of a system with narrow-banded random response. In particular, it was applied to a simple harmonic oscillator subjected to a modulated Gaussian random process. For a special case of the damage law, a closed form expression was formulated for the expected damage rate.

In Chapter V, the degree of damage in a simple structure subjected to excitation specified by a response spectrum was determined. Two types of structure were considered: a steel structure and a reinforced concrete structure. The damage law was defined from cyclic bending tests

performed on steel and reinforced concrete structural members. The response spectrum consistent random processes computed earlier were used as input to the system.

It was observed that the damage of a linear structure initially increases rapidly with increasing duration, and then approaches a constant positive slope corresponding to the steady-state damage rate. A steel structure is capable of sustaining much greater levels of ductility without failure than a reinforced concrete structure. Damage for a reinforced concrete structure displays a much stronger dependence on the ductility level of the response than the damage for a steel structure. When system softening is accounted for through statistical linearization, results are found similar to the linear system, but with lesser degrees of damage.

A relatively straightforward analytical procedure has been presented to estimate the effect of earthquake duration on the damage of a structure. Based on the results presented herein, it is found that the duration of excitation and the design ductility level of the response can have a strong effect on the expected damage of the structure. Use of the response spectrum alone to specify a design input ground motion accounts for the dependence of the damage on the ductility factor of the response, but ignores the effects of the duration of the excitation. Therefore, it is recommended that some measure of duration be provided more often in earthquake design specifications and utilized in the analysis of structural reliability.

REFERENCES

1. Lin, Y.K., Probabilistic Theory of Structural Dynamics, New York: McGraw Hill, 1967.

2. Rice, S.O., "Mathematical Analysis of Random Noise," in Selected Papers on Noise and Stochastic Processes, Nelson Wax, ed., New York: Dover Publications, Inc., 1954.

3. Mason, A.B., Some Observations on the Random Response of Linear and Nonlinear Dynamical Systems, Ph.D. Thesis, California Institute of Technology, 1979.

4. Crandall, S.H., "First-Crossing Probabilities of the Linear Oscillator," Journal of Sound and Vibration, vol. 12, no. 3, 1970, pp. 285-299.

5. Mark, W.D., "On False-Alarm Probabilities of Filtered-Noise," Proceedings of IEEE, vol. 54, 1966, pp. 316-317.

6. Vanmarcke, E.H., "On the Distribution of the First-Passage Time for Normal Stationary Random Processes," Journal of Applied Mechanics, ASME, vol. 42, ser. E, no. 1, 1975, pp. 215-220.

7. Vanmarcke, E.H., "Properties of Spectral Moments with Application to Random Vibration," Journal of the Engineering Mechanics Division, ASCE, vol. 98, no. EM2, 1972, pp. 425-446.

8. Mason, A.B.,Jr. and Iwan, W.D., "An Approach to the First Passage Problem in Random Vibration," Journal of Applied Mechanics, ASME, vol. 50, no. 3, 1983, pp. 641-646.

9. Corotis, R.B., Vanmarcke, E.H., and Cornell, C.A., "First Passage of Nonstationary Random Processes," Journal of the Engineering Mechanics Division, ASCE, vol. 98, no. EM2, 1972, pp. 401-414.

10. Crandall, S.H., Chandiramani, K.L., and Cook, R.G., "Some First-Passage Problems in Random Vibrations," Journal of Applied Mechanics, ASME, vol. 33, ser. E, no. 3, 1966, pp. 532-538.

11. Booton, R.C., "The Analysis of Nonlinear Control Systems with Random Input," Proceedings of the Symposium on Nonlinear Circuit Analysis, Brooklyn, New York, 1953, vol. 2.

12. Caughey, T.K., "Equivalent Linearization Techniques," Journal of the Acoustical Society of America, vol. 35, no. 11, 1963, pp. 1706-1711.

13. Kryloff, N. and Bogoliuboff, N., Introduction to Nonlinear Mechanics, Princeton, New Jersey: Princeton University Press, 1947.

14. Foster, E.T.,Jr., "Semilinear Random Vibrations in Discrete Systems," Journal of Applied Mechanics, ASME, vol. 35, ser. E, no. 3, 1968, pp. 560-564.

15. Iwan, W.D., and Yang, I-M., "Statistical Linearization for Nonlinear Structures," Journal of the Engineering Mechanics Division, ASCE, vol. 97, no. EM6, 1971, pp. 1609-1623.

16. Yang, I-M., Stationary Random Response of Multidegree-of-Freedom Systems, Ph.D. Thesis, California Institute of Technology, 1970.

17. Atalik, T.S., and Utku, S., "Stochastic Linearization of Multi-Degree-of-Freedom Non-Linear Systems," Earthquake Engineering and Structural Dynamics, vol. 4, no. 4, 1976, pp. 411-420.

18. Clough, R.W., and Penzien, J., Dynamics of Structures, New York: McGraw-Hill, 1975.

19. Nigam, N.C., and Jennings, P.C., "Calculation of Response Spectra from Strong-Motion Earthquake Records," Bulletin of the Seismological Society of America, vol. 59, no. 2, 1969, pp. 909-922.

20. Jennings, P.C., Housner, G.W., and Tsai, N.C., Simulated Earthquake Motions, Earthquake Engineering Research Laboratory, California Institute of Technology, Pasadena, California, 1968.

21. Saragoni, G.R., and Hart, G.C., "Simulation of Artificial Earthquakes," Earthquake Engineering and Structural Dynamics, vol. 2, 1974, pp. 249-267.

22. Housner, G.W., "Design Spectrum," in Earthquake Engineering, R.L. Wiegel, ed., Englewood Cliffs, N.J.: Prentice Hall, Inc., 1970.

23. Regulatory Guide 1.60, U.S. Atomic Energy Commission, December 1973.

24. Newmark, N.M., Blume, J.A., and Kapur, K.K., "Seismic Design Spectra for Nuclear Power Plants," Journal of the Power Division, ASCE, vol. 99, no. PO2, 1973, pp. 287-303.

25. Iwan, W.D., and Gates, N.C., "The Effective Period and Damping of a Class of Hysteretic Structures," Earthquake Engineering and Structural Dynamics, vol. 7, no. 3, 1979, pp. 199-211.

26. Iwan, W.D., "Estimating Inelastic Response Spectra from Elastic Spectra," Earthquake Engineering and Structural Dynamics, vol. 8, no. 4, 1980, pp. 375-388.

27. Bertero, V.V., and Popov, E.P., "Effect of Large Alternating Strains on Steel Beams," Journal of the Structural Division, ASCE, vol. 91, no. ST1, 1965, pp. 1-12.

28. Yamada, M., "Low Cycle Fatigue Fracture Limits of Various Kinds of Structural Members Subjected to Alternately Repeated Plastic Bending under Axial Compression as an Evaluation Basis or Design Criteria for Aseismic Capacity," Proceedings of the Fourth World Conference on Earthquake Engineering, Santiago, Chile, 1969, vol. 1, B-2, pp. 137-151.

29. Yamada, M., "Effect of Cyclic Loading on Buildings," Proceedings of the International Conference on the Planning and Design of Tall Buildings, Bethlehem, Pennsylvania, 1972, vol. II, pp. 725-739.

30. Travernelli, J.F., and Coffin, L.F.,Jr., "Experimental Support for Generalized Equation Predicting Low Cycle Fatigue," with discussion by S.S. Manson, Journal of Basic Engineering, ASME, vol. 84, ser. D, no. 4, 1962, pp. 533-541.

31. Miner, M.A., "Cumulative Damage in Fatigue," Journal of Applied Mechanics, ASME, vol. 12, ser. A, no. 1, 1945, pp. 159-164.

32. Palmgren, A., "Die Lebensdauer von Kugellagern," Ver. deut. Ingr., vol. 68, 1924, pp. 339-341.

33. Roberts, J.B., "Structural Fatigue under Non-Stationary Random Loading," Journal of Mechanical Engineering Science, vol. 8, no. 4, 1966, pp. 392-405.

34. Miles, J.W., "On Structural Fatigue under Random Loading," Journal of Aeronautical Sciences, vol. 21, no. 11, 1954, pp. 753-762.

35. Kasiraj, I. and Yao, J.T.P., "Fatigue Damage in Seismic Structures," Journal of the Structural Division, ASCE, vol. 95, no. ST8, 1969, pp. 1673-1692.

36. ASCE Committee on Fatigue and Fracture Reliability, "Fatigue Reliability," Journal of the Structural Division, ASCE, vol. 108, no. ST1, 1982, pp. 3-88.

CALIFORNIA INSTITUTE OF TECHNOLOGY

Reports Published

by

Earthquake Engineering Research Laboratory*
Dynamics Laboratory
Disaster Research Center

Note: Numbers in parenthesis are Accession Numbers assigned by the National Technical Information Service; these reports may be ordered from the National Technical Information Service, 5285 Port Royal Road, Springfield, Virginia, 22161. Accession numbers should be quoted on orders for reports (PB --- ---). Reports without this information either have not been submitted to NTIS or the information was not available at the time of printing. An N/A in parenthesis indicates that the report is no longer available at Caltech.

1. Alford, J.L., G.W. Housner and R.R. Martel, "Spectrum Analysis of Strong-Motion Earthquakes," 1951. (Revised August 1964). (N/A)

2. Housner, G.W., "Intensity of Ground Motion During Strong Earthquakes," 1952. (N/A)

3. Hudson, D.E., J.L. Alford and G.W. Housner, "Response of a Structure to an Explosive Generated Ground Shock," 1952. (N/A)

4. Housner, G.W., "Analysis of the Taft Accelerogram of the Earthquake of 21 July 1952." (N/A)

5. Housner, G.W., "A Dislocation Theory of Earthquakes," 1953. (N/A)

6. Caughey, T.K., and D.E. Hudson, "An Electric Analog Type Response Spectrum," 1954.(N/A)

7. Hudson, D.E., and G.W. Housner, "Vibration Tests of a Steel-Frame Building," 1954. (N/A)

8. Housner, G.W., "Earthquake Pressures on Fluid Containers," 1954. (N/A)

9. Hudson, D.E., "The Wilmot Survey Type Strong-Motion Earthquake Recorder," 1958. (N/A)

10. Hudson, D.E., and W.D. Iwan, "The Wilmot Survey Type Strong-Motion Earthquake Recorder, Part II," 1960. (N/A)

---

* To order directly by phone the number is 703-487-4650.

11. Caughey, T.K., D.E. Hudson, and R.V. Powell, "The CIT Mark II Electric Analog Type Response Spectrum Analyzer for Earthquake Excitation Studies," 1960. (N/A)

12. Keightley, W.O, G.W. Housner and D.E. Hudson, "Vibration Tests of the Encino Dam Intake Tower," 1961. (N/A)

13. Merchant, Howard Carl, "Mode Superposition Methods Applied to Linear Mechanical Systems Under Earthquake Type Excitation," 1961. (N/A)

14. Iwan, Wilfred D., "The Dynamic Response of Bilinear Hysteretic Systems," 1961. (N/A)

15. Hudson, D.E., "A New Vibration Exciter for Dynamic Test of Full-Scale Structures," 1961. (N/A)

16. Hudson, D.E., "Synchronized Vibration Generators for Dynamic Tests of Full-Scale Structures," 1962. (N/A)

17. Jennings, Paul C., "Velocity Spectra of the Mexican Earthquakes of 11 May and 19 May 1962," 1962. (N/A)

18. Jennings, Paul C., "Response of Simple Yielding Structures to Earthquake Excitation," 1963. (N/A)

19. Keightley, Willard O., "Vibration Tests of Structures," 1963. (N/A)

20. Caughey, T.K. and M.E.J. O'Kelly, "General Theory of Vibration of Damped Linear Dynamic Systems," 1963. (N/A)

21. O'Kelly, M.E.J., "Vibration of Viscously Damped Linear Dynamic Systems," 1964. (N/A)

22. Nielsen, N. Norby, "Dynamic Response of Multistory Buildings," 1964. (N/A)

23. Tso, Wai Keung, "Dynamics of Thin-Walled Beams of Open Section," 1964. (N/A)

24. Keightley, Willard O., "A Dynamic Investigation of Bouquet Canyon Dam," 1964. (N/A)

25. Malhotra, R.K., "Free and Forced Oscillations of a Class of Self-Excited Oscillators," 1964.

26. Hanson, Robert D., "Post-Elastic Response of Mild Steel Structures," 1965.

27. Masri, Sami F., "Analytical and Experimental Studies of Impact Dampers," 1965.

28. Hanson, Robert D., "Static and Dynamic Tests of a Full-Scale Steel-Frame Structure," 1965.

29. Cronin, Donald L., "Response of Linear, Viscous Damped Systems to Excitations Having Time-Varying Frequency," 1965.

30. Hu, Paul Yu-fei, "Analytical and Experimental Studies of Random Vibration," 1965.

31. Crede, Charles E., "Research on Failure of Equipment when Subject to Vibration," 1965.

32. Lutes, Loren D., "Numerical Response Characteristics of a Uniform Beam Carrying One Discrete Load," 1965. (N/A)

33. Rocke, Richard D., "Transmission Matrices and Lumped Parameter Models for Continuous Systems," 1966. (N/A)

34. Brady, Arthur Gerald, "Studies of Response to Earthquake Ground Motion," 1966. (N/A)

35. Atkinson, John D., "Spectral Density of First Order Piecewise Linear Systems Excited by White Noise," 1967. (N/A)

36. Dickerson, John R., "Stability of Parametrically Excited Differential Equations," 1967. (N/A)

37. Giberson, Melbourne F., "The Response of Nonlinear Multi-Story Structures Subjected to Earthquake Excitation," 1967. (N/A)

38. Hallanger, Lawrence W., "The Dynamic Stability of an Unbalanced Mass Exciter," 1967.

39. Husid, Raul, "Gravity Effects on the Earthquake Response of Yielding Structures," 1967. (N/A)

40. Kuroiwa, Julio H., "Vibration Test of a Multistory Building," 1967. (N/A)

41. Lutes, Loren Daniel, "Stationary Random Response of Bilinear Hysteretic Systems," 1967.

42. Nigam, Navin C., "Inelastic Interactions in the Dynamic Response of Structures," 1967.

43. Nigam, Navin C. and Paul C. Jennings, "Digital Calculation of Response Spectra from Strong-Motion Earthquake Records," 1968.

44. Spencer, Richard A., "The Nonlinear Response of Some Multistory Reinforced and Prestressed Concrete Structures Subjected to Earthquake Excitation," 1968. (N/A)

45. Jennings, P.C., G.W. Housner and N.C. Tsai, "Simulated Earthquake Motions," 1968.

46. "Strong-Motion Instrumental Data on the Borrego Mountain Earthquake of 9 April 1968," (USGS and EERL Joint Report), 1968.

47. Peters, Rex B., "Strong Motion Accelerograph Evaluation," 1969.

48. Heitner, Kenneth L., "A Mathematical Model for Calculation of the Run-Up of Tsunamis," 1969.

49. Trifunac, Mihailo D., "Investigation of Strong Earthquake Ground Motion," 1969. (N/A)

50. Tsai, Nien Chien, "Influence of Local Geology on Earthquake Ground Motion," 1969. (N/A)

51. Trifunac, Mihailo D., "Wind and Microtremor Induced Vibrations of a Twenty-Two Steel Frame Building," EERL 70-01, 1970.

52. Yang, I-Min, "Stationary Random Response of Multidegree-of-Freedom Systems," DYNL-100, June 1970. (N/A)

53. Patula, Edward John, "Equivalent Differential Equations for Nonlinear Dynamical Systems," DYNL-101, June 1970.

54. Prelewicz, Daniel Adam, "Range of Validity of the Method of Averaging," DYNL-102, 1970.

55. Trifunac, M.D., "On the Statistics and Possible Triggering Mechanism of Earthquakes in Southern California," EERL 70-03, July 1970.

56. Heitner, Kenneth Leon, "Additional Investigations on a Mathematical Model for Calculation of the Run-Up of Tsunamis," July 1970.

57. Trifunac, Mihailo D., "Ambient Vibration Tests of a Thirty-Nine Story Steel Frame Building," EERL 70-02, July 1970.

58. Trifunac, Mihailo and D.E. Hudson, "Laboratory Evaluations and Instrument Corrections of Strong-Motion Accelerographs," EERL 70-04, August 1970. (N/A)

59. Trifunac, Mihailo D., "Response Envelope Spectrum and Interpretation of Strong Earthquake Ground Motion," EERL 70-06, August 1970.

60. Keightley, W.O., "A Strong-Motion Accelerograph Array with Telephone Line Interconnections," EERL 70-05, September 1970.

61. Trifunac, Mihailo D., "Low Frequency Digitization Errors and a New Method for Zero Baseline Correction of Strong-Motion Accelerograms," EERL 70-07, September 1970.

62. Vijayaraghavan, A., "Free and Forced Oscillations in a Class of Piecewise-Linear Dynamic Systems," DYNL-103, January 1971.

63. Jennings, Paul C., R.B. Matthiesen and J. Brent Hoerner, "Forced Vibrations of a 22-Story Steel Frame Building," EERL 71-01, February 1971. (N/A) (PB 205 161)

64. Jennings, Paul C., "Engineering Features of the San Fernando Earthquake of February 9, 1971," EERL 71-02, June 1971. (PB 202 550)

65. Bielak, Jacobo, "Earthquake Response of Building-Foundation Systems," EERL 71-04, June 1971. (N/A) (PB 205 305)

66. Adu, Randolph Ademola, "Response and Failure of Structures under Stationary Random Excitation," EERL 71-03, June 1971. (N/A) (PB 205 304)

67. Skattum, Knut Sverre, "Dynamic Analysis of Coupled Shear Walls and Sandwich Beams," EERL 71-06, June 1971. (N/A) (PB 205 267)

68. Hoerner, John Brent, "Modal Coupling and Earthquake Response of Tall Buildings," EERL 71-07, June 1971. (N/A) (PB 207 635)

69. Stahl, Karl John, "Dynamic Response of Circular Plates Subjected to Moving Massive Loads," DYNL-104, June 1971. (N/A)

70. Trifunac, M.D., F.E. Udwadia and A.G. Brady, "High Frequency Errors and Instrument Corrections of Strong-Motion Accelerograms," EERL 71-05, 1971. (PB 205 369)

71. Furuike, D.M., "Dynamic Response of Hysteretic Systems with Application to a System Containing Limited Slip," DYNL-105, September 1971. (N/A)

72. Hudson, D.E. (Editor), "Strong-Motion Instrumental Data on the San Fernando Earthquake of February 9, 1971," (Seismological Field Survey, NOAA, C.I.T. Joint Report), September 1971. (PB 204 198)

73. Jennings, Paul C. and Jacobo Bielak, "Dynamics of Building-Soil Interaction," EERL 72-01, April 1972. (PB 209 666)

74. Kim, Byung-Koo, "Piecewise Linear Dynamic Systems with Time Delays," DYNL-106, April 1972.

75. Viano, David Charles, "Wave Propagation in a Symmetrically Layered Elastic Plate," DYNL-107, May 1972.

76. Whitney, Albert W., "On Insurance Settlements Incident to the 1906 San Francisco Fire," DRC 72-01, August 1972. (PB 213 256)

77. Udwadia, F.E., "Investigation of Earthquake and Microtremor Ground Motions," EERL 72-02, September 1972. (PB 212 853)

78. Wood, John H., "Analysis of the Earthquake Response of a Nine-Story Steel Frame Building During the San Fernando Earthquake," EERL 72-04, October 1972. (PB 215 823)

79. Jennings, Paul C., "Rapid Calculation of Selected Fourier Spectrum Ordinates," EERL 72-05, November 1972.

80. "Research Papers Submitted to Fifth World Conference on Earthquake Engineering, Rome, Italy, 25-29 June 1973," EERL 73-02, March 1973. (PB 220 431)

81. Udwadia, F.E. and M.D. Trifunac, "The Fourier Transform, Response Spectra and Their Relationship Through the Statistics of Oscillator Response," EERL 73-01, April 1973. (PB 220 458)

82. Housner, George W., "Earthquake-Resistant Design of High-Rise Buildings," DRC 73-01, July 1973. (N/A)

83. "Earthquakes and Insurance," Earthquake Research Affiliates Conference, 2-3 April, 1973, DRC 73-02, July 1973. (PB 223 033)

84. Wood, John H., "Earthquake-Induced Soil Pressures on Structures," EERL 73-05, August 1973. (N/A)

85. Crouse, Charles B., "Engineering Studies of the San Fernando Earthquake," EERL 73-04, March 1973. (N/A)

86. Irvine, H. Max, "The Veracruz Earthquake of 28 August 1973," EERL 73-06, October 1973.

87. Iemura, H. and P.C. Jennings, "Hysteretic Response of a Nine-Story Reinforced Concrete Building During the San Fernando Earthquake," EERL 73-07, October 1973.

88. Trifunac, M.D. and V. Lee, "Routine Computer Processing of Strong-Motion Accelerograms," EERL 73-03, October 1973. (N/A) (PB 226 047/AS)

89. Moeller, Thomas Lee, "The Dynamics of a Spinning Elastic Disk with Massive Load," DYNL 73-01, October 1973.

90. Blevins, Robert D., "Flow Induced Vibration of Bluff Structures," DYNL 74-01, February 1974.

91. Irvine, H. Max, "Studies in the Statics and Dynamics of Simple Cable Systems," DYNL-108, January 1974.

92. Jephcott, D.K. and D.E. Hudson, "The Performance of Public School Plants During the San Fernando Earthquake," EERL 74-01, September 1974. (PB 240 000/AS)

93. Wong, Hung Leung, "Dynamic Soil-Structure Interaction," EERL 75-01, May 1975. (N/A) (PB 247 233/AS)

94. Foutch, D.A., G.W. Housner, P.C. Jennings, "Dynamic Responses of Six Multistory Buildings During the San Fernando Earthquake," EERL 75-02, October 1975. (PB 248 144/AS)

95. Miller, Richard Keith, "The Steady-State Response of Multidegree-of-Freedom Systems with a Spatially Localized Nonlinearity," EERL 75-03, October 1975. (PB 252 459/AS)

96. Abdel-Ghaffar, Ahmed Mansour, "Dynamic Analyses of Suspension Bridge Structures," EERL 76-01, May 1976. (PB 258 744/AS)

97. Foutch, Douglas A., "A Study of the Vibrational Characteristics of Two Multistory Buildings," EERL 76-03, September 1976. (PB 260 874/AS)

98. "Strong Motion Earthquake Accelerograms Index Volume," Earthquake Engineering Research Laboratory, EERL 76-02, August 1976. (PB 260 929/AS)

99. Spanos, P-T.D., "Linearization Techniques for Non-Linear Dynamical Systems," EERL 76-04, September 1976. (PB 266 083/AS)

100. Edwards, Dean Barton, "Time Domain Analysis of Switching Regulators," DYNL 77-01, March 1977.

101. Abdel-Ghaffar, Ahmed Mansour, "Studies on the Effect of Differential Motions of Two Foundations upon the Response of the Superstructure of a Bridge," EERL 77-02, January 1977. (PB 271 095/AS)

102. Gates, Nathan C., "The Earthquake Response of Deteriorating Systems," EERL 77-03, March 1977. (PB 271 090/AS)

103. Daly, W., W. Judd and R. Meade, "Evaluation of Seismicity at U.S. Reservoirs," USCOLD, Committee on Earthquakes, May 1977. (PB 270 036/AS)

104. Abdel-Ghaffar, A.M. and G.W. Housner, "An Analysis of the Dynamic Characteristics of a Suspension Bridge by Ambient Vibration Measurements," EERL 77-01, January 1977. (PB 275 063/AS)

105. Housner, G.W. and P.C. Jennings, "Earthquake Design Criteria for Structures," EERL 77-06, November 1977. (PB 276 502/AS)

106. Morrison, P., R. Maley, G. Brady, R. Porcella, "Earthquake Recordings on or Near Dams," USCOLD, Committee on Earthquakes, November 1977. (PB 285 867/AS)

107. Abdel-Ghaffar, A.M., "Engineering Data and Analyses of the Whittier, California Earthquake of January 1, 1976," EERL 77-05, November 1977. (PB 283 750/AS)

108. Beck, James L., "Determining Models of Structures from Earthquake Records," EERL 78-01, June 1978. (PB 288 806/AS)

109. Psycharis, Ioannis, "The Salonica (Thessaloniki) Earthquake of June 20, 1978," EERL 78-03, October 1978. (PB 290 120/AS)

110. Abdel-Ghaffar, A.M. and R.F. Scott, "An Investigation of the Dynamic Characteristics of an Earth Dam," EERL 78-02, August 1978. (PB 288 878/AS)

111. Mason, Alfred B., Jr., "Some Observations on the Random Response of Linear and Nonlinear Dynamical Systems," EERL 79-01, January 1979. (PB 290 808/AS)

112. Heimberger, D.V. and P.C. Jennings (Organizers), "Strong Ground Motion: N.S.F. Seminar-Workshop," SL-EERL 79-02, February 1978.

113. Lee, David M., Paul C. Jennings and George W. Housner, "A Selection of Important Strong Motion Earthquake Records," EERL 80-01, January 1980. (PB 80 169196)

114. McVerry, Graeme H., "Frequency Domain Identification of Structural Models from Earthquake Records," EERL 79-02, October 1979.

115. Abdel-Ghaffar, A.M., R.F. Scott and M.J. Craig, "Full-Scale Experimental Investigation of a Modern Earth Dam," EERL 80-02, February 1980.

116. Rutenberg, Avigdor, Paul C. Jennings and George W. Housner, "The Response of Veterans Hospital Building 41 in the San Fernando Earthquake," EERL 80-03, May 1980.

117. Haroun, Medhat Ahmed, "Dynamic Analyses of Liquid Storage Tanks," EERL 80-04, February 1980.

118. Liu, Wing Kam, "Development of Finite Element Procedures for Fluid-Structure Interaction," EERL 80-06, August 1980. (PB 184078)

119. Yoder, Paul Jerome, "A Strain-Space Plasticity Theory and Numerical Implementation," EERL 80-07, August 1980.

120. Krousgrill. Charles Morton, Jr., "A Linearization Technique for the Dynamic Respone of Nonlinear Continua," EERL 80-08, September 1980.

121. Cohen, Martin, "Silent Boundary Methods for Transient Wave Analysis," EERL 80-09, September 1980. PB82-201831

122. Hall, Shawn A., "Vortex-Induced Vibrations of Structures," EERL 81-01, January 1981, PB-

123. Psycharis, Ioannis N., "Dynamic Behavior of Rocking Structures Allowed to Uplift," EERL 81-02, August 1981, PB-

124. Shih, Choon-Foo, "Failure of Liquid Storage Tanks Due to Earthquake Excitation," EERL 81-04, May 1981, PB-

125. Lin, Albert Niu, "Experimental Observations of the Effect of Foundation Embedment on Structural Response," EERL 82-01, May 1982, PB-84-163252

126. Botelho, Dirceau L.R., "An Empirical Model for Vortex-Induced Vibrations," EERL 82-02, August 1982, PB-84-161157

127. Ortiz, L. Alexander, "Dynamic Centrifuge Testing of Cantilever Retaining Walls," SML 82-02, August 1982, PB-84-162312

128. Iwan, W.D., Editor, "Proceedings of the U.S. National Workshop on Strong-Motion Earthquake Instrumentation, April 12-14, 1981, Santa Barbara, California," California Institute of Technology, Pasadena, California, 1981.

129. Rashed, Ahmed, "Dynamic Analysis of Fluid-Structure Systems," EERL 82-03, July 1982, PB-

130. National Academy Press, "Earthquake Engineering Research-1982."

131. National Academy Press, "Earthquake Engineering Research-1982, Overview and Recommendations."

132. Jain, Sudhir Kumar, "Analytical Models for the Dynamics of Buildings," EERL 83-02, May 1983, PB-84-161009

133. Huang, Moh-jiann, "Investigation of Local Geology Effects on Strong Earthquake Ground Motions," EERL 83-03, July 1983, PB-

134. McVerry, G.H. and J.L.Beck, "Structural Identification of JPL Building 180 Using Optimally Synchronized Earthquake Records," EERL 83-01, August 1983, PB-

135. Bardet, J.P., "Application of Plasticity Theory To Soil Behavior: A New Sand Model," SML 83-01, September 1983, PB-84-162304

136. Wilson, John C., "Analysis of the Observed Earthquake Response of a Multiple Span Bridge," EERL 84-01, May 1984, PB-

137. Hushmand, Behnam, "Experimental Studies of Dynamic Response of Foundations," SML 83-02, November 1983, PB-

Strong-Motion Earthquake Accelerograms
Digitized and Plotted Data

Uncorrected Accelerograms

Volume I

Part	Report No.	NTIS Accession No.
A	EERL 70-20	PB 287 847
B	EERL 70-21	PB 196 823
C	EERL 71-20	PB 204 364
D	EERL 71-21	PB 208 529
E	EERL 71-22	PB 209 749
F	EERL 71-23	PB 210 619
G	EERL 72-20	PB 211 357
H	EERL 72-21	PB 211 781
I	EERL 72-22	PB 213 422
J	EERL 72-23	PB 213 423
K	EERL 72-24	PB 213 424
L	EERL 72-25	PB 215 639
M	EERL 72-26	PB 220 554
N	EERL 72-27	PB 223 023
O	EERL 73-20	PB 222 417
P	EERL 73-21	PB 227 481/AS
Q	EERL 73-22	PB 232 315/AS
R	EERL 73-23	PB 239 585/AS
S	EERL 73-24	PB 241 551/AS
T	EERL 73-25	PB 241 943/AS
U	EERL 73-26	PB 242 262/AS
V	EERL 73-27	PB 243 483/AS
W	EERL 73-28	PB 243 497/AS
X	EERL 73-29	PB 243 594/AS
Y	EERL 73-30	PB 242 947/AS

Strong-Motion Earthquake Accelerograms
Digitized and Plotted Data

Corrected Accelerograms and Integrated
Ground Velocity and Displacement Curves

Volume II

Part	Report No.	NTIS Accession No.
A	EERL 71-50	PB 208 283
B	EERL 72-50	PB 220 161
C	EERL 72-51	PB 220 162
D	EERL 72-52	PB 220 836
E	EERL 73-50	PB 223 024
F	EERL 73-51	PB 224 977/9AS
G	EERL 73-52	PB 229 239/AS
H	EERL 74-50	PB 231 225/AS
I	EERL 74-51	PB 232 316/AS
J,K	EERL 74-52	PB 233 257/AS
L,M	EERL 74-53	PB 237 174/AS
N	EERL 74-54	PB 236 399/AS
O,P	EERL 74-55	PB 239 586/AS
Q,R	EERL 74-56	PB 239 587/AS
S	EERL 74-57	PB 241 552/AS
T	EERL 75-50	PB 242 433/AS
U	EERL 75-51	PB 242 949/AS
V	EERL 75-52	PB 242 948/AS
W,Y	EERL 75-53	PB 243 719

Analyses of Strong-Motion Earthquake Accelerograms
Response Spectra

Volume III

Part	Report No.	NTIS Accession No.
A	EERL 72-80	PB 212 602
B	EERL 73-80	PB 221 256
C	EERL 73-81	PB 223 025
D	EERL 73-82	PB 227 469/AS
E	EERL 73-83	PB 227 470/AS
F	EERL 73-84	PB 227 471/AS
G	EERL 73-85	PB 231 223/AS
H	EERL 74-80	PB 231 319/AS
I	EERL 74-81	PB 232 326/AS
J,K,L	EERL 74-82	PB 236 110/AS
M,N	EERL 74-83	PB 236 400/AS
O,P	EERL 74-84	PB 238 102/AS
Q,R	EERL 74-85	PB 240 688/AS
S	EERL 74-86	PB 241 553/AS
T	EERL 75-80	PB 243 698/AS
U	EERL 75-81	PB 242 950/AS
V	EERL 75-82	PB 242 951/AS
W,Y	EERL 75-83	PB 243 492/AS

Analyses of Strong-Motion Earthquake Accelerograms
Fourier Amplitude Spectra

Volume IV

Part	Report No.	NTIS Accession No.
A	EERL 72-100	PB 212 603
B	EERL 73-100	PB 220 837
C	EERL 73-101	PB 222 514
D	EERL 73-102	PB 222 969/AS
E	EERL 73-103	PB 229 240/AS
F	EERL 73-104	PB 229 241/AS
G	EERL 73-105	PB 231 224/AS
H	EERL 74-100	PB 232 327/AS
I	EERL 74-101	PB 232 328/AS
J,K,L,M	EERL 74-102	PB 236 111/AS
N,O,P	EERL 74-103	PB 238 447/AS
Q,R,S	EERL 74-104	PB 241 554/AS
T,U	EERL 75-100	PB 243 493/AS
V,W,Y	EERL 75-101	PB 243 494/AS
Index Volume	EERL 76-02	PB 260 929/AS